



ScuDo
Scuola di Dottorato ~ Doctoral School
WHAT YOU ARE, TAKES YOU FAR



Doctoral Dissertation
Doctoral Program in Materials Science (31.th cycle)

Low-Pressure Plasma treatments for Cleaning and Protecting metallic heritage artefacts

Ahmed Mahmoud Mostafa Elsayed

* * * * *

Supervisors

Prof. Emma Angelini, Supervisor
Prof. Sabrina Grassini, Co-supervisor

Doctoral Examination Committee:

Prof. Panayota Vassilou - University of Athens, Reviewer
Prof. Tilde de Caro - Italian National Resource Council, Reviewer

Politecnico di Torino
July, 2019

This thesis is licensed under a Creative Commons License, Attribution - Noncommercial-NoDerivative Works 4.0 International: see www.creativecommons.org. The text may be reproduced for non-commercial purposes, provided that credit is given to the original author.

I hereby declare that, the contents and organisation of this dissertation constitute my own original work and does not compromise in any way the rights of third parties, including those relating to the security of personal data.

.....
Ahmed Mahmoud Mostafa Elsayed
Turin, July, 2019

Summary

Restoration and conservation of Cultural heritage is a multidisciplinary field that takes advantage of engineering and material science for developing tailored strategies for long-lasting conservation by means of innovative and reversible materials for restoration, non-invasive analytical techniques. Cleaning Metallic artefacts is a primary step in the restoration and conservation processes. For this reason Low-pressure Plasma is proposed as an effective and environmentally friendly technique for cleaning different materials such as metals artefacts. Moreover, strategies for preventive conservation have to be considered as next step. The metallic artefacts are sensitive to the atmospheric corrosion in indoor environments as museum. A new smart monitoring system to assess the environmental conditions and the atmosphere aggressiveness in a museum indoor environment has been developed and tested. The main objectives of this thesis are to examine the efficiency of the plasma for cleaning metallic artefacts and to test a new real-time monitoring system. The thesis consists of five chapters: Chapter 1 deals with the state of the art of low-pressure plasma in the field of cleaning and protecting metallic artefacts. Chapter 2 deals with an experimental study on plasma cleaning of copper and silver samples aged by electrochemical treatment for copper-based alloys and tarnished by H_2S exposure for silver samples. Several parameters in plasma cleaning using hydrogen and argon were modified in order to optimize the procedure. Plasma cleaning shows a higher efficacy silver-based alloy samples than on copper-based alloys. Chapter 3 is a study of the corrosion mechanisms of copper-based alloys and Silver-based alloys. A case study is considered, the characterization of some ancient coins found in an excavation site in AL-Fustat in Egypt, with a deeping on interaction between the soil and the corrosion products and the production methods of the artefacts. The analytical techniques employed were FESEM coupled with EDS, optical microscopy, XRD. The results showed that all the coins were made of bronze with variable amounts of tin. The production method was hammering into molds. Moreover, the corrosion products were copper oxides and copper chloride due to long-term burial period in a soil which is rich in chloride ions. Chapter 4 is a study of the indoor environment aggressivity by means of the smart sensors environmental monitoring system and of a set of reference samples, constituted by copper specimens coated with nano-structured thin film. Chapter 5 deals with the environmental monitoring system, based on a wireless network composed of small sensors, designed to satisfy the requirements for their employment in

the Cultural Heritage field. The sensors are stand-alone devices able to measure temperature and relative humidity for three years, connected through a wireless link to a small receiver for routing data to a cloud system. The proposed system contains a set of copper reference specimens coated with a Cu nano-structured films deposited by plasma sputtering to be located close to the sensors to assess the atmosphere aggressiveness. A monitoring campaign was performed for one year in the museum of the Faculty of Archaeology at Sohag University in Egypt and allowed to obtain a map of the climatic conditions in the museum and to develop strategies for improving the stability of the environmental conditions. Furthermore, from a material science point of view, the higher sensitivity of the Cu-nano-structure thin film to the atmosphere with respect to bulk copper, due to the increase of the number of the grain boundaries, allows to proposed them as proper reference materials . Moreover an artificial ageing of copper specimens coated with nano-structured thin film following the ISO 3231-1993 standard method for the determination of resistance to humid atmospheres containing sulphur dioxide was performed.

Acknowledgements

At the outset, I submit my deepest gratitude to ‘Almighty Allah’, whose blessings enabled me to accomplish this endeavour successfully. Then I am grateful to the Egyptian Ministry of Higher Education for their financial support for my Ph.D.’s scholarship.

I would like to extend my sincere gratitude to my Supervisors Prof. Emma Angelini and Sabrina Grassini for their continuous support, motivation, enthusiasm, assiduous guidance, constructive criticism and constant encouragement throughout this research study.

I would like to thank Prof. Marco Parvis from the Department of Electronics and Telecommunications for his continuous support in laboratory experiments and his great cooperation in the environmental monitoring system, as well as Dr. Simone Corbellini for his cooperation in developing of sensors, Mobile application and the website of the environmental monitoring of the museum of Faculty of archaeology, Sohag university, Egypt.

I extend my sincere thanks to my colleagues in the research group; Luca Lombardo, Leonardo Iannucci, Alessio Gullino, and Elisabetta Di Francia for all-time support and standing with me during my stay at Politecnico di Torino.

Special thanks to my big family; the soul of my father, my mother, My brother and my sister for their continued support and prayers. Further, I extend my thanks to my small family; Asmaa, Heba, and my lovely kids; Marwan, Fairoz, and Farida.

Many Thanks for all my Professors my Collogues at my home; the department of conservation, faculty of archaeology, Sohag University, Egypt.

*I would like to dedicate
this thesis to the soul of
my father, my mother,
my brother and sister, my
small family; Asmaa,
Heba, and my lovely kids
Marwan, Fairoz and
Farida*

Contents

List of Tables	x
List of Figures	xi
1 Introduction	1
2 Low Pressure Plasma Technologies	9
2.1 Introduction to Plasma	9
2.2 Plasma Typologies	11
2.3 Low-pressure Plasma treatment of Metallic artefacts	11
2.3.1 Cleaning of iron artefacts	11
2.3.2 Cleaning of copper-based artefacts	32
2.3.3 Cleaning of silver artefacts	34
3 Plasma cleaning of metallic artefacts	37
3.1 Plasma discharge for cleaning metallic artefacts	37
3.1.1 Principles of the plasma discharge	37
3.1.2 Plasma cleaning of metallic artefacts	43
3.1.3 Plasma Cleaning Tests	45
3.2 Results and discussion	53
3.2.1 High resolution photos	54
3.2.2 FSEM and EDS	66
3.2.3 XRD	77
3.3 Conclusions	79
4 Case Studies	81
4.1 The Corrosion Mechanism of ancient Coins	81
4.1.1 Materials and Methods	84
4.1.2 Results and Discussion	84
4.1.3 Conclusions	93

5	Assessment of atmospheric corrosion effects	95
5.1	The environmental monitoring campaign in the Museum of the Faculty of Archaeology of the Sohag University (Egypt)	95
5.1.1	Materials and Methods	101
5.1.2	Sensors description	106
5.1.3	Cu nanostructured reference specimens	107
5.2	Result and discussion	109
5.2.1	Day/ night measurement	110
5.2.2	One year environmental monitoring data	112
5.2.3	Surface characterization of Cu reference specimens	112
5.3	Conclusions	117
5.3.1	Assessment of the atmospheric corrosion of copper at nanoscale	118
5.3.2	Materials and methods	118

List of Tables

2.1	Plasma treatment for iron artefacts	27
2.2	The Parameters of Plasma treatment for Bronze artefacts	33
2.3	The Parameters of Plasma treatment for silver artefacts	34
3.1	Chemical composition of the reacted surface as a function of the atmosphere[146].	49
3.2	Pre test for plasma cleaning parameters	53
3.3	Plasma cleaning parameters	54
4.1	XRD results of the coins corrosion products	91
5.1	Corrosivity categories of indoor atmospheres	102
5.2	Levels for average of relative humidity	103

List of Figures

2.1	Matter chagement of state.	10
2.2	Discharge prototype of Hauksbee in 1705.	10
2.3	Short-circuit discharge prototype of Volta, 1775.	11
2.4	Space and laboratory plasmas on a $\log n$ versus $\log T_e$ diagram	12
2.5	Rate of removal organic materials in O_2/Ar plasma.	13
2.6	Effects of O_2/ Ar plasma	14
2.7	Effects of H_2/Ar plasma.	14
2.8	Pyrex glass plasma apparatus[30].	15
2.9	Time-dependence of the surface layer composition of a thermally oxidized iron platelet during treatment in hydrogen plasma at about $380^\circ C$ [30].	16
2.10	Free energy of the reduction of iron oxides with molecular and atomic hydrogen[32].	17
2.11	Free energy of the reduction of iron and sodium chlorides with molecular and atomic hydrogen[32].	18
2.12	The plasma chamber with the bell-jar. The cross-bow bolt is hanging in a connecting wire and functions as cathode between the two perforated anodes[34].	19
2.13	Experimental set-up of the VHF-GD reactor used with gas supply, pumping system, VHF-power supply, and the set-up for optical emission spectroscopy (OES). [45].	21
2.14	Plasma layout. [48].	23
2.15	Schematic of plasma operating in liquid, 1-treated sample, 2-Powered electrode, 3-water solution, 4-insulator, 5-grounded electrode; right-electrode head	29
3.1	Electron-atom elastic collision	39
3.2	Electron impact ionization	40
3.3	Electron impact excitation	40
3.4	Relaxation or de-excitation	41
3.5	Recombination	41
3.6	Gas phase reactions involving electrons and heavy species	42
3.7	Plasma etching profiles, (A) is Isotropic, (B) is anisotropic	44
3.8	The plasma reactor in the Plasma Lab of Politecnico di Torino	46

3.9	Artificial corrosion of copper samples	50
3.10	Artificial tarnishing of silver alloy samples	51
3.11	Photo of the copper and silver samples inside the chamber at the treatment time	52
3.12	Schematic of the Aluminium foil mask on the half of the sample	53
3.13	Sample C1, (A) before and after treatment, (B) histogram of patches before treatment and (C) histogram of patches after treatment.It shows the sputtering of copper nanoparticles from the target on the surface	57
3.14	Sample C2, (A, B) before and after treatment, (C, D) histogram of patches before and after treatment.It shows the sputtering of copper nanoparticles from the target on the surface	58
3.15	Sample C3, (A) before and after treatment, (B, C) histogram of patches before and after treatment.It shows the sputtering of copper nanoparticles from the target on the surface.	58
3.16	Sample C4, (A) before and after 30 minutes of treatment, (B, C) histogram of patches before and after treatment.	59
3.17	Sample C4, (A) before and after 60 minutes of treatment, (B, C) histogram of patches before and after treatment.	59
3.18	Sample Cup3, (A) before and after 30 minutes of treatment, (B, C) histogram of patches before and after treatment.	60
3.19	Sample Cup2, (A) before and after 1 hours of treatment, (B, C) histogram of patches before and after treatment.	60
3.20	Sample Cup1, (A) before and after 2 hours of treatment, (B, C) histogram of patches before and after treatment.	61
3.21	Sample Oxy3, (A) before and after 30 min of treatment, (B, C) histogram of patches before and after treatment.	61
3.22	Sample Oxy2, (A) before and after 2 hours of treatment, (B, C) histogram of patches before and after treatment.	62
3.23	Sample Oxy1, (A) before and after 3 hours of treatment, (B, C) histogram of patches before and after treatment.	62
3.24	Sample Ag1, (A) before and after 30 minutes of treatment, (B, C) histogram of patches before and after treatment.	63
3.25	Sample Ag2, (A) before and after 30 minutes of treatment, (B, C) histogram of patches before and after treatment.	63
3.26	Sample Ag2, (A) before and after 30 minutes of treatment, (B, C) histogram of patches before and after treatment.	64
3.27	Sample Ag4, (A) before cleaning, (B) after 30 minutes of treatment, (C, D) histogram of patches before and after treatment.	64
3.28	Sample Ag5, (A) before cleaning, (B) after 30 minutes of treatment, (C, D) histogram of patches before and after treatment.	65
3.29	Sample Ag6, (A) before cleaning, (B) after 30 minutes of treatment, (C, D) histogram of patches before and after treatment.	65

3.34	FESEM image and EDS analysis of sample Cup2 before treatment. . . .	68
3.35	FESEM image and EDS analysis of sample Cup2 after 1 hour of treatment. . . .	68
3.30	FESEM image of sample Cup2 before and after 1 hour of treatment. . . .	69
3.31	FESEM image of sample Cup3 before and after 2 hours of treatment. . . .	70
3.32	FESEM image of sample Oxy3 before and after 30 minutes of treatment. . . .	71
3.33	FESEM image of sample Oxy1 before and after 3 hours of treatment. . . .	72
3.36	FESEM image and EDS analysis of sample Cup3 before treatment. . . .	73
3.37	FESEM image and EDS analysis of sample Cup3, after 2 hours of treatment. . . .	73
3.38	FESEM image and EDS analysis of sample Oxy1 (A) before treatment. . . .	73
3.39	FESEM image and EDS analysis of sample Oxy1 (B) before treatment. . . .	74
3.40	FESEM image and EDS analysis of sample Oxy1, after 3 hours of treatment. . . .	74
3.41	FESEM image and EDS analysis of sample Oxy3 before treatment. . . .	74
3.42	FESEM image and EDS analysis of sample Oxy3, after 30 minutes of treatment.	75
3.43	FESEM image and EDS analysis of sample Ag2 before treatment.	75
3.44	FESEM image and EDS analysis of sample Ag2, after 30 min of treatment.	75
3.45	FESEM image and EDS analysis of sample Ag3 before treatment.	76
3.46	FESEM image and EDS analysis of sample Ag3, after 30 min of treatment.	76
3.47	FESEM image and EDS analysis of sample Ag4, after 30 min of treatment.	76
3.48	FESEM image and EDS analysis of sample Ag5, after 30 min of treatment.	77
3.49	FESEM image and EDS analysis of sample Ag6, after 30 min of treatment.	77
3.50	XRD spectra of sample Cup3, before and after 30 minutes treatment.	78
3.51	XRD spectra of sample OX1, before and after 3 hours of treatment.	78
4.1	(a) Copper–water and (b) copper–chloride–water Pourbaix diagrams. The diagrams show the different products that can exist when copper is in contact with water in the absence and presence of chloride. The regions where solid products exist are marked with bold and dissolved products are marked in normal font (reprinted with permission from author)[88]	83
4.2	High resolution image of Coin C1	85
4.3	High resolution image of Coin C2	85
4.4	High resolution image of Coin C3	86
4.5	FESEM and EDS analysis of the outer layer of Coin C1	86
4.6	FESEM and EDS analysis of the inner layer of Coin C1	87
4.7	EDS map of Coin C1	87
4.8	FESEM and EDS analysis of the inner layer of Coin C2	88
4.9	FESEM and EDS analysis of the outer layer of Coin C2	88
4.10	FESEM and EDS analysis of the inner layer of Coin C3	89
4.11	FESEM and EDS analysis of the outer layer of Coin C3	89
4.12	Metallographic microscope images for the microstructure of the coins	90
4.13	schematic show the coin production in ancient ages	91
4.14	XRD pattern of coin C1	92

4.15	XRD pattern of coin C2	92
4.16	XRD pattern of coin C3	93
5.1	Sohag location at the map of Egypt	97
5.2	The museum structure	98
5.3	The Faculty museum	99
5.4	The Faculty museum	99
5.5	Some artefacts in the museum	100
5.6	Thermo-hygrometer to measure T and RH in the museum and silica gel for reduce the RH inside the showcases	101
5.7	Sensors distribution inside and outside the showcases	105
5.8	Sensors and Cu nanostructured specimens distribution inside and out- side the showcases	106
5.9	(A) small sensor, (B) WiFi data receiver	107
5.10	Schematic showing nanomaterials	107
5.11	scheme of the preparation of Cu nanostructured thin film specimens	108
5.12	Scheme of a DC glow discharge apparatus in which gas atoms are ion- ized by an electron filament and either deposit on a substrate or cause sputtering of a target	109
5.13	T and RH measurements collected for about two days in summer from the smart sensors inside (S161, S162, S163, S165, S166) and outside (S164) the showcases.	111
5.14	T and RH measurements collected for about two days in Winter from the smart sensors inside (S161, S162, S163, S165, S166) and outside (S164) the showcases.	111
5.15	T and RH measurements collected for one year of measurement with the smart sensors inside (S161, S162, S163, S165, S166) and outside (S164) the showcases.	112
5.16	FESEM images of the Cu nanostructured reference specimens exposed for 2 months inside showcases (S162, S163, S165) and outside in the room exhibition (S164)	113
5.17	FESEM images of the Cu nanostructured reference specimens exposed for 6 months inside showcases (S162) as an example and outside in room exhibition (S164)	114
5.18	EDS analysis of chemical composition of corrosion products for the Cu nanostructured reference specimens exposed for (A) 2 months & (B) 6 months inside showcases (S162)	115
5.19	FESEM images of the Cu nanostructured reference specimens exposed for year inside showcases (S165) as an example and outside in the room exhibition (S164)	116
5.20	EDS analysis of chemical composition of corrosion products for the Cu nanostructured reference specimens exposed for 1 year (A) inside show- case S165 and (B) exhibition room S162	117

5.21	Schematic classification of the information content of different imaging and analytical techniques in terms of their lateral and depth resolutions	119
5.22	FESEM image of the Cu nanostructured thin film with different nanoparticles size with different power	120
5.23	Diagram showing correlation between nanotechnology with corrosion	121
5.24	Difference in the mass increase between the two samples related to the time of the test	122
5.25	Mass changes of the samples due to the accelerated ageing test	122
5.26	Optical microscope images, shows the morphology of the three groups (samples 100w and 500w) after the accelerating ageing test	124
5.27	FESEM image of sample 100w-1, showing the brochantite and cuprite on the sample surface	125
5.28	FESEM image for sample 500w-1, it shows the brochantite and cuprite on the sample surface	126
5.29	schematic of cuprite layer on the nanostructured thin film and the form of brochantite with evaporating water on the cuprite layer due to the humid air through the test	126
5.30	Schematic of the relation between the nanoparticles size and sensitivity to corrosion	127

Chapter 1

Introduction

Protecting, preserving, and interpreting metals from museums in the Mediterranean Basin:

Heritage is our legacy from the past, what we live with today, and what we pass on to future generations. Our cultural and natural heritage are both irreplaceable sources of life and inspiration. The United Nations Educational, Scientific and Cultural Organisation (UNESCO) seeks to encourage the protection, preservation, interpretation of cultural and natural heritage around the world, as they are considered to be of outstanding value to humanity [1, 2].

Among the tangible cultural heritage, metallic artefacts such as weapons, tools, machinery, decorative art objects as statues, and jewelry, have always been of primary importance. The growth of ancient metallurgy is related to the development of trade in highly valued and attractive ancient metal objects such as those produced in the Mediterranean basin by skilled craftspeople.

The study of these ancient metal objects has contributed to understanding the great importance of the history of the region where many great civilizations have flourished such as the Egyptians, Minoans, Mycenaeans, Greeks, Romans, Byzantines, and Arabs have flourished, making an encyclopedia of human history in the area where three continents, Europe, Asia, and Africa meet [3].

The important role of the Mediterranean basin is reflected in the many books, journals, and societies that exist today to emphasize the Mediterranean culture as the foundation of world culture. Today, the vast and attractive geographical features of the Mediterranean basin face immense environmental pressures, as they are under threat due to intense human activity such as maritime traffic or even mass tourism.

The changing world climate has forecast that this region will suffer the most from major risks such as fires and droughts and reduction of water resources; the latter has

already begun to have an impact on the region. The culture and history of the region represents a strong factor for unity and economic prosperity necessitating the respect of sustainable development for cultural and natural heritage resources. Technological innovation is considered as the key element to economic development in the region that requires cooperation.

This thesis is developed in the field of preservation of cultural heritage devoted to find innovative strategies to protect, preserve, and interpret the material culture made of metals, which is in museums of the Mediterranean basin. The significance of metals cultural heritage from the Mediterranean region is underlined. Metallurgical science today is considered under the auspices of materials science, but up to the eighteenth century it mainly concerned the practices of metallurgy consisting of the traditional methods of smelting, melting and working of metals.

The study of the spread of this knowledge is extremely meaningful, because this knowledge has been strictly dependent on the ability of the various civilizations to invent new and exploit known techniques. Great civilizations from about the fourth millennium BC succeeded in smelting metals from their ores, working and casting them into metal objects.

The metal age developed along the valleys of the Nile and Euphrates, the Middle East, and Anatolia, rapidly progressing to countries across the Mediterranean. Archaeological evidence from the fourth millennium BC shows that the Sumerian craftsman from the Tigris-Euphrates valley of Mesopotamia had remarkable skills in metal working. Similar evolutionary stages were found in early Egypt, where there is evidence of metal processing from 4000 to 3000 BC.

Still little is known about the early metalworkers in the Nile valley and whether their influence came from Mesopotamia or elsewhere. However, the Greek world obviously benefited from being close to these great civilizations, starting in Crete and the Cyclades where copper alloy production was known from the third millennium BC and then followed by Cyprus [4, 5].

The types of alloys used with copper progressed from the prehistoric and classical periods to the Roman times. The occurrence of the types of metal alloys throughout the ages was greatly influenced by the trade of metals in these regions. For example, no silver mines were found in ancient Egypt and so silver had to be imported from Mesopotamia, Crete, and Cyprus.

Mines with tin used in copper alloys were also non-existent in Egypt and mainland Greece and had to be imported. The activity of metals production shows the interaction between great civilizations of antiquity in terms of trade around the shores of the

Mediterranean. The well-marked metallic sequence occurring over widely spaced areas of the globe could be consistent with a diffusion process: for example the sequence copper-arsenical copper-bronze-iron occurs in different areas at times separated by over 2000 years. However, some argue that care is needed not to oversimplify the diffusion case as, for example, when considering the ancient finds of the Vinča culture in the Balkan region, where it may be argued that metallurgy developed independently, several centuries before it reached a comparable state of development in the Aegean. Nonetheless, alloying was not practiced in the Balkans until the Bronze Age, around 2500 BC, at about the same time as it began in the Aegean and the Near East [6].

Notwithstanding the cultural transmissions for copper metallurgy, geology suggests other possible reasons for the development of the metallic sequence, such as the fact that the main primary copper ores have weathered into a succession of layers with an oxidized zone containing native copper and oxidized minerals like malachite at the top and an enriched sulfide zone with arsenic impurities at the bottom; however, the theory of the diffusion of ideas and techniques is generally accepted. For example, the technique of copper smelting developed in Anatolia as early as 5000 BC and reached the British Isles and China by the beginning of 2000 BC; the appearance of smelted copper in South and Central America at the beginning of the first millennium could be an independent development. In Anatolia, the Iron Age started between 1500 and 1000 BC and reached China and Britain by 400 BC.

North and South America obtained their knowledge of iron-working with European colonization beginning from 1400 AD. The remains of the past history of the Mediterranean have filled our museum collections around the world with evidence of this great metals production. Ancient metal objects from these great civilizations are displayed in many foreign Western museums, since they represent the progression of man from the Stone Age [7, 8].

Still today, as our cities grow in the Mediterranean basin, salvage excavations take place at a fast pace filling our museums with vast quantities of objects. The socio-economic impact involved in preserving such collections needs to be considered, and viable solutions specific to the region need to be found, which will respect its sustainable development. The problems museum curators/restorers face in the Mediterranean basin are really wide.

Curators of museums are responsible for protecting, preserving, interpreting, enriching, enhancing, and disseminating their collections. They may also run an establishment or service for which there must be wide public access. To fulfill this curatorial mission, a good knowledge of the composition and manufacturing techniques of the finds of the collections is necessary. This information is of primary importance for improving the archaeological/historical data of the collection and for conducting a survey of the metallic collections to allow the set up of a coherent conservation and restoration

policy. Taking into account environmental data and the degradation mechanisms, the curator will need to develop and implement a coherent conservation plan [9].

In some cases, the plan shows that conservation-restoration work must take place because of the presence of active corrosion on a metal object. At the end of the conservation treatment, a protection coating must be applied to slow down the exchange between the metal and the corrosive media. With the application of these protective coatings, a maintenance program must be set up to prevent the degradation of the coating and to determine the time between two applications. Unfortunately, most of those methods cannot be easily pursued because of the lack of qualified persons in the institutions; consequently it is difficult to have a coherent conservation and restoration policy since, except for large institutions, the curator has to hire a conservator-restorer(s) as well as search for funds.

As explained previously, good knowledge of the composition of the ancient metals can be a decisive factor for their preservation, because some alloys are more sensitive to changes in the environment than others. Thus, it is often important to perform early diagnostic analysis to identify the mechanisms that lead to the degradation of collections. Furthermore, the caretakers of these collections need to make clear the full extent of the difficulties involved in implementing national policies at their museums for the protection of their cultural property from the environment.

There are specific problems for metals collections in the Mediterranean region. As a matter of facts, despite their apparent solidity, metallic artefacts do corrode and can be vulnerable to physical and chemical damages. Because of the huge range of uses for metals, objects containing metals or fully made of metals are all around us and comprise a large part of many collections housed in museums, galleries and some libraries.

Archaeological collections : Many museum collections in the Mediterranean region are located at the archaeological sites where the excavations take place. The archaeologists or curators are responsible for the care of both the archaeological site and excavated objects. The restoration of buildings and structures associated to the site often take precedence over the conservation-restoration of the objects stored in the museum, since they are more visible to the public and monies are more easily raised (either private or public) for them than the objects. Furthermore, archaeologists may not be able to offer proper care and handling of the objects during excavations, so that, when objects are removed from wet burial environment, they are allowed to dry out. To compound this problem, they are often stored inadequately, and it may be decades before any conservation treatment takes place.

As a result, archaeological finds most sensitive to changes in the environment after excavation such as iron, copper, or silver alloy artefacts suffer a great deal. The best that

can be hoped for is that the excavated metal artefacts are found completely mineralized and contain no metal so that they will remain stable and not turn to dust in the end. [10]

Historical collections : Historical collections are usually on display or stored in historical locations and buildings, such as forts or castles. These historic buildings may not be ideal as museums for maintaining their collections, and it may be very difficult to upgrade their facilities, because large amounts of monies may be required to create an ideal environment for the preservation of these collections. Furthermore, the curators of these museums may display their objects in a manner that emphasizes the historic building rather than best preserves the objects. Often, old display cases made of wood, which are not suitable for metals, are used in displaying such objects since they are considered as a historical element of the museum [11].

Usually, in the Mediterranean region these historical buildings are located near the sea, where salt aerosols are abundant in the atmosphere and, with relative humidity (RH) being greater than 60 per cent, result in water vapor with chlorides settling on the bare metal surfaces and stimulating electrochemical corrosion. As a result, historical metals most sensitive to such conditions, such as iron, copper or silver alloys suffer a great deal. Such collections need constant maintenance and care from a conservator-restorer.

Museum environment : In an ideal museum environment, treated archaeological metal objects or metals collections of historic, ethnographic or artistic value must be displayed or stored in a controlled environment to prevent further damages to the collection. For stable metal objects that do not exhibit active signs of corrosion, it is generally accepted to store or display them with a RH ranging between 35 to 55 per cent. Above RH of 55 per cent, problems begin to occur for metal objects, since water vapor settles on the objects and begins the cycle of electrochemical corrosion. Below RH of 35 per cent, problems occur for the storage of objects made of organic materials, common for the display of mixed collections.

Currently, only a few museums provide a controlled environment in terms of maintaining the RH and temperature at standard values with minimal fluctuations, as well as preventing outdoor air pollutants from affecting the collections, either on display or in storage. What is worse, many museums display up to 80% of their collections, and those stored in their reserves are not properly protected with the necessary packaging to create a microclimate specific for preserving those objects [12, 13].

While governments do invest in building new state-of-the-art museums, such as the new Acropolis museum in Athens, Greece, or the prospective Egyptian museum in Giza, Egypt, to house some of the most famous collections, the cost involved in meeting building requirements for state-of-the-art museums is prohibitive for most economies. As a result, one would expect museums to invest a great deal in preventive conservation,

by upgrading and maintaining buildings that house their collections, or by storing, to the extent that this is possible, their collections with proper materials to maintain a microclimate specific to the objects.

Ironically, while preventive conservation has been a hot topic in the conservation field since the 1970s, still today, many museums in Europe and abroad do not have policies for adopting such effective preventive conservation and maintenance plans for their buildings and collections. and proper lifting, handling, and packaging for archaeological metals must be carried out in order to ensure minimal damage to the finds as a result of excavation.

Archaeological metals may be very brittle from corrosion with time and contain contaminants and corrosion products that stimulate further damage upon changes from their burial environment, since artefacts now come in contact with an open environment with an abundance of oxygen, fluctuating moisture, and light. With such environmental changes, soluble corrosion products at the metal interface may change and become insoluble or oxidized, growing inside to more voluminous corrosion products, corroding further the remaining metal, and breaking open the body of the artefact.

Thus, the artefacts with remaining metal begin to disintegrate into dust, a common problem for archaeological iron artefacts that are not properly treated. In fact, most conservators-restorers prefer to deal with excavated iron artefacts that are completely mineralized, since with no more metal remaining, electrochemical corrosion is now impossible.

The iron has now reverted back to its original oxidized state, as is commonly found in nature [14, 15, 16].

In this case, the conservator-restorer has minimal work, namely to clean the artefact so that it returns to its original shape, without the need to prevent the corrosion of any remaining metal using protective methods, such as coatings or preventive measures. With metal remaining, the conservator-restorer's goal is very difficult, since prior to conservation treatment, they must create a microclimate for the metal artefacts similar to the burial conditions in order to ascertain minimal changes prior to treatment. Then treatment requires the complete removal of any contaminants, such as chlorides or sulphates, which would otherwise continue the cyclic corrosion in the presence of even a minimal amount of moisture. If the wet artefacts were allowed to dry out prior to treatment, the soluble salts would become insoluble and change, thus making it more difficult to remove them using traditional stabilization treatments.

Furthermore, mechanical cleaning is ineffective at removing these contaminants, since they are found below the original surface of the artefact and can only be removed by stripping away at the layers of the artefact containing important technological and anthropological information. Specialized chemical or electrochemical treatments are required to diffuse the soluble contaminants from the pores of the corrosion products, while still retaining the corrosion layers that make-up the original shape and surface of the object.

After such stabilisation treatments, the object is cleaned to its original surface, and then protection is offered by storing the object in controlled conditions or special packaging to create a microclimate specific for maintaining such objects. However, for most Mediterranean museums, the objects are stored and displayed in uncontrolled environments, and monies are not spent for materials for the special packaging of such objects.

Furthermore, since most objects in museum collections are on display, conservator-restorers use organic coatings, such as varnishes or waxes to protect the surface of the object from fluctuating moisture and other pollutants in the open environment. These coatings offer some protection with time, but will eventually fail or become irreversible if they are not maintained on a regular basis [17, 18].

Historical metals: Metal objects of historic, ethnographic, or artistic value as part of a museum collection are very different from archaeological metal objects. First, in order for them to survive with time, their past users may have offered their own cleaning and protection methods as is evident on the wear of the surface of the metal. Here, we usually find objects that survived indoors and are usually free from thick corrosion layers, since through time shiny metal surfaces may have been desired during the use of the object, especially for ceremonial purposes. Typical examples are iron armory, knife and sword, and silverware collections to name a few. Depending on their storage throughout the ages, these objects tend to be in better condition than archaeological objects, that is less brittle from corrosion, and with less pollutant contaminants absorbed onto the surface of the objects.

Stabilization treatments are not commonly used by conservator-restorers for such objects, but removal of surface corrosion products during cleaning needs careful consideration. First, many historical objects in museums tend to be intricately decorated and/or consist of other materials rendering them composite objects. How much to clean needs to be considered very carefully as well as the manner to clean such objects so as not to damage the metal or decorative features [19, 20].

Mechanical cleaning using traditional methods may remove too much information and, what is worse, may scratch and wear away at the metal surface. Chemical cleaning is more difficult to control and, if any residual chemical remains on the surface after rinsing, it will continue to attack the metal object. Special and advanced technologies such as electrolytic cleaning, hydrogen plasma reduction, and laser technology have all been applied successfully in the cleaning of historical metals. There are advantages and disadvantages related to the use of such technologies.

However, the most important aspect after cleaning of such objects is the protection of the surface from any further corrosion. Traditionally, coatings are applied to protect the surface from further corrosion, but more and more, museums are starting to invest in maintaining special environments for such objects so as to avoid the reapplication of coatings with time or other problems of corrosion that occur due to coating failures. However, for the Mediterranean region, this tends to be the exception, and coatings are

commonly used for protecting the artefacts in museum display or in storage [19, 20, 21].

Survey and damage assessment: The only way to establish and to promote a proper conservation strategy for the Mediterranean region is to develop prototype portable diagnostic and/or monitoring systems and protection methods, to identify each specific degradation factor for the many museum collections of precious metals, iron and copper alloys, and then carry out the preservation.

This thesis on plasma cleaning procedures will contribute to the efforts to extend the life of the witnesses of human metallurgical activities that, although defined by Georgius Agricola in *De re metallica* of 1566 as : “rem metallicam fortuitum quiddam esse, & sordidum opus, atque omninò eiusmodi negotium quod non tam artis indigeat quàm laboris” (metal working is a fortuitous & sordid work, and the related actions do not need an artistic attitude but labor) allowed mankind to produce wonderful artefacts.

Chapter 2

Low Pressure Plasma Technologies

Plasma technologies gained in recent years increasing popularity in different application fields as well as in the Cultural Heritage area for cleaning and protecting the metallic artefacts. This chapter deals with the state of the art about the nature of the plasma and the applications of plasma in the field of restoration and conservation of metallic artefacts.

2.1 Introduction to Plasma

Plasma, the fourth state of matter, is a ionized gas which contains equal positively charged ions and negatively charged electrons in a sea of neutral atoms or molecular [22, 23]. Plasmas compose quite 90% of visible matter within the universe. Some examples of the natural plasma state are stars, interior part of the Sun, solar corona, and lightning. When the solid-state materials are heated, they transform to liquid-state. Thereafter when the liquids are heated the particles start to evaporate to form the gas state. Subsequently, when applying a high energy such as electrical discharge on a gas the plasma generate. In this case electrons escape from the atom or molecule and move freely see 2.1. Scientists tried to understand plasma starting from the 17th century. Natural plasmas like lightning and polar lights are usually determined and have intrigued individuals for several centuries. The early researchers tried to understand the mechanism governing plasma generation by the invention of the discharge device [24].

According to André Anders, in 1705 Hauksbee tried rubbing substances other than mercury inside evacuated jars. He eventually decided to see what would happen if he simply rubbed an evacuated glass globe. He built a machine in which a glass sphere could be rapidly spun on an axle by a great wheel. The axle was hollow and connected to the globe through a valve and on the other end to a vacuum pump. A glow appeared when he spun the sphere in the dark, rubbing it with his bare hand (fig. 2.2) [25].

For many years scientists tried to store the electricity in different ways. In 1775

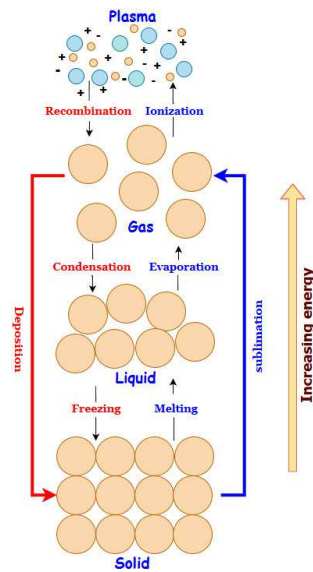


Figure 2.1: Matter change of state.

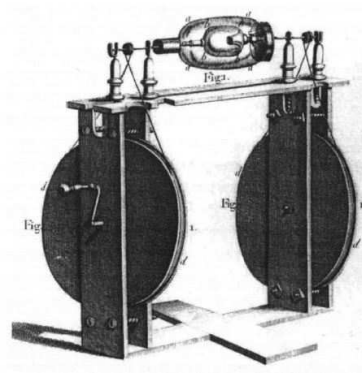


Figure 2.2: Discharge prototype of Hauksbee in 1705.

Alessandro Volta invented an short-circuit discharge of a Leyden jar, producing a spark by connecting two metal electrodes and a charge storage, see f. 1.32.3[24] [25]. In 1879 Sir William Crookes discovered the plasma when he invented a cathode ray tube. Meanwhile, he observed the charges in the gases and decided that this phenomenon should be considered as a state of matter. Thereafter, in 1923, Irving Langmuir gave the name "plasma" to this state of the matter [26]. In the 20th century many work done for developing some devices to create plasma in laboratories for deep study of it as a state of matter. Low-pressure plasma with radio frequency were used for different industrial application as deposition and etching in electronic device fields. In 1990s atmospheric pressure plasmas are widely used for environmental applications, surface modification

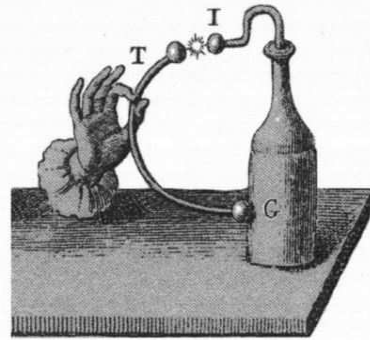


Figure 2.3: Short-circuit discharge prototype of Volta, 1775.

of materials, medicine applications, etc. [24].

2.2 Plasma Typologies

The different plasma typologies can be described in relation to different parameters as density, ionization degree, thermodynamic equilibrium, and so on; plasma can be generated in space or in laboratory. For both laboratory and space plasmas, there is a huge range of densities and temperatures. The most important type for the field of cultural heritage is low-pressure plasma which is characterized by $T_e \approx 1-10$ V, $T_i \ll T_e$ and $n \approx 10^8 - 10^{13} \text{ cm}^{-3}$, pressure 1 mTorr- 1 torr 2.4, [27].

2.3 Low-pressure Plasma treatment of Metallic artefacts

Several studies were performed for evaluating the effectiveness of cleaning the different types of metals such as iron, silver, copper and bronze.

2.3.1 Cleaning of iron artefacts

D. F. O’Kane and K. L. Mittal compared the effectiveness of the use of plasma cleaning with argon and helium/oxygen mixture and the cleaning with organic solvents of metal surfaces. The plasma conditions were power 10 - 200 W, time treatment 1-6 min, gas pressure 1 Torr. The plasma cleaning was more effective than the solvents cleaning. The results were good for rhodium specimens cleaning with argon gas after 6 min with 40W power and caused a 45% decrease in the amount of carbon and sulphur. Moreover, the best results for Fe-Co samples cleaning were obtained with a mix of helium-oxygen at power 10, 80 and 200 for 1 min [28].

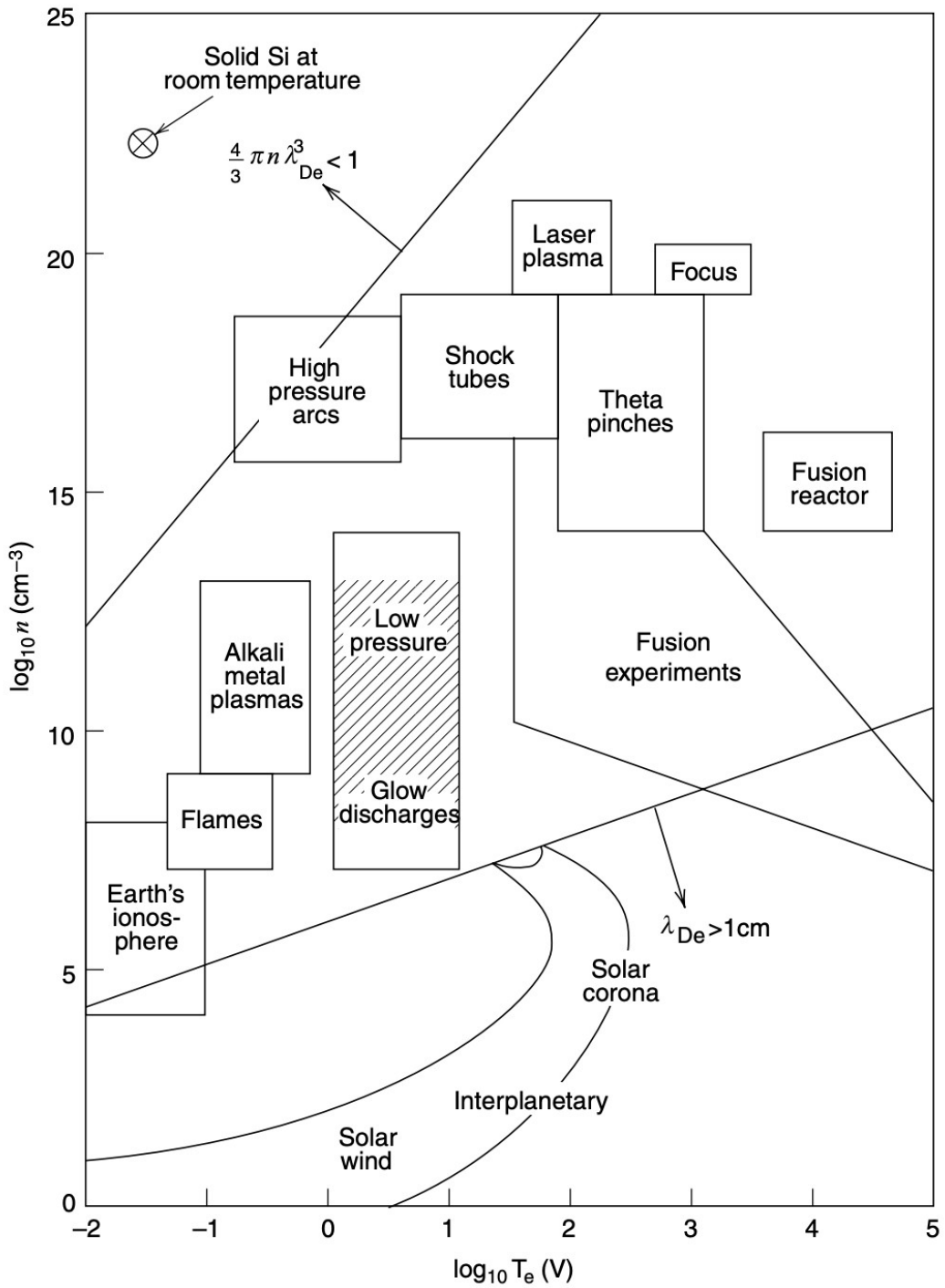


Figure 2.4: Space and laboratory plasmas on a $\log n$ versus $\log T_e$ diagram

In 1979 V.D. Daniels et al described the plasma glow discharge and what exactly happen through applying high energy on a gas. Glow discharge excited by d.c power supplies or a radio frequency these two methods cause ionizing the gas. The types of gases used were Oxygen, Hydrogen and mixture of 1: 1 argon-oxygen. The Oxygen plasma is able to oxidize organic materials at the room temperature to form carbon monoxide and water, whereas hydrogen plasma is able to reduce different corrosion products back to metal. After the experimental test they described the efficiency of the plasma cleaning for different materials as follow in figure 2.5 the oxygen plasma causes oxidization for all organic materials tested. For inorganic materials there were some residues but it was easy to clean them by brush after the treatment. The amount of removing organic materials was not changed with the treatment time.

<i>Material</i>	<i>Density (Mgm⁻³)</i>	<i>Rate of removal</i>	
		<i>By weight g h⁻¹m⁻²</i>	<i>By thickness μm h⁻¹</i>
Shellac (heat cured varnish)	1.1	1.6	1.4
Araldite (AV/HV 100) cured complete epoxy	1.14	3.3	2.8
Araldite (rapid cure) systems	1.14	3.7	3.2
Colloidal carbon (from aqueous dispersion)	—	2.0	—
Cellulose acetate (plasticized)	1.3	2.2	1.7
Nitrocellulose lacquer (Frigilene)	1.23	6.5	5.2
Poly (styrene)	1.05	2.7	2.6
Poly (ethylene terephthalate)	1.15	4.6	4.0
Poly (ethylene)	0.92	2.5	2.7
Poly (vinyl acetate)	1.2	3.4	2.8
Regenerated cellulose film (plasticized)	1.45	2.4	1.6
Poly (ethylene glycol) Carbowax 8000	1.1	2.5	2.3
Microcrystalline wax	0.9	1.4	1.6

Figure 2.5: Rate of removal organic materials in O₂/Ar plasma.

As seen in figure 2.6 the oxygen plasma cause slight oxidation of the copper and high oxidation of the silver and formed Ag₂O . On the other hand when they used 1:1 hydrogen/argon plasma for 1 hour no detectable changes happened on the metal surface 2.7. The operating conditions were 600 V at 40 mA and 7 Pa pressure of 1:1 H₂/Ar mixture. The conclusion of this experimental work is that the hydrogen plasma has a good efficiency for cleaning tarnished silver. as well as for cleaning organic materials from the metals surfaces[29].

In 1985, S. Vepřek et al performed a test for cleaning iron artefacts using low-pressure hydrogen plasma. The used apparatus was a Pyrex glass discharge tube (15 cm inner diameter and 45 cm length) connected with two external water-cooled electrodes. The tube is connected with a high frequency power generator of 80 MHz, 2 kW. The rotary pump produced vacuum 10⁻³ Torr. The hydrogen purity 99.99% and the used a mercury thermometer covered iron sheet see 2.8. The condition of the test for cleaning some iron artefacts performed at 1 Torr pressure and hydrogen flow of~100 Torr

<i>Material</i>	<i>Effect of O₂/Ar plasma (1 hour)</i>
Gold (24 ct)	No detectable change
Steel (Cu-steel)	No detectable change
Tin	No detectable change
Copper	Slight surface oxidation
Lead	Slight surface oxidation
Zinc	No detectable change
Silver	Extensive oxidation to Ag ₂ O (matt black)
Soda glass	No detectable change
Bottle glass—green	No detectable change
Bottle glass—brown	No detectable change
Pottery—Etruscan buchero	No detectable change
—Bronze age pot	No detectable change
—Greek black figure	No detectable change
—Greek white ground	No detectable change
Paper	Gradual erosion, no discoloration
Felt tip pen inks	Almost complete bleaching on all those tried

Figure 2.6: Effects of O₂/ Ar plasma

<i>Material</i>	<i>Effect of H₂/Ar plasma</i>
Paper	No detectable change (mesh electrodes) see text
Araldite (rapid and AY100 system)	No detectable change
Shellac	No detectable change
Gold (24 ct)	No detectable change
Steel (Cu-steel)	No detectable change
Silver	No detectable change
Zinc	No detectable change
Lead	No detectable change
Copper	No detectable change
Tin	No detectable change
Soda glass	No detectable change
Bottle glass—green and brown	No detectable change
Pottery—Etruscan buchero	No detectable change
—Bronze age pot	No detectable change
—Greek black figure	No detectable change
—Greek white ground	No detectable change
Haematite	Reduced to black magnetite
Magnetite	No detectable change
Lead acetate	Grey coating on surface
Basic lead carbonate	
Old corroded lead	Blackening of surface which went brown in air overnight
Cuprous oxide	Brown layer formed on surface
Cupric acetate	
Malachite	
Paratacamite	
Silver sulphide	Reduced to silver
Tarnished silver paint (silver flake in gum arabic)	Partially reduced to silver
Silver chloride	Reduced to silver

Figure 2.7: Effects of H₂/Ar plasma.

ml/sec⁻¹. The temperature was between 350-380°C. The time of the treatment depends on the corrosion products, the thickness of the layers and was typically between 20-70

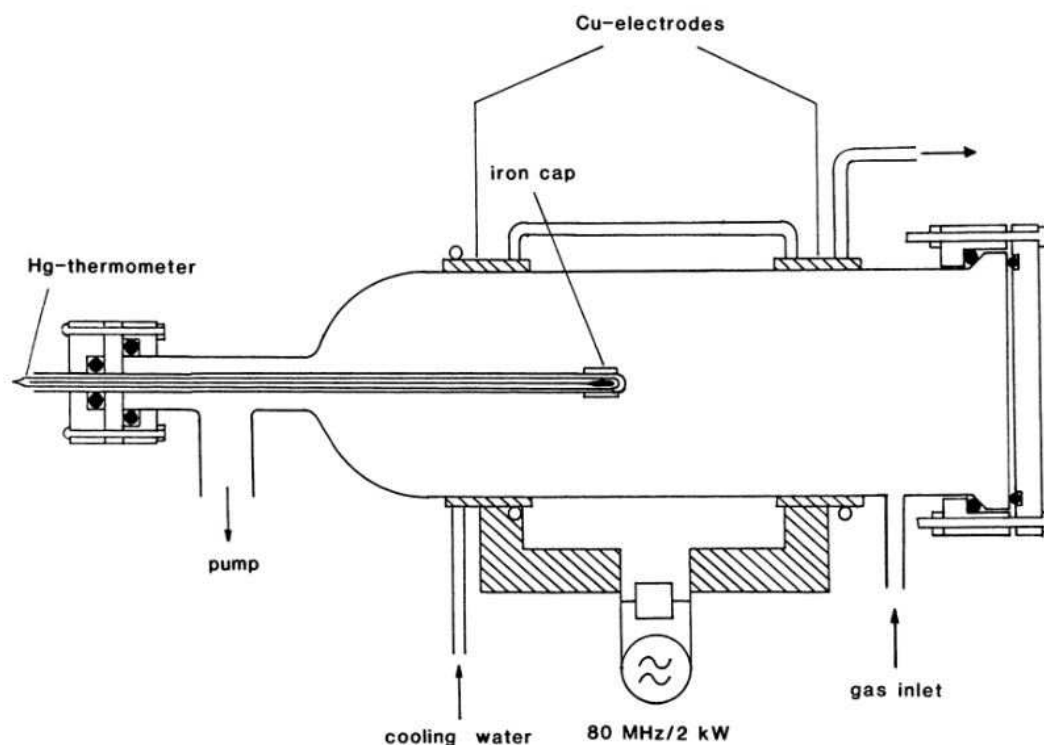


Figure 2.8: Pyrex glass plasma apparatus[30].

hours. The results were satisfactory due to the disappearance of the hematite (Fe_2O_3) after 1 hour of treatment substituted by wüstite (FeO). This work improved the good efficiency of the low-pressure hydrogen plasma in cleaning of iron artefacts, which is especially efficient in the removal of chlorides, and in the reduction of the oxide layer due to the time of the treatment.

In 1986 J. Patscheider and S. Vepřek performed some other work for cleaning the iron artefacts using low-pressure plasma. In this work they mentioned the difference between using of the low pressure plasma and atmospheric plasma. There are two disadvantages in the use of atmospheric plasma:

1. The possibility of explosion due to the interaction between hydrogen and air
2. The temperature in this condition above $\sim 500^\circ C$

In the case of iron artefacts cleaning using Low-pressure plasma the glow discharge pressure is between 0.3-1 torr and the temperature between $300-400^\circ C$. In addition, low-pressure plasma is safe for the artefacts and it has a significant efficiency for cleaning the chlorides and oxides from the iron artefacts surface. Due to the treatment time hematite (Fe_2O_3) is removed completely but magnetite (Fe_3O_4) and wüstite (FeO) increased as

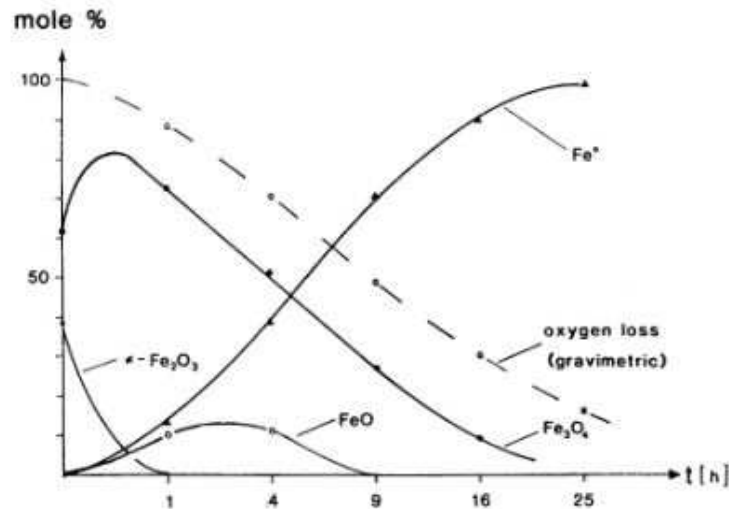


Figure 2.9: Time-dependence of the surface layer composition of a thermally oxidized iron platelet during treatment in hydrogen plasma at about 380°C [30].

described in figure 2.9.

In the same work the reduction of chlorides is tested to evaluate the efficiency of hydrogen low-pressure plasma. The artificial iron oxychloride (FeOCl) was treated by plasma and after 25 h it was removed completely faster than the oxides [30, 31].

In 1988, S. Vepřek, et al. tested radio-frequency (RF) generator (27 MHz, 4 kW) coupled with the plasma discharge by two external water-cooling electrodes fixed along the pyrex tube. They performed the cleaning of different metals as iron, silver, and bronze artefacts. They used mixture of gases. The first mixture was hydrogen with 25 mol.% methane for the reduction of oxides. The second mixture used to remove the chlorides content was ($\sim 39\text{mol.}\%$ hydrogen + $\sim 17\text{mol.}\%$ Methane + $\sim 22\text{mol.}\%$ Nitrogen + $\sim 22\text{mol.}\%$ Argon). The treatment time was between 2-20 hours. S. Vepřek described in figure 2.10 his experiments as follow " the free energy of the reduction of iron oxides with molecular and atomic hydrogen. Accordingly, the reduction of hematite (Fe_2O_3), to magnetite (Fe_3O_4), occurs easily with molecular hydrogen, but the further reduction to FeO and to iron requires high temperatures and a large excess of hydrogen. The free energy of the reaction with atomic hydrogen is strongly negative for the FeO reduction as well as for the other iron oxides. This means that the rate-limiting step in the reduction under plasma conditions, when the degree of dissociation reaches several at.% or more and the corresponding fluxes of atomic hydrogen to the surface exceed a value of $1 - 10^{19} \text{cm}^{-2} \text{s}^{-1}$, should be the bulk diffusion of hydrogen into the oxide and/or the diffusion of the reaction product from the reduced surface layer".

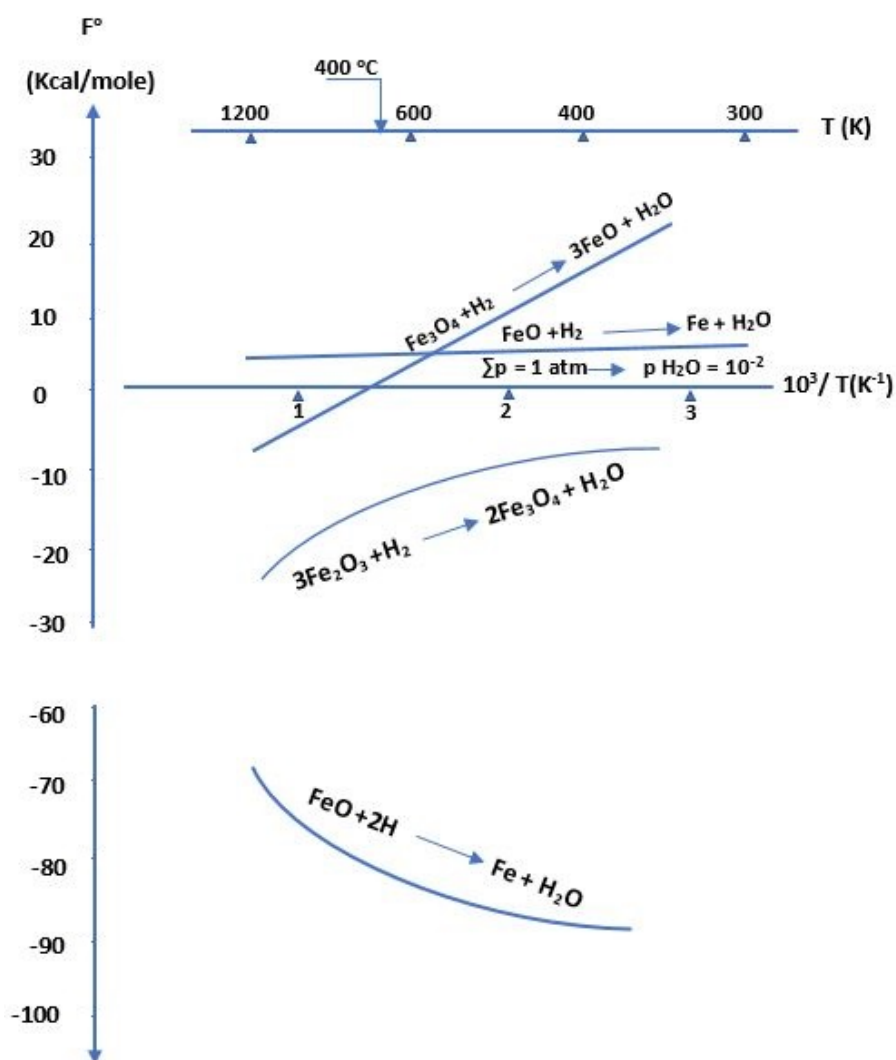


Figure 2.10: Free energy of the reduction of iron oxides with molecular and atomic hydrogen[32].

The same thing is found related to the removal of chlorides. The molecular H_2 is able to reduce $FeCl_3$ to $FeCl_2$. The dichloride is more unstable than the trichloride. Moreover, it is more easy to remove at a low temperature below $400^\circ C$. Additionally, the only possibility of the reduction of Fe^{2+} to Fe^0 with molecular hydrogen at high temperature and high amount of hydrogen however it takes place easily with hydrogen atoms figure 2.11. Otherwise, the atomic hydrogen cannot reduce sodium chloride below $400^\circ C$ except if there is a large amount of hydrogen[32].

In 1991, S. Keene mentioned the gas plasma reduction as one of the methods for cleaning the iron and other metals. The paper describes the plasma reduction as a very

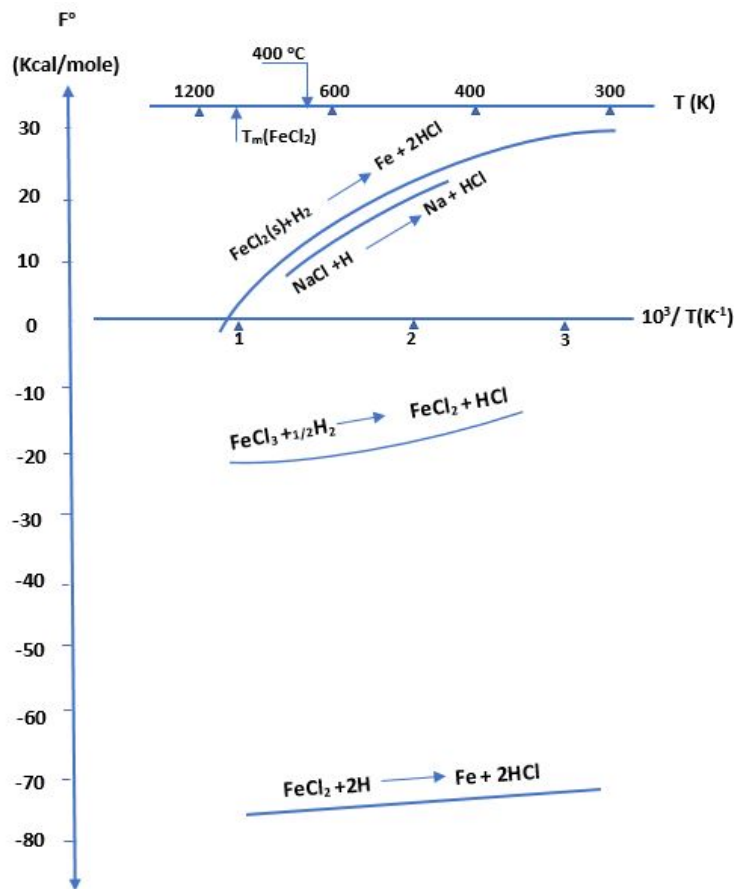


Figure 2.11: Free energy of the reduction of iron and sodium chlorides with molecular and atomic hydrogen[32].

aggressive treatments method with the hydrogen reduction and chemical reduction methods. She reported that all these methods may affect the metallurgical evidence and may remove the patina from the metal surface [33]. Anker Sjøgren and Vagn F. Buchwald, in 1991 used the hydrogen plasma for cleaning iron meteorite fragments, and ancient wrought iron. Iron meteorite is a coarse-grained iron-nickel alloy with plentiful iron-nickel phosphide crystals (schreibersite $(FeNi)_3P$). Sometimes there are some iron sulphide (troilite FeS) and iron chrome-oxide (chromite $FeCr_2O_4$) inclusions. This type of iron shows less corrosion resistance than the wrought iron. Meteorites are basically fragments from asteroids. Usually the corrosion products of the iron meteorites are Goethite (α - $FeOOH$), Lepidocrocite γ - $FeO(OH)$, Maghemite $\gamma - Fe_2O_3$, Magnetite (Fe_3O_4) and Akaganite (β - $FeOOH$) which form under deep-freeze when the chlorine became active and interact with the iron oxide to form akaganite [34, 35, 36, 37, 38, 39].

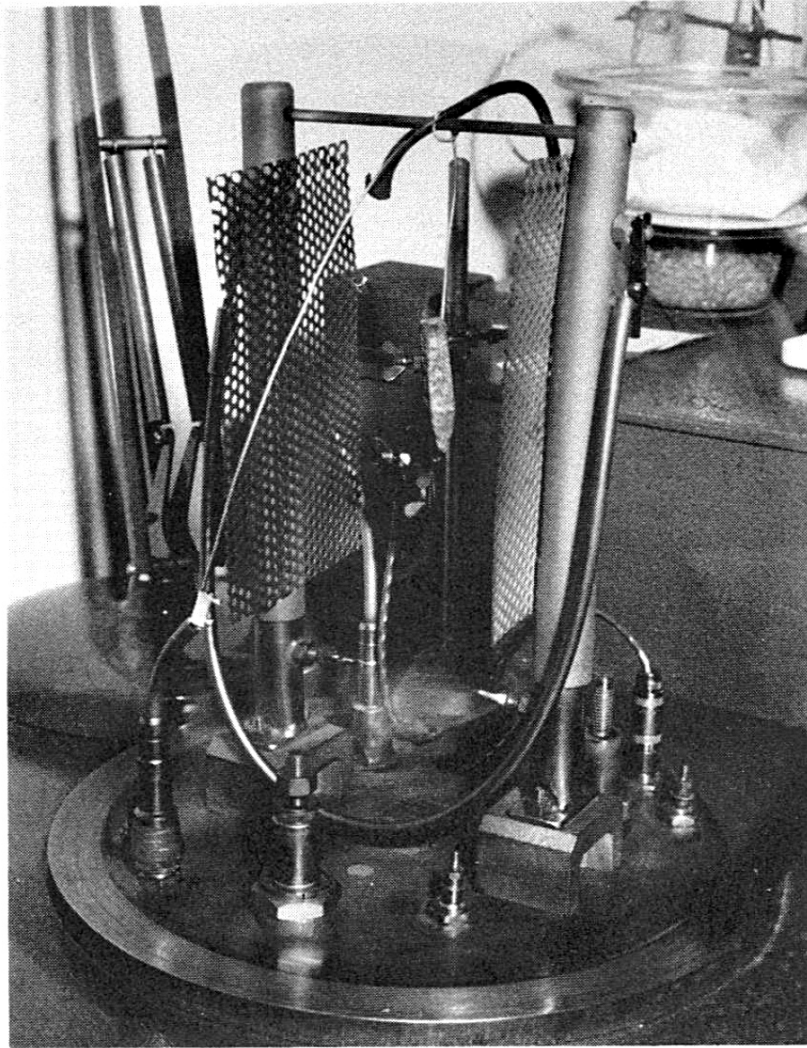


Figure 2.12: The plasma chamber with the bell-jar. The cross-bow bolt is hanging in a connecting wire and functions as cathode between the two perforated anodes[34].

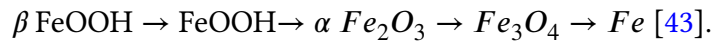
In addition, the ancient wrought irons tested are more than thirteen different objects excavated from Danish soil. The apparatus was 25 l Pyrex 300mm diameter bell-jar sealed by a rubber gasket to a 360 mm diameter iron base plate. The pressure inside the chamber was 0.1 mb evacuated using two-stage vacuum pump and controlled by an Edwards thermocouple 1 . The gas controlled by Edwards LV5 needle valve. The temperature measured by iron constantane thermocouples and it possible to attached to the object or it can be placed in the Faraday dark Space near the object see 2.12 . The D.C power supply was an electronic engineering unit of 3- 4.5kv a.c 150mA, 400mH. The d.c range were 300- 2500V, and the unit connected to the mains at 220V, 50Hz. The energy

consumption under continuous operation is 500-600W. For the treatment of the iron meteorites, the conditions was 13 days of treatment in hydrogen plasma for a Tunorput specimen. The minerals before the treatment were akaganeite, goethite, maghemite, magnetite and after treatment were mainly magnetite and no reduction to free iron. The concentration of chlorine before treatment was 6.7wt% and after treatment was < 0.1wt%. The second sample was Jerslev specimen and after 13 days of treatment. The minerals before treatment were akaganeite, goethite, maghemite, and magnetite. The minerals after treatment was only magnetite. The chlorine concentration was 7.4wt% before treatment, and after treatment was < 0.1wt% . The tests for the archaeological objects treatment was performed on three artefacts. The first one was cross-bow bolt. The corrosion products were mainly goethite, magnetite and lepidocrocite $\gamma\text{-FeO(OH)}$, in addition, the active corrosion zone of akaganeite. The cross-bow bolt was exposed to a 95% RH at 20°C in a chamber for five days before the plasma treatment. After that the object was connected in the plasma discharge as cathode and treated for 9 days with hydrogen plasma, then 10 days in a chamber at 95% RH. The results were a success of reduction of some minerals which were found before treatment as akaganeite, goethite, lepidocrocite, and magnetite and after treatment was only magnetite. Moreover, the chlorine concentration before treatment was 4.4wt% and after treatment was <0.1wt%. Furthermore the other two object were treated using the same system but with different time of plasma treatment [34, 40, 41].

In 1999, D. L. Hamilton wrote about the hydrogen plasma treatment as one of the most efficient methods for cleaning the archaeological metals from underwater sites. He mentioned that the magnetite and ferric oxide converted to metallic iron after the treatment without any changes in the metallic structure. A disadvantage of this technique is the high cost of the plasma equipment [42].

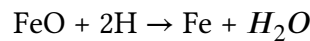
P. Arnould-Pernot et al tested the reduction of dechlorination of ferrous archaeological objects by hydrogen plasma in 1994. The treated object were covered mainly with goethite, $\alpha\text{-FeOOH}$, magnetite, Fe_3O_4 , lepidocrocite, $\gamma\text{-FeOOH}$. The outer layer is a mixture of goethite and minerals from landfill (sand-clay) . When the object extracted from the burial soil the chlorides activated due to the humid air which can deteriorate the object completely in a few years and the corrosion continued after excavation[43, 44]. Due to their work the efficiency of low-pressure plasma treatment depends on three major factors (Time, Temperature, nature of plasma). The equipment which they used is composed of a vacuum chamber, a DC generator from a current alternative (50Hz) with hydrogen and argon gas tubes. The main tube is a Quartz cylinder. the electrical discharge was 400V and the pressure was 10 mbar and the maximum temperature was 450°C. After each treatment, the samples are systematically cooled under hydrogen flow up to 100°C. The treatment performed in hydrogen plasma for eight days at 300°C and four days at 400°C at 10 mbar of pressure. The reaction of dechlorination is clearly much faster at 400°C than at lower temperatures. Moreover, the concentration of akaganite decreased together with the simultaneous appearance of magnetite. In addition, there is a significant change the morphology of the surface The eight days of

treatment at 200°C wasn't enough and the presence of oxyhydroxide, FeOOH, confirms an intermediation of the reaction decomposition of Akaganeite. Between 300 – 350°C treatment they observed the existence of small microns of hematite which transformed to magnetite due to the high temperature. Finally after five days of treatment at 400° and or two days at 450°C they arrived to pure iron as the following equation:



akaganeite → Oxyhydroxyde → Hematite → Magnetite → iron

In 1997, H. Keppner et al tested the advantages of adding argon with hydrogen using very high frequency discharge process (VHF-GD). They mentioned that the atomic hydrogen is the main radical produced in the hydrogen plasma which causes a chemical reduction of the corrosion products of the metals. Whereas there is a real need to what they called "soft" plasma sources which allow to produce a high radical density and avoid high ion energy not to cause any damage to the metals surface. Usually the reduction of iron oxide using atomic hydrogen can be described by the following equation:



While the atomic hydrogen can be produced using "cold" low-pressure plasma, the electron effect separation of molecular hydrogen happens. Usually using DC or RF plasma Power source, the plasma process shows a good efficacy. In addition, to avoid the overheating and strong ion bombardment of the object some changes on the metal surface occur. [45, 46]

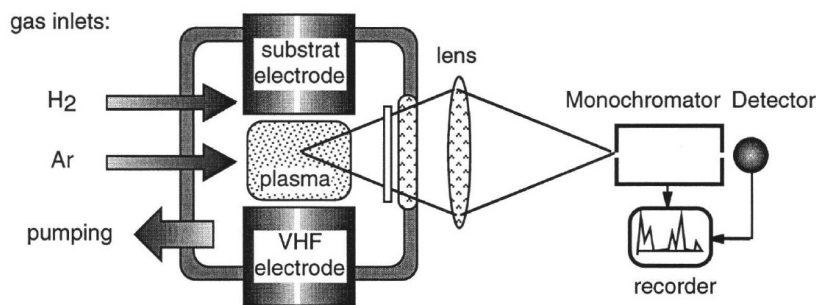
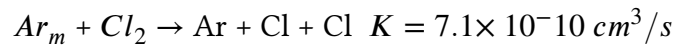


Figure 2.13: Experimental set-up of the VHF-GD reactor used with gas supply, pumping system, VHF-power supply, and the set-up for optical emission spectroscopy (OES). [45].

VHF-GD parallel plate reactor is shown in figure 2.13, it generates very high excitation frequencies (VHF 20 – 150 MHz). Moreover the excitation frequency increases

while the sheath voltage decreases rapidly. This gives the possibility of much higher RF power into the plasma however keep the sheath voltage moderate which protect the metal surface or the thin films from damage[47]. So Keppener said that adding argon to the discharge helps to stabilize the plasma. In addition, if there are chloride containing artefacts the reaction will follow the equation:



Cl_2 is a very good "quencher" and some little traces of it could cause a bad reaction of the treated metal artefact with the atomic chlorine. There is a possibility of the atomic chlorine could take place as strong etching instead of a surface reduction by the atomic hydrogen. Finally the authors summarized that due to the effect of argon metastable quenching of hydrogen and can modifying the process better if the hydrogen diluted in argon but should take care about unwanted reactions through the process [45].

In 1997 A. Voûte performed some tests to use low-pressure plasma in the Swiss National museum. The work was focused on the observation and improvement of the plasma reactor to have a clear idea about what can be happen through the treatment process. So he added several additional measuring devices to measure temperature inside the chamber, temperature of the object surface, gas flow, safety of the hydrogen flow and etc. For example they added a pyrometer to measure the temperature of the object surface using infrared. In addition, they used the generator connected with safety circuit to check the oven temperature and safety of the hydrogen valve. Their monitoring system was so complicated but they accept that as a good way to have all the information they need for the treatment see 2.14[48].

In the same year K. Schmidt-Ott did some assessment for the low-pressure plasma treatment of some objects which were performed at the Swiss National Museum. Before performing the treatment the Swiss national museum was concerned about using a standard treatment method. Hence they put in their minds some questions about the plasma treatment as follow:

1. Is this a kind treatment and conservation for the artefacts or damaging way?
2. In which condition the artefact is more stable, before or after treatment?
3. Does the method completely keep the archaeological and metallurgical evidence of the treated artefacts?
4. Is the plasma treatment is efficient regarding the time and the cost?

So this paper compared some treatment methods such as the mechanical cleaning, protective coatings, stable storing conditions and many applications of the plasma. The result was there no single method can solve all the problems. In the first stage of the plasma treatment of iron artefacts, they were a typical steps for the treatment followed by the Swiss museum until the year 1989 :

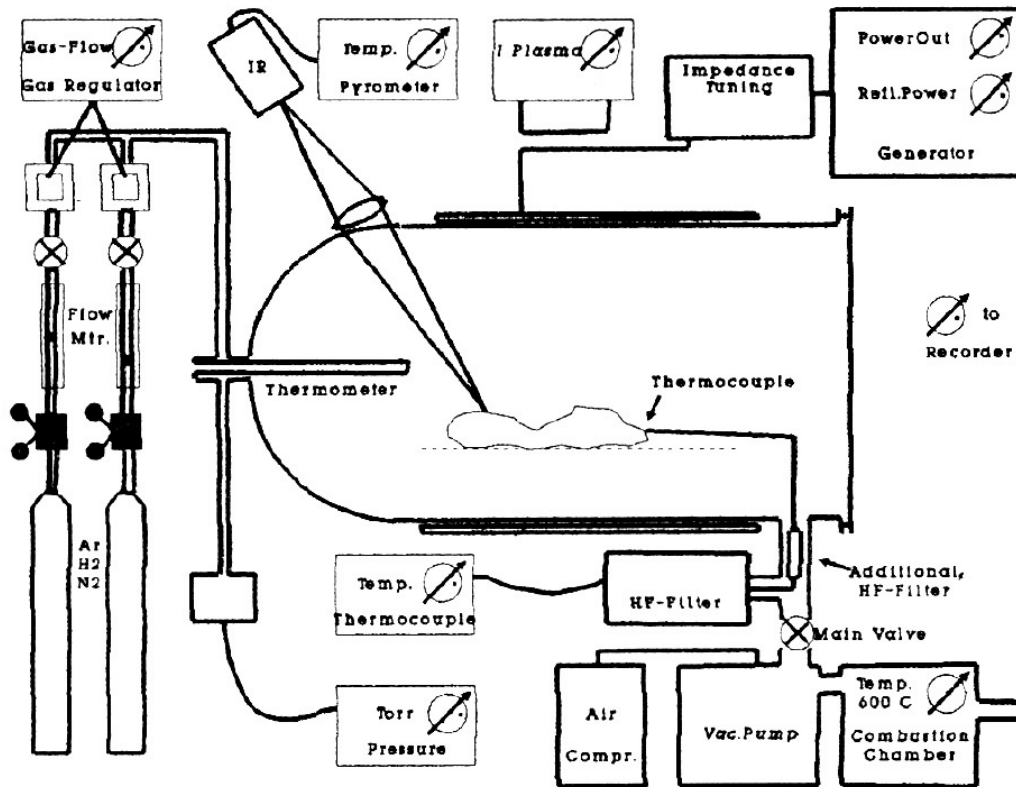


Figure 2.14: Plasma layout. [48].

1. Apply two hours of hydrogen-methane plasma treatment.
2. Mechanical cleaning using scalpel or ultrasonic.
3. Perform a plasma treatment for 18-20 hours at (approx 400°C).
4. Apply protective coating of microcrystalline wax.

The uses of the two hours of H_2-CH_4 plasma was a pre-treatment before the mechanical cleaning. Moreover, the 18-20 hours plasma treatment performed to remove the chlorides, furthermore passivate the surface and protect from the post-corrosion. Finally coating with the wax. After that from 1990- 1993 the Swiss National museum team formulated a new treatment procedures:

1. Put the artefacts in a vacuum oven at 75°C for drying.
2. 7-8 hours of plasma treatment using hydrogen, methane, nitrogen and argon at temperature average of 190 – 260°C.

3. Mechanical cleaning with abrasives or ultrasonic scaler.
4. Apply protective coating of microcrystalline wax.

The results were satisfactory and the artefacts were stabilized. They mentioned that the removal of chlorides requires very long time of treatment at high temperature (300–450°C). On the other hand the use of high temperature could lead to structural changes of the artefacts. Furthermore there were some additional observation recorded during the plasma cleaning. The use of nitrogen and methane caused irreversible colour change on the surface of some treated artefacts. From 1994 the museum team modified the conservation and plasma treatment steps as follows:

1. Put the artefacts in a vacuum oven at 75°C for pre-drying.
2. 7 hours of plasma treatment using hydrogen and argon at temperature of 120°C.
3. Slow cooling of artefacts in nitrogen.
4. Mechanical cleaning with micro sandblasting or scalpel.
5. Desalination in alkaline sulphite.
6. Mechanical cleaning using scalpel or sandblasting.
7. Application of protective coating of acrylic resin (Paraloid B72).
8. Finally, dry storage.

The Swiss museum team tried to standardize the plasma treatment steps. It has become default to desalinate the iron artefacts in alkaline sulphite after plasma treatment and mechanical cleaning with a scalpel and sandblasting to increase chlorides removal [49]

P. Sankot and A. Havlinova performed some plasma treatment in the year of 1997 due to the co-operation between the Swiss national Museum and the Museum of Central Bohemia in Roztoky town, Czech Republic. The same plasma apparatus of the Swiss National museum were installed in the Museum of central Bohemia with little modification. The generator was cooling by alcohol/water solution in a closed cycle. Moreover, the safety system improved to decrease the possibility of the human errors. One of the cleaned objects was a scabbard. It had some important decoration so the treatment should take into the historical information of this decoration through the chlorides removal process. Hence the best conditions tested for the plasma treatment are in two steps:

1. 2 hours of plasma treatment in pressure 140 Pa with 40 sccm hydrogen flow at maximum T 325°C.

2. 18 hours of plasma treatment in pressure 140 Pa with hydrogen 30 sccm at temperature between 240 – 250°C.

After treatment the artefacts were saturated in polyacrylate copolymer and coated with Wax to protect the object from any active corrosion. The results were satisfactory, however this procedure may not be convenient for the very fine and decorative objects[50].

In 1997, S. Bradley et al treated some iron objects from the British Museum. The plasma apparatus was a pyrex glass chamber with external copper electrodes connected with a 27MHz, 4k Watt RF generator. There were two rotary pump to vacuum the chamber to 0.5 Torr. The objects underwent to the following treatment steps:

1. A plasma pre-treatment in a mixture of hydrogen and methane of 100-120 Torr/60-70 Torr for 2.5 or 4 hours at 250, 260 and 270°C.
2. Clean the and remove the corrosion manually by scalpels and air abrasive to reach the original surface.
3. Passivate the object surface by mixture of hydrogen/methane/nitrogen at 50/20/110-130 Torr at 270°C for 12-13.75 hours. Other objects passivated by 60/20/120 Torr at 260°C for 15 hours.
4. Apply protective coating of Paraloid B72.

The visual assessment of the objects before and after cleaning treatment may be evaluated taking into account: •Colour •Number of pieces •Presence of flaking •Active Corrosion/ Mineral preserved organic remains •Soil deposits •Metal core•Previous conservation treatment includes: •Stabilisation and •Surface coatings.

The colour change before treatment from orange-brown to dark and after treatment the colour became dark charcoal grey or black. Moreover, mineral preserved organic remains found in some treated artefacts. After treatment many of the objects were more fragile with some visual cracks than before. Furthermore, after XRD analysis detected the existence of chlorides in some objects without any changes in some objects and decreased in others. Hence Akageneite $\beta - FeOOH$, was present due to the presence of chlorides [51].

In 2002, K. Schmidt-Ott and V. Boissonnas evaluated the use of low-pressure hydrogen plasma in Swiss National museum for assessment the cleaning efficacy. To avoid any structural change, they reduced the treatment temperature from 400 to 120°C. They measured the temperature using three different ways; Liquid thermometer, infrared pyrometer and thermocouple. Furthermore, they decreased the treatment time to six hours as average. These parameters proved the success of the plasma treatment for iron artefacts and the corrosion products density decreased after the treatment without any problems for the artefacts. The treatment steps done as follow:

1. A hydrogen plasma treatment about 6 hours at 120°C.
2. Mechanical cleaning by a micro sandblasting unit using aluminum oxide (Biloxite F 280) , diameter $\pm 37 \mu\text{m}$ or glass beads $< 50 \mu\text{m}$.
3. Desalination Process in alkaline sulphite.
4. Apply protective coating of Paraloid B44.
5. Stored the treated objects at low RH condition using silica gel and oxygen absorbers.

In conclusion the results were acceptable. The low treatment temperature of 120°C reduced the amount of chlorides but not much. The results facilitate the following mechanical cleaning process to remove the chlorides. Moreover, the desalination by alkaline sulphite was four times faster after the plasma treatment. Overall the hydrogen plasma treatment was more effective in the cleaning and stabilization of corroded iron artefacts [52].

In 2002, Z. Rašková et al used a low-pressure hydrogen plasma to clean some silver and iron artefacts. Their question was how to characterize the efficiency of the plasma treatment and what is the best cleaning time? They decided to use the kinetic point of view. In this case the oxide and chloride molecules reduction is the main goal. The OH radical was illustrated in the optical emission spectra. Moreover, it is well known that the OH emission could not be overlapped by any other radiation. For this reason they used the OH integral intensity in the range of 300- 330 nm to indicate the oxides reduction efficiency. As a function of the treatment the integral intensity of OH they performed the plasma cleaning test. The intensity of OH modified strongly in the first 10- 15 minutes of the plasma treatment due to the artefact temperature. After that the intensity decreased slowly so during the first step of treatment the reduction completed in the first two hours, the the oxide reduction became much slower and almost reach a constant value. The final result were OH intensity value decreased of 10% as maximum value during the treatment. Moreover the integral OH radical spectral intensity can be used as an indicator for the plasma treatment in the range of 305-330 nm. The time also can be used to provide some informations how many stages needed for the full removal of oxides [53].

In 2004, K. Schmit-Ott investigated the effect of plasma reduction by optical emission spectroscopy and metallographic examination for silver and iron artefacts. The used plasma produced by 27MHz power generator in a 0.7 m^3 quartz vessel and the gas pressure between 15- 50 Pa (0.1-0.4 Torr). The results of the iron artefacts proved the effectiveness of the hydrogen and hydrogen-argon plasma especially in low temperature about 80°C the efficiency increase. In addition, the low temperature treatment avoid the metallographic changes of the artefacts [54].

In 2009 C. L. Xaplanteris and E. Filippaki treated some metallic artefacts in Plasma

physics laboratory of NCSR "Demokritos", Athens, Greek. They reported that the procedures of the plasma cleaning are chaotic because of the multi-parameter behaviour of the plasma and the complicated corrosion of metallic objects. So, the cleaning of every piece consider unique due to the multi-parametric chaotic. Mainly the work confirmed the good results of using external d. c electric current for the plasma treatment because the current passes through the plasma and object. On the other hand, the rf plasma accelerate the electrons much more than the ions because the electrons mass is very small. Moreover, the electrons loss their energy due to the collisions with ions or neutrals but this loss is negligible because of the small value of the ratio m_e/m_i . This means the temperature of the electrons increases significantly (10.000- 100.000 K°) however, the temperature of the ion and neutral decreases (500 K° for ions, 300 K° for neutrals). Accordingly, plasma is not in thermodynamic equilibrium, whereas the high temperature of electrons make the plasma more efficient for removing and reduction the oxides. In their experimental work the factors and parameters which can affect the plasma cleaning were classified as the kind of the metal, the corrosion depth which can divided to three categories, lightly corroded, moderately corroded and heavy corded. So in the table 2.1 they described different parameters they used to clean some iron artefacts depends on the gas type, plasma pressure and density, rf power, ion temperature, treatment times were used [55].

Table 2.1: Plasma treatment for iron artefacts

	light corroded	medium corroded	Heavey corroded
Gas	H_2	H_2	H_2
Pressure (Torr)	0.8	0.9	0.7
Power (kW)	0.7	1 to 1.2	0.7
Time	8-10h	10-20h	more than 20h
Temperature	200 to 300° C	250 to 350 ° C	200 °C
Gas	H_2, N_2	H_2, N_2	H_2, N_2
Pressure (Torr)	0.4, 0.2	0.8, 0.4	0.4, 0.2
Power (kW)	0.8	1.1 to 1.2	0.7
Time	8-10h	10-20h	more than 20h
Temperature	200 to 300° C	250 to 350 ° C	200 °C
Gas	N_2	N_2	N_2
Pressure (Torr)	0.7	0.9	0.5
Power (kW)	0.8	1.0	0.5
Time	more than 20h	10-20h	more than 20h
Temperature	200 to 300° C	250 to 350 ° C	200 °C

V. Sazavska et al in 2010, tested the using of RF hydrogen low-pressure plasma treatment of artificial corroded iron. The samples were artificially corroded by HCl vapour

for one week and dipping for 5 seconds HNO_3 and H_2SO_4 acids and one week storage in desiccator. The reactor was Quartz and the outer electrodes connected with RF discharge in pure hydrogen. The pressure was 170 Pa. The treatment time was 40-120 minutes. They used 400 and 500 W for the treatment and the results confirmed that when the power increased the corrosion removal became faster for the chlorine and nitrate corrosion layers except the cleaning of the nitrate corrosion is slower. whereas, removal of the sulphuric corrosion layers is more difficult. At the end, the conclusion of the work confirmed the the decrease of the corrosion salts contents from the surface significantly but not fully removed [56].

In 2012, S. Sif Einarsdo'ttir discussed the reason for use argon with hydrogen for cleaning the iron artefacts. The mixture of hydrogen with argon were used an electrolyte in plasma reduction. The argon used to stabilize the plasma and improve the effect of the surface interaction. The iron artefacts became more warmer during the plasma cleaning by using of argon[57].

V. Mazankova et al, in 2013 used the RF low-pressure hydrogen plasma for cleaning some artificially corroded iron. The work deals with measure the OH radical integral intensity represented quantitative ablation of oxygen from a corrosion layer. The tested samples were corroded by HCL vapour for five weeks of exposure in desiccator. Then the samples were kept for 24h in Vacuum. The quartz reactor was coupled with outer copper electrodes. The RF (13.56 MHz) power supply was operated in a continuous or pulsed system in a duty cycle of 75%, 50% and 25% at repetition frequency of 1000 Hz. The gas was a pure hydrogen with gas flow 50 sscm and pressure of 200 Pa. The OH radical spectra were used in region of 305-325 nm to monitor the process because atomic hydrogen reacts with oxygen from the corrosion layer then form excited OH radicals. The spectrum of that OH can be used to measure the effectiveness of the corrosion removal. The treatment time were 90 minutes and the power was 400 W. The results confirmed that intensity of the OH radicals decreased with decreasing effective power so the reduction of the corrosion is slow. While when the power increases the efficiency of reduction increases. After the experiments they proved that the 200°C is safe for the iron artefacts to avoid any metallographic changes. In addition, due to in increase to power it was confirmed the use of 400 W power was better than 100, 200, 300 W for the cleaning process. Finally the result were the duty cycle was varied from contentious to 25% pulse. Whereas, after measuring the OH radicals intensity and temperature the corrosion agents as chlorine and oxygen were decreased in the condition of 400 W and 75% pulsed system in temperature not more than 200°C [MAZANKOVA2013plasma].

F. Krčma et al continued the work for testing the low pressure hydrogen plasma for cleaning metallic artefacts. In 2014 they published some new results of their work. the work was carried out using two different systems. The first one was ow temperature low-pressure Rf plasma. the reactor was quartz cylinder with two surrounded external copper electrodes connected by a radio frequency generator (13.56 MHz). The linked gas tubes was pure hydrogen or mixture of hydrogen-argon at pressure of 160 Pa with gas flow 50 sscm. The tested power were 100, 200, 300 and 400 W and the pulsed duty cycle

were 25-100% with 1 kHz frequency and the treatment time was up to 120 minutes. The second system was plasma operating in liquid 2.15. This system is a high-performance instrument and commonly used in biomedicine nowadays. This system allows a direct contact between with the tested samples. The system is a multi-electrode setup with a driving circuit producing 100kHz RF at relatively low voltage signals (up to 600 V).

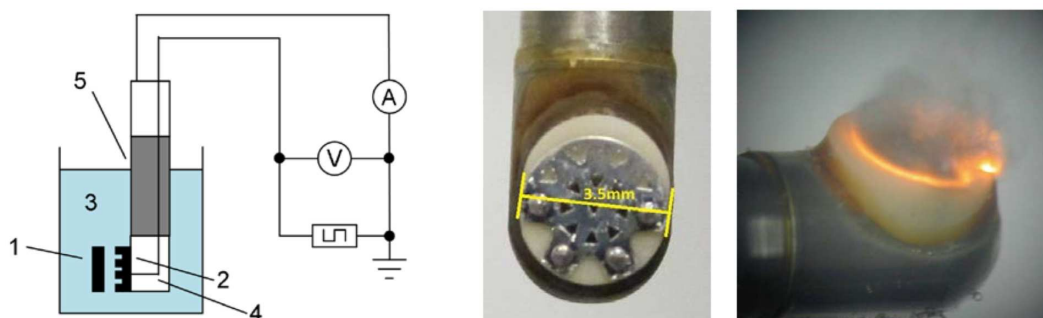


Figure 2.15: Schematic of plasma operating in liquid, 1-treated sample, 2-Powered electrode, 3-water solution, 4-insulator, 5-grounded electrode; right-electrode head

The idea of the cleaning depends on the solution conductivity which rely upon temperature and the concentration of add salt. Moreover, the distance between the cleaned sample and the electrode. The used solution was 0.9% sodium chloride and the solution conductivity was 13 mS.cm^{-1} . They mentioned that the best distance between the electrode and the treated sample is 1 mm and the optimal applied power was 5 W. The efficiency of the two systems always affected by the applied power. The OH radical intensity and the temperature can give an idea about the corrosion removal from the surface of the treated iron sample. The tested sample were corroded iron with and without incrustation. The results proved that the intensity of the OH radical increased in the beginning of the treatment process in both systems. In the case of the incrustated sample the intensity increased faster. On the other hand, while the slightly bounded oxygen is removed at incrustation layers, the rest of these incrustation works as a shield for the artefacts, so the active particles of the plasma cannot interact with the corroded surface. Another observation about was noted which is the temperature of the non-incrusted samples increased in the first 30 minutes of the treatment then it remains constantly. Both of the two plasma systems were used in this paper and both of them succeeded in the treatment process. Furthermore, in the case of the planner shape of the objects and incrustation layer the temperature increases. Additionally, the objects must be cleaned by mechanical removal way through the plasma treatment to remove any incrustation. The pulsed plasma regime increases the removal energy efficiency and decreases the maximal sample temperature. In case of oxides removal it can happen by the reaction with the neutral species whereas the hydrogen charged particles can remove the chlorides [58].

In 2015, H. Grossmannová and F. Krčma they used low-pressure plasma to treat some artificially corroded iron samples. The pure mineral of lepidocrocite (γ -FeOOH) which was formed in laboratory was treated with by plasma with two real pieces. Commonly the lepidocrocite and akaganeite formed due to the chloride corrosion and usually found on the surface of the artefacts as orange points or bores. After the treatment the lepidocrocite is visually transformed to goethite as powder on the surface of the sample. In addition, notable amount of akaganeite is formed. The XRD confirmed the transformation of the corrosion products. The lepidocrocite and goethite transformed to magnetite and it's amount increased in both the artificial samples and the real objects. On the other hand, there was some morphological changes in the samples moreover, the analysis indicate the presence of chlorides and sulfur crystals on the surface of the objects [Grossmannová2015plasm].

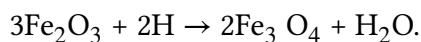
In 2015, S. K. Pradhan et al used H_2 - Ar plasma for clean old Indian coin from 1960. The treatment was performed with RF plasma reactor connected with two mass flow of argon and hydrogen with maximum power 50W, the vacuum pressure was 10–6 Torr. The chamber pressure controlled by a gate valve operated manually. the operating pressure was 1.2-170 mTorr and gas flow was 10 sccm for the argon and hydrogen. The treatment time was 1 hour. The coin was an alloy which composed of Cu, Ag, Ni, Fe, Cr. After performing different tests the coin cleaned very well and became shiny. The effective conditions was 50 W and 50% H_2 in Ar and the ideal pressure was 20-100 mTorr for the process [60].

In 2016, Vera Sazavska et al, performed some cleaning tests using RF low-pressure hydrogen plasma for some metallic objects. They used optical emission spectroscopy to measure the OH radical which result due to the reaction between atomic hydrogen with oxygen from the corrosion layer in the excited state. The spectral region of the OH radicals was 305-325 nm, so its integral intensity was used for the quantitative analysis of oxygen removal from the corrosion layer of the treated objects. During the plasma treatment the temperature was constant about (600 K). The observations were noted and the integral intensity of OH radicals increased fast to the maximum value at the beginning of the treatment then the reduction process slow down gradually. They stopped the treatment when the value of relative intensity of OH radicals reached one tenth of maximum OH radical intensity. This maximum intensity helps for the reduction of oxides from the corrosion layer. Furthermore, in the pulsed regime (200W, 75% pulse) maximum of OH radicals was lower and the reduction process was less strong in the pulsed regime than the continual regime. The pulsed regime was preferred due to lower heating of the objects through the treatment. In addition, the pulsed regime good for sensitive objects to the heating. The treatment time were from 60-120 minutes depending of the duty cycle[61].

In 2018, Xaplanteris. C.L, and Xaplanteris S.C performed low-pressure plasma treatments on some iron objects exposed for 10 years to the environment. They tested four types of plasma treatment described as follow:

- A reducing plasma treatment of 100% H_2 at a pressure of 1 to 1.2Torr, and at a temperature range of 240°C to 280°C. The purpose of the experiment is to confirm the agreement between results and the theoretical foresights.
- A plasma treatment of 100% H_2 at a pressure of 1 to 1.2Torr, and at a temperature range of 240°C to 280°C, while an external D.C. potential was applied to the treated coupons, so that each coupon behaves as the negative and the positive electric pole of a closed d.c. electrical circuit.
- A plasma treatment of 100% N_2 at a pressure of 0.50Torr and at a temperature range of 260°C to 300°C. The purpose is now to check the effect of nitrogen plasma on the samples; the purpose is also to show the difference from the hydrogen action, as well as to study the nitriding of objects.
- A plasma treatment of 100% N_2 at a pressure of 0.50 Torr and at a temperature range of 260- 300°C, while an external D.C. potential was applied to the treated coupons, so that each coupon behaves as the negative and the positive electric pole of a closed D.C. electrical circuit. The aim of this experiment is also the research of the effectiveness of the external potential on cleaning and restoration when the plasma gas is nitrogen.

through all these different treatment parameters the oxide layer became porous and soft due to the transformation or transformation and reduction in the uses of H_2 . In addition, the layer was removed mechanically by scalpel until the original surface. Before the treatment the identified corrosion products were mainly goethite $FeO(OH)$ and hematite $\alpha-Fe_2O_3$. The results after applied the treatment were good in the case of use hydrogen plasma than nitrogen plasma. The treated samples by hydrogen without d.c potential illustrated the presence of goethite and appearance of magnetite whereas the sample with negative potential, shows magnetite only due to dehydration of iron hydroxide to trivalent iron oxide Fe_2O_3 (hematite or magnetite) which result as the follow reaction $2FeOOH \rightarrow Fe_2O_3 + H_2O$. Further, the final products were found after hydrogen plasma were hematite and magnetite which consider most stable oxide of iron and it produced due to the reduction of hematite according to the following reaction:

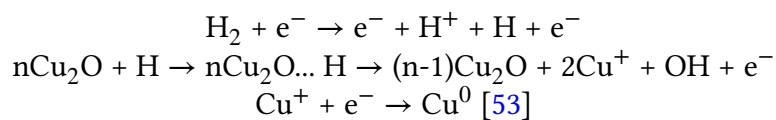


On the other hand, the nitrogen plasma was less effective in presence of hematite and maghemite $\gamma-Fe_2O_3$. Moreover, in the case of the nitrogen plasma the electron released electron from the nitrogen atom and it became ions so the nitrogen plasma less action than hydrogen. But in the case of pure metal the nitrogen plasma has a significant effects. As a final result, the effectiveness of the treatment is different depending on the nature of the plasma gas. While the gas is hydrogen, an intense chemical action is noticed. Whereas, in the case of nitrogen, the action is weak and no reduction is noticed because hydrogen atoms gives more electrons for the reduction process than

the nitrogen. In addition, the nitrogen cannot reduce the oxides from the iron[62]. In 2018, R. Tino et al described the treatment of the metallic artefacts by low-pressure plasma, for removing corrosion products. The authors noted that the main compounds of the corrosion products contains oxygen and /or chlorine which can be removed by the reaction of the species of hydrogen plasma (atoms, ions, both in excited states and highly excited molecules). The reaction can be described as follow: $(AO + H \rightarrow A + OH)$ where AO is the metal-based compounds containing an oxygen atom, and A is the same compound with less oxygen atom. OH is converted by another hydrogen atom to the water in the next step. A, similar reaction is possible in one step with highly excited molecule hydrogen is reacting instead of two hydrogen atoms consequently $(ACl + H \rightarrow A + HCl)$. Where ACl is a compound containing chlorine atom and A is the same compound with one less chlorine atom. Due to the strong electronegativity of a chlorine atom. This reaction is much more effective with atomic ions. The products of the two actions are volatile and therefore, they are leaving from the surface. In this case the active particles can penetrate the pores and the holes in the treated sample surface. In case of remove organic pollution from inorganic surfaces. The reaction based on the oxidation in the oxygen plasma but the problem of using oxygen in cleaning of metallic artefacts is the possible oxidation for the treated metal so the hydrogen plasma is preferred in this case [63].

2.3.2 Cleaning of copper-based artefacts

In 1979 D. Daniels et al performed plasma cleaning. They mentioned that using the Oxygen argon for cleaning the copper artefacts cause a slight surface oxidation but in the case of cleaning bronze artefacts there wasn't detectable changes on the surface after the treatment. Whereas, in the case of using hydrogen/ argon plasma they mentioned that in the case of cleaning cuprous oxide, cupric acetate, malachite and paratacamite from the surface of the copper and bronze artefacts there was a brown layer formed on the surface[29]. In 2002 Z. Rašková and Krcma discussed the possible reactions between atomic hydrogen with the oxygen in the corrosion layer of the copper artefacts with the creation of OH- radicals in the active discharge. The possible reduction of oxides from the copper surface can be done following this scheme:



In 2007, E. Angelini et al carried out the cleaning of bronze artefacts using hydrogen plasma (20 sccm of H_2 , 1.3×10^{-2} mbar, 50 W power, 20-60 min treatment time). This work confirmed the effectiveness of plasma in reducing the thickness of the corrosion layer and in removing copper chlorides from the bronze surface by the formation of volatile hydrogen chloride due to the reaction between hydrogen atoms and patina.

In 2009 C. L. Xaplanteris and E. Filippaki performed plasma treatments of bronze artefacts. They defined the treatment plasma parameters to be adopted by conservators for cleaning of metallic artefacts. The suggested condition for cleaning bronze artefacts are described in the following table[55]:

Table 2.2: The Parameters of Plasma treatment for Bronze artefacts

	light corroded	medium corroded	heavily corroded
Gas	H_2	H_2	H_2
Pressure (Torr)	0.8	1.2	-
Power (kW)	0.65	1.0	-
Time	4-6h	2-4h	-
Temperature	170 to 190°C	230 to 2400 ° C	-

In 2009 J. Novakovic et al investigated the efficacy of hydrogen plasma in cleaning of bronze artefacts artificially aged in soil enriched in chlorides. The treatment parameters were: RF glow discharge, 100% of H_2 , 0.65 kW power, at 190- 200° C, 0.8 Torr pressure, treatment time 1, 2, 4 hours. No metallographic change of the samples was observed after plasma cleaning. By means of XRD analysis, they found that the peaks intensity of tenorite, malachite and paratacamite decreased after one hour treatment, while cuprite signals increased as well as the ones of metallic copper. After 2 hours of treatment the peaks of malachite and paratacamite disappeared completely and the cuprite and copper peaks increased. Finally after 4 hours treatment, a minor decrease of cuprite peaks and a lower increase of copper peaks was observed, thus indicating an increase of the efficacy of the treatment with the time. [64].

In 2014, F. Krčma et al described the cleaning of bronze sample using hydrogen plasma with 300 W in continuous regime. The samples were previously corroded in HCl vapour in sandy environment. They compared the effect of plasma cleaning due to the temperature with different applied power and the duty cycle. They found that corrosion products removal is enhanced by increasing the applied power and decreased at shorter duty cycle, which means that if the mean energy is too low the corrosion removal is too slow. On the other hand, when the mean energy is high the cleaning is faster, but also the temperature is high and this should be consider to avoid any crystallographic changes. [58].

In 2016 P. Fojtíková et al used hydrogen plasma for cleaning bronze samples patinated by exposure of the samples to vapour of hydrochloric acid for 14 days. The plasma parameters were: power from 50- 400 W, flow rate of hydrogen 50 sccm. The EDX analysis confirmed the decrease of oxygen and chlorine from the first two minutes of treatment. The mentioned that the advantages of using hydrogen plasma is to void contact with aggressive chemicals [65].

In 2016 C. Soto et al tested the mixture of Ar/ H_2 for cleaning two types of artificial

patina, a cuprite layer and malachite and nantokite layer. They utilized different parameters, gas ratio, applied RF power, pressure, 20-60 min treatment time. The cleaning of cuprite samples induced a partial removal of the patina as confirmed by XRD with the cuprite intensity peaks decrease after plasma cleaning. In the case of malachite patina, after cleaning a change of the patina color from green to brown and dark brown was observed but the time was not enough to remove all the malachite/nantokite crystals. In conclusion the effectiveness of plasma cleaning depends on the time and the power. [66].

2.3.3 Cleaning of silver artefacts

Dealing with plasma cleaning of silver artefacts, in 1979 V. D. Daniels used oxygen/argon plasma causing a little oxidation of Ag_2O on the silver surface, meanwhile with a hydrogen/argon plasma the silver sulphide and silver chloride were reduced easily to silver. [29]. In 2004 K. Schmidt-Ott used hydrogen plasma for cleaning silver artefacts. His work also confirmed the removal of sulphide and chloride from silver samples, artificially corroded, without any damage for the samples surface. He also performed the cleaning on two silver artefacts. The first one was a silver/ gold spoon, treated for 90 min in a pure hydrogen plasma (hydrogen 4 In/h, 20 Pa, 770 Watt, maximum temperature of the artefact 82°C). The second was a silver chalice treated for 2.5 hours (hydrogen 6 In/h, 29 Pa, 1030 Watt, maximum temperature of the artefact 85°C). The silver spoon was cleaned and the tarnish layer removed without noticeably affecting other chemical elements of the spoon. The tarnished layer was completely removed except some small darker areas in the depth. In the case of the chalice the tarnish layer was removed gradually within half an hour with some dark areas still remaining but after an additional hour of cleaning all these dark areas were completely removed and the chalice became shiny [54].

As mentioned before, C. L. Xaplanteris and E. Filippaki in 2009 in addition to plasma treatments for iron and bronze, they carried out the same cleaning on Silver artefacts. The suggested condition for cleaning the silver artefacts were described in the following table[55]:

Table 2.3: The Parameters of Plasma treatment for silver artefacts

	light corroded	medium corroded	heavily corroded
Gas	H_2	H_2	H_2
Pressure (Torr)	0.8	0.8	0.8
Power (kW)	0.7	0.7	0.7
Time	2-4h	6-8h	10- 12h
Temperature	210° C	210° C	210°

In 2010 B. T. Goras et al performed a cleaning of a silver coin using hydrogen plasma. The HF discharge of 13.5MHz frequency was used under conditions of temperature 35-40°, pressure 3.5×10^{-4} bar, electric field intensity 20-50 V/cm for 30 min of treatment. Moreover, they continued the work in 2013 on other silver coins. In both papers they conclude that the HF plasma treatment is very good for cleaning silver artefacts quickly and safely without any damage of the coins surface [67, 68]. In the same year of 2010 E. Ioanid et al used O₂ and H₂ plasma for cleaning some silver coins. These coins contained little amount of other metals such as copper and magnesium. The maximum treatment time was 20 min in the case of oxygen plasma and 30 min for hydrogen plasma, the power was 100 W. They performed the oxygen plasma treatment as the first step to remove the organic contaminants then they cleaned the surface of the coin with natural hair brush to remove any impurities that were not eliminated by the vacuum system. The EDS analysis confirmed the removal of Ag₂O and Cu₂S from the surface and the crusts of CuCO₃Cu(OH)₂ and CaCO₃ became fragile and have been removed by repeated brushing process after each treatment cycle. They also mentioned that using oxygen plasma allowed the oxygen to interact with organic compounds and through this oxidation reactions the results were the production of volatile compounds (CO, CO₂, H₂O) which were removed by the evacuation system after the first 20 min of treatment. In addition, after using the hydrogen plasma the coins partially recovered the specific gloss of silver[69]

In 2013 E. Angelini et al used hydrogen plasma for cleaning silver-based artefacts. The cleaning conditions were (20 sccm of H₂, 1.3×10^{-2}) mbar, 50 W of power, 20- 60 min of treatment). They tested the plasma cleaning on artificially tarnished silver-copper alloy buried in soil in the archaeological site of Tharros in Sardinia, Italy, for six months. Moreover, they added 5 wt% NaCl to accelerate the the corrosion degradation. The patina was constituted by chloroargyrite (AgCl) and paratacamite. The paper confirmed the effect of using hydrogen plasma for cleaning silver-based artefacts. The work assumed that the H atoms react directly with the patina and remove the dangerous copper chloride due to the formation of volatile HCL inside the plasma sheath. Otherwise, the silver ions (Ag⁺) back to silver (Ag⁰). After 30 min of treatment the thickness of the patina decreases from 13.4 m to 6.4m. They mentioned that it is possible to use the hydrogen plasma for cleaning gilded artefacts without damaging the surface decoration [70]

Chapter 3

Plasma cleaning of metallic artefacts

Several studies in the field of Safeguard of Cultural Heritage focus on the methods for cleaning and protecting the metallic artefacts. In the first paragraphs of this chapter some generalities on low-pressure plasma and on its employment in the field of restoration and conservation of metallic artefacts are reported. In the second part, the results of the experimental work carried out on the plasma cleaning of copper and silver based alloy samples artificially corroded are reported. The used gas were hydrogen and argon in different time cycles. The results of plasma cleaning are satisfactory both on silver alloy and on copper alloy samples although with different treatment time.

3.1 Plasma discharge for cleaning metallic artefacts

Cleaning is an important step in the conservation of metallic artefacts. The methods utilized have to be tailored in order to avoid any damage to the metals surface, as the one caused by too invasive methods as chemical cleaning especially when the metallic artefacts are very thin. Moreover, the conservation and protection methods should use reversible materials and proper methodologies that do not change the aesthetic appearance of the artefacts [122]

3.1.1 Principles of the plasma discharge

The low pressure plasma is a non-equilibrium, homogeneous and highly anisotropic medium[123]. By applying high power on a gas between to metal electrodes at low pressure (10-100 Pa), an electrical current (d.c or RF) will begin to flow when the applied voltage reaches a critical value. In this case a light emission appears inside the chamber and this phenomena called a glow discharge. The gas particles excited by the RF or d.c power supply and the electrons are accelerated to enough energy to ionize this gas molecules then, the positive ions formed and charged enough energy to extract the electrons from the cathode. In this case the light reign or the plasma reign will have an equal number of positive and negative charges and chemical reactions are happening.

A charged particles bombardment occurs on the metal surface and clean the corrosion products in different ways due to the type of the gas, type of the metal, the corrosion products and the cleaning time. [29] The process is based on the reduction of the corrosion products from metals surface by reactive reducing species as hydrogen atoms in the glow discharge at low pressure and low temperature. The reduced layer becomes fragile, and conservators can easily remove it. Furthermore, chloride ion - containing phases can be destabilized and chlorides can be removed from the discharge gaseous phase[64]. Many scientists studied the effect of the low-pressure plasma cleaning for the metallic artefacts. Some of them mentioned the advantages of the plasma treatment and why it is usually preferred by the conservator:

- Dry Process and easy to apply.
- No shape problem.
- REtching process controlled and selective
- Production of nano thin-films protective coating and homogeneous on the metal surface.
- Low plasma temperature
- No destruction of the artefacts.
- The chemical reactions produce stable compounds on the artefact surface.
- The size of the reactor allows to treat the different sizes of the artefacts. [122, 55]

There are some factors that can affect the cleaning process:

- The plasma production parameters, the nature of the gas, plasma density, temperature, pressure, ect.
- The alloys composition and microstructure
- The type of the corrosion products in dependence of the the burial environment and burial time[55].

There are two types of collisions that can occur in the plasma:

1. Elastic collisions, occur in cold plasma and are very efficient when the mass difference between the colliding partners is high, produce neutral excitation with formation of emitting species as well as fragmentation into atoms and radicals. In this case when the electron collides with the atom just changes its direction without markedly changing speed because the transferred energy is negligible due to the different masses between the electron and any atom.

2. Inelastic collisions occur in thermal plasma (hot plasma) when the pressure inside the reactor is low (0.001-1torr) in this condition the elastic electron-molecule collisions, largely inefficient because of the mass difference between the colliding partners and are characterised by low collision frequency and result in efficient energy transfer. In this case the electron collisions are considered inelastic. In addition, the importance of the glow discharge is electron impact ionization [124]. The ionization degree can vary from 100% (fully ionized gases) to very low values (e.g. 10^{-4} – 10^{-6} ; partially ionized gases)[125] The primary electrons can remove an electron from the atom and produce a positive ion and two electrons as follow: $(e + Ar \rightarrow 2e + Ar^+)$ 3.2 [124]

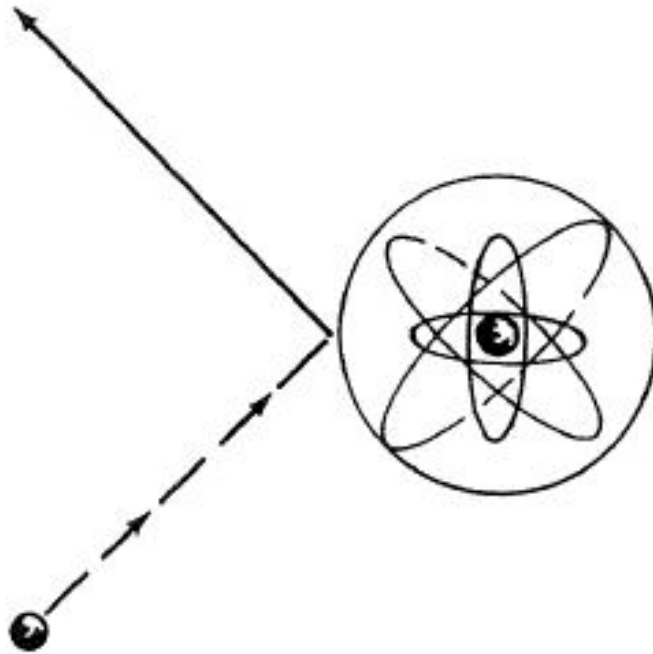


Figure 3.1: Electron-atom elastic collision

There are four main basics for the inelastic collision Which are simply:

- Excitation, which means that in the ionization process there is a bound electron ejected from the atom. A less transfer of energy to the bound electron would empower the electron to jump to a high energy level inside the atom a corresponding quantum absorption of energy 3.3.
- Relaxation, when the discharge glows that's the behaviour of the relaxation of electronically excited atoms and molecules, so after the excitation the electron

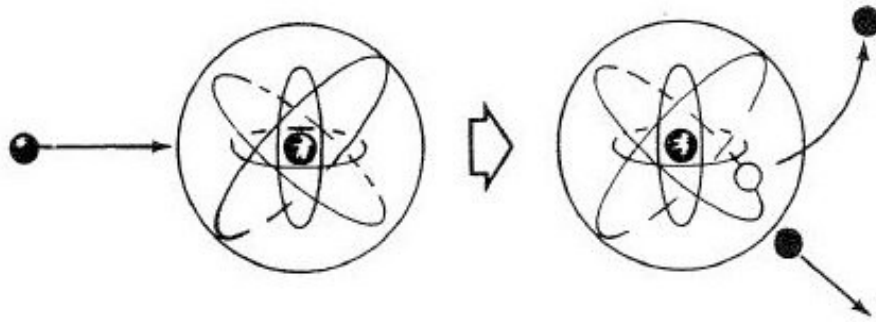


Figure 3.2: Electron impact ionization

configuration backs to its original ground state in one or several transitions from nanoseconds to seconds.

- Ionization
- Recombination, it is opposite of the excitation as relaxation, so it is to ionization an electron coalescence with a positive ion to create a neutral atom^{3.5} [124].

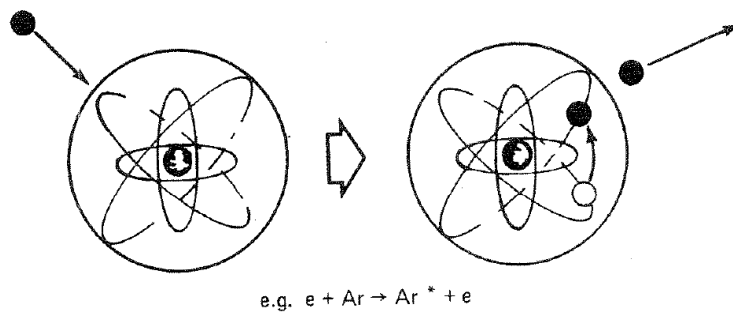


Figure 3.3: Electron impact excitation

Many mechanisms may occur in low-pressure plasma which modify the materials properties such as:

- Etching: it allows the ablation of artefacts surfaces by the reaction with active species generated in a plasma discharge to form volatile products.
- Grafting: performed in inert or reactive gases, such as Ar, H₂ it modifies the hydrophilic or hydrophobic character of a surface, its acid or basic behaviour.

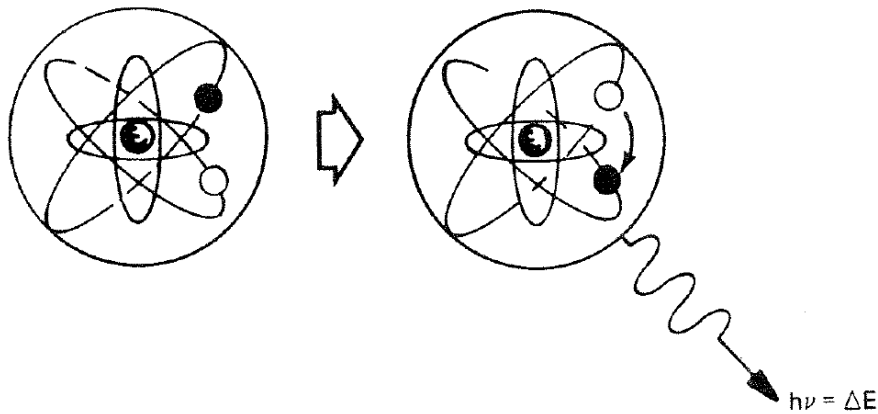


Figure 3.4: Relaxation or de-excitation

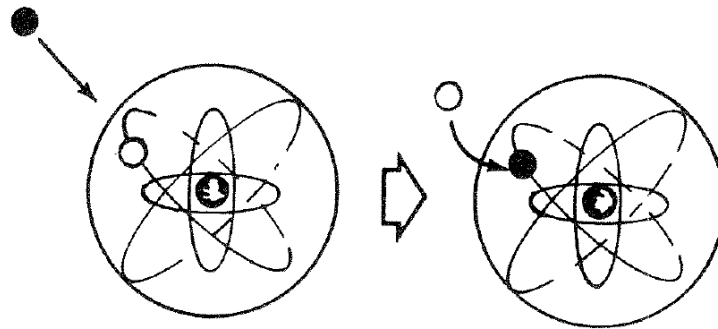


Figure 3.5: Recombination

- Deposition: the substrate positioned on both electrodes or on a suitable substrate holder inside or outside the plasma region. After evacuated the reactor, the mixture of the reactant gas is introduced into the system, the pressure is adjusted to selected value (0.01-1 torr) by means of a suitable device and plasma created by applying the RF potential to the electrodes is evident because of a typical glow emission.
- Coating: the organic molecule forms reactive species for collisions with energetic electrons. These reactive species can react with the exposed surface to the plasma and create a coating. The other possibility, in the gas phase with other species, sometimes deliberately added to the gas feed to form new film precursors.
- PECVD: it allows the deposition of thin films (100-10.000 Å) as polymers and silica-like coatings with good barrier properties against the aggressive agents and

vapours.

Name	Reactions	Description
Etching	$AB + C_{\text{solid}} \rightarrow A + BC_{\text{vapour}}$	Materials erosion
Adsorption	$M_g + S \rightarrow M_s$ $R_g + S \rightarrow R_s$	Molecules or radicals a plasma come in contact with a surface exposed to the plasma and are adsorbed on surface.
Deposition	$AB \rightarrow A + B_{\text{solid}}$	Thin film formation.
Recombination	$S-A + A \rightarrow S + A_2$ $S-R + R_1 \rightarrow S + M$	Atoms or radicals from the plasma can react with the species already adsorbed on the surface to combine and form a compound.
Excitation	$S + A^* \rightarrow A$	Excited species on collision with a solid surface return to the ground state
Sputtering	$S-B + A^+ \rightarrow S^+ + B + A$	Positive ions accelerated from the plasma towards the surface with sufficient energy can remove an atom from the surface.
Polymerization	$R_g + R_s \rightarrow P_s$ $M_g + R_s \rightarrow P_s$	Radicals in the plasma can react with radicals adsorbed on the surface and form polymers.

Figure 3.6: Gas phase reactions involving electrons and heavy species

The types of electrical power sources can be used for applying a current in the plasma discharge are (DC) direct current and (RF) radio frequency. In the field of culture heritage conservation it is better to use rf system because the use of d.c only can be done with the conductive materials, so the two electrodes have to be conducting but in the case of rf it doesn't matter if they are conducting or not. However, it is difficult to operate a stable DC glow discharge with the artefacts covered with corrosion products occurring at the non-uniform surface of the object. On the other hand by using RF discharge the operation is more stable and it can be done for large objects with thin or thick layers of corrosion products. Moreover, it is more efficient in promoting ionization, self-bias of the plasma. Due to the very small electron mass, the RF plasma gives to the electrons much more acceleration than to the ions. In addition, the loss of electron energy from ion or neutral collisions is negligible due to the low value of the ratio m_e/m_i . In this way, the temperature of the electron increases considerably (10,000-100,000 k), while the ion and neutral temperatures remain at low ion (500 k) and neutral (300 K).

Therefore, plasma is not in thermodynamic equilibrium, because the high temperature of the electron makes plasma more effective in reducing oxides [32, 126, 55].

3.1.2 Plasma cleaning of metallic artefacts

Plasma cleaning is a process that removes any organic contaminants and corrosion products from the metal surface. The principle of the glow discharge cleaning means placing the material or the substrate to be cleaned in the glow discharge chamber and bombarding by many plasma species: Electrons, ions, photons and neutral species that may be chemically unstable (e.g. radicals) or excited state. The precise energy of the bombardment depends on whether the substrates are isolating or conducting, if the discharge is excited rf or dc, and if the substrates are subjected to a high-energy negative bombardment of particles from the target sheath [124, 127].

There are three main parameters for etching process:

1. Etch rate uniformity, the geometry of the electrode assembly at the wafer perimeter is most important for the uniformity of the etch rate in capacitively coupled systems, especially in the wafer edge region.
2. Anisotropic etching means that the material is only removed vertically, while the horizontal etching rate is zero. In contrast, isotropic etching is characterized and proceeds at the same rate in all directions [3, 7].
3. Selectivity, which means removing one type of material without affecting other materials. It seems that it is not easy to design highly selective plasma etch processes. In fact, the design of a plasma etch process often competes with selectivity and anisotropy [66, 128, 124]

Different mechanisms can be observed for the low-pressure etching as follows:

1. The sputter-etching mechanism is comparable to the deposition of the sputter, however the discharge parameters are now customized to efficiently remove the material from the target instead of depositing the sputtered atoms on the substrate. It can be considered as non-selective process, so the sputtering yield depending on the energy of the bombarding species, The projectile and target species masses and the binding energy of the surface. Consequently, the sputter yields for different materials do not differ greatly. Sputtering, however, is an anisotropic process that greatly depends on the incidence angle of the bombing ions.
2. Pure chemical etching. Atoms or radicals from the plasma discharge can chemically react to projectiles in the gas phase with the target surface. Chemical etching is essentially isotropic, as the etching atoms are almost uniformly angularly distributed on the target surface. Anisotropic etching is only possible if the reaction

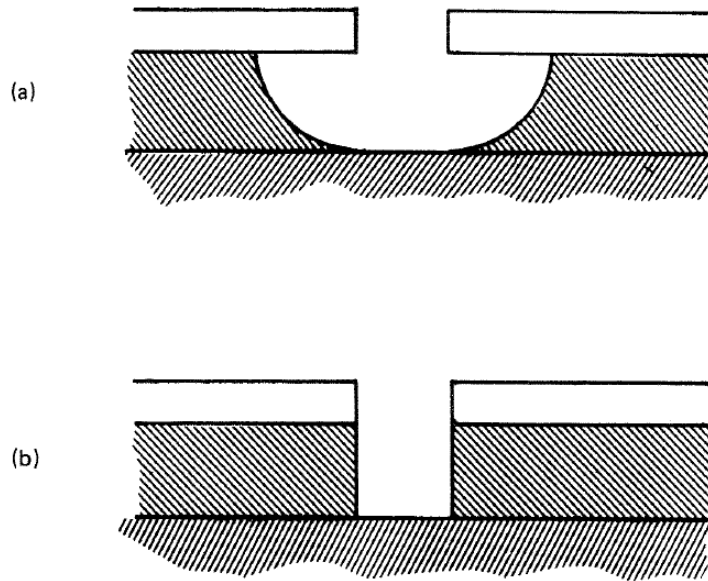


Figure 3.7: Plasma etching profiles, (A) is Isotropic, (B) is anisotropic

between etching atoms and a crystal depends on the crystallographic orientation of the etching rate. The etch rate is not usually determined by the flow of etching atoms, but by the set of surface reactions.

3. Energy etching enhanced by ions. The discharge provides the etching process with etching particles and energy ions. The combination of etching atoms and energetic ions appears to be much more effective than the separate sputter and chemical etching mechanisms. The etching process itself is probably chemical, but it is determined by the energy bombardment of ions with a reaction rate. This etching method can also be very anisotropic, but generally the selectivity is lower than with chemical etching.
4. Inhibitor etching enhanced by ions. The discharge not only provides etching atoms and energetic ions, but also so-called precursor molecules for inhibitors. To form a protective layer, the latter are deposited on the target material. In the absence of ion bombardment and the inhibitor, the etching atoms are selected to obtain a high chemical etch rate. The bombarding ion flux prevents the formation of an inhibitor layer and removes this layer in order to expose the target surface to the etching atoms. The target surface is therefore only etched if there is no layer of inhibitors. The ion-enhanced etching of the inhibitor is therefore very selective and anisotropic. However, the contamination of the surface and the removal of the protective film after the etching step are possible problems with ion enhanced inhibitor etching. In order to achieve a compromise between parameters such as

efficiency, accuracy, selectivity and anisotropy, the various etching mechanisms can be combined (parallel or after)[66, 124].

3.1.3 Plasma Cleaning Tests

Some laboratory tests carried out to evaluate the efficiency of rf low-pressure plasma discharge to clean some copper and silver alloy samples are described. The samples were artificially corroded and successively cleaned in the Department of Applied Science and Technology of Politecnico di Torino.

Instrumentation

The plasma cleaning was carried out in a parallel plate reactor capacitively coupled with an asymmetric electrode configuration. It consists of a vacuum chamber made of stainless steel, an electrical electrode connected to the RF power supply (13.56 MHz) via an impedance unit and a ground electrode. Gas flow rates are controlled by mass-flow controllers, while a turbo-molecular pump supported by a rotating pump, a throttle valve and a pressure gauge allow the selected value to be maintained??

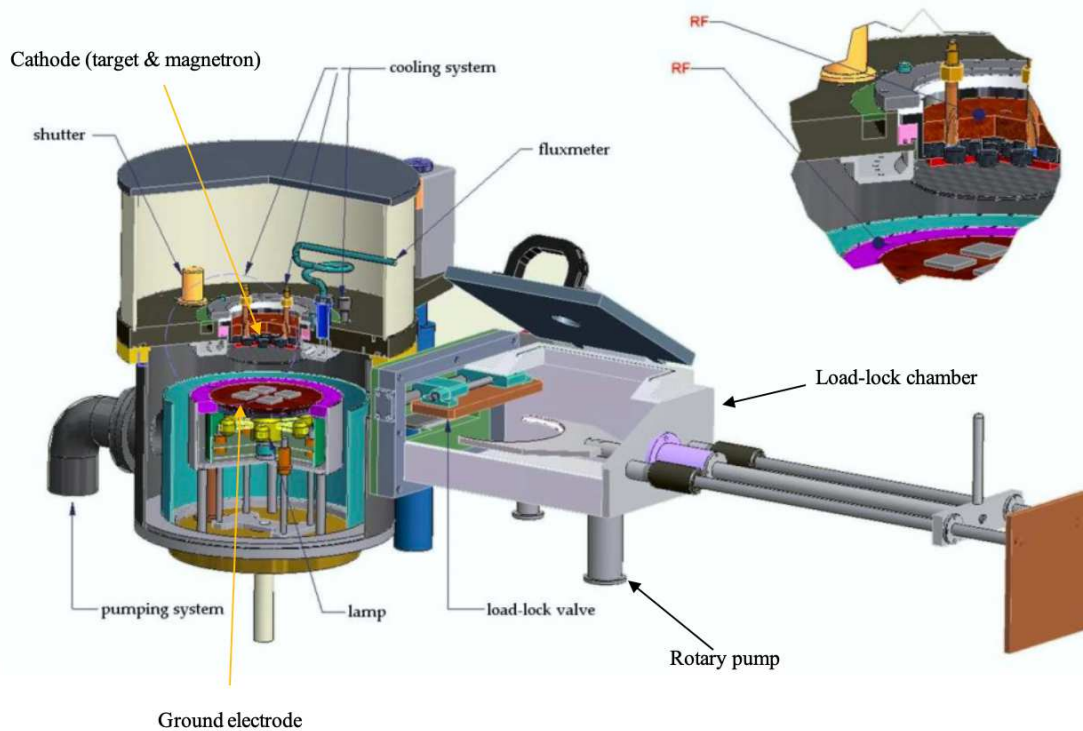
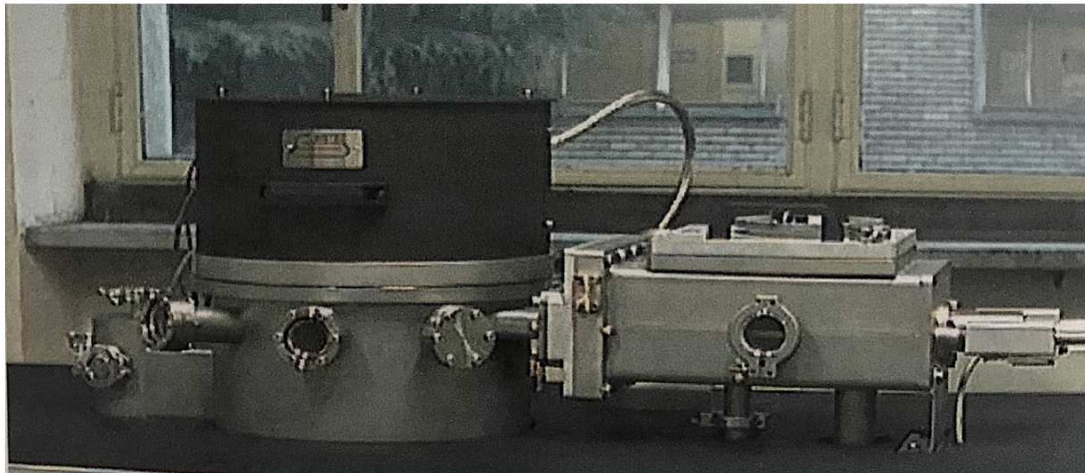


Figure 3.8: The plasma reactor in the Plasma Lab of Politecnico di Torino

Experimental Parameters

The tests were carried out on 10 copper samples divided into two groups with different corrosion products. The first group was artificially corroded in order to obtain a cuprite layer and the second group was artificially corroded in order to obtain a copper oxychlorides layer. Moreover a set of silver alloy samples was artificially tarnished with

silver sulfide. The used gas for the cleaning was mixture of Hydrogen and argon and the conditions described in Table

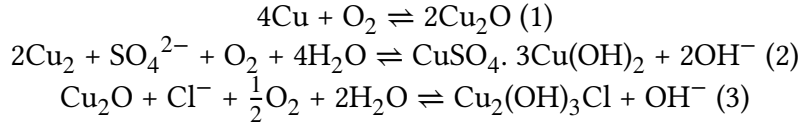
Artificial Ageing of the samples

The copper and copper alloys can give rise to different corrosion products in dependence of the environmental conditions. Cuprite is the first corrosion layer which can be formed due to the interaction between copper and oxygen. The cuprite layer can behave as a protective film for the artefacts. Furthermore, the copper patina typically consists of two distinct layers cuprite and external porous layer of basic copper sulphate, brochantite ($\text{Cu}_4\text{SO}_4(\text{OH})_5$), or basic copper chloride% atacamite ($\text{Cu}_2\text{Cl}(\text{OH})_3$). Brochantite patinas are more common whereas, atacamite is found in marine patina [121, 129, 130]. The copper samples (99.99 wt %) had the following dimensions 3: 3.5 x 1.5 x 0.5 cm. The samples were polished with SiC paper 180, 320, 500 and 800, cleaned by ethanol in ultrasonic bath for 15 min. The artificially ageing of the first group of copper samples was performed by means of electrochemical techniques in order to obtain a cuprite layer. The copper-based samples were polarized anodically at 80 mV (versus a saturated Ag/AgCl reference electrode) for 16 hours in (400ml) a 0.1 M Na_2SO_4 solution. The second group were patinated by a type of corrosion products were little complex mixture of carbonates, chlorides and sulphides. Before start the patination we left the samples in the cell to stabilize for 30- 40 minutes before applying the current to the cell until the potential for free E_{corr} , the potential of the working electrode compared to the reference electrode when there is no current or potential existing in the cell, it has not reached steady state. Then start the patination by applying the current. The samples were obtained initially immersing in Na_2SO_4 0.01 M (400 ml) for 2 hours to create a layer of cuprous oxide (cuprite) 3.9. Then start the patination by applying an 80 mV anodic potential (vs Ag / AgCl). Then after create the cuprite layer we followed the standard method for corrosion tests ASTM D 1384 by immerse the samples in corrosive water and apply the anodic potential of 380 mV for 7 days (168 hours) [131]. Then the anodic potential increased to 880 mV for 3 days (72 hours). The electrolyte contained 100 ppm each of sulfate, chloride, and bicarbonate ions introduced as sodium salts, dissolved in 1 L of distilled water at 20° C:

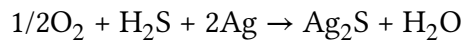
1. Sodium sulfate 148mg.
2. Sodium chloride 165 mg.
3. Sodium bicarbonate 138 mg [132].

In this case the cuprite film created on the sample surface, then the interaction with chlorides results in the formation of nantokite (CuCl) which transforms to atacamite or paratacamite. Moreover, in this case there is a possibility of create of brochantite which can be confirm due to the existence of Sulfur in the EDS analysis. The reactions can be

done according to the following equations [133, 134, 135, 136, 137, 138, 139, 140]



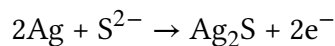
Since ancient times, silver has been used in the manufacture of decorative and functional objects due to its working properties and pleasant colour and brightness, either as pure metal or in conjunction with other metals such as copper or gold. Although highly lustrous when polished, silver and silver alloys gradually darken and become less bright for a long time when they are exposed to the atmosphere. Indeed, due to the interaction with sulphur-containing compounds in the environment, the well-known tarnishing reaction begins almost immediately. The main compound responsible for silver tarnishing is hydrogen sulphide (H_2S), but other organic sulphides, such as carbonyl sulphide, can react faster with silver and contribute to the degradation process, even if they are present in lower concentrations. Many mechanisms can be happen and cause tarnishing of the silver depending on the environmental conditions such as temperature and relative humidity, type of gases together with other corrosion processes that may occur at the same time 3.1. However, the main product of silver tarnishing is silver sulphide (Ag_2S). In this case the silver sulfide is a corrosion product which can be found in the museum's atmosphere and may occur due to the atmospheric Corrosion. For that matter, the tarnishing of silver in a display case of a museum is a result of H_2S transport to the silver surface of the artefact.due to the formation proceeds according to the following electrochemical reaction. If the hydrogen sulphide present in the museum environment even if in a small amount 0.2 ppm it cause a visible tarnish layer in a few weeks or months and form silver sulphide.



With high relative humidity the silver tarnishing is accelerated. Moreover, when the thickness of Ag_2S increases, the colour, initially white, will turn yellow at 10 nm, violet at 26 nm, blue at 47 nm and finally dark gray thus interfering with the readability of surface details. Even though silver sulfide tarnish is a surface phenomenon, it does not tend to threaten the mechanical integrity of an object. It can, however, be aesthetically unpleasant and interfere with the readability of surface details.[141, 142, 143]

[144, 145, 146]

[147]



The Silver based alloy are in different chemical compositions

Table 3.1: Chemical composition of the reacted surface as a function of the atmosphere[146].

Atmosphere	Film composition
H_2S	Ag_2S
OCS	Ag_2S
$H_2S + SO_2$	98% Ag_2S + 2% Ag_2O
$H_2S + Cl_2$	90% Ag_2S + 10% $AgCl$
$H_2S + SO_2 + Cl_2 + NO_2$	40% Ag_2S + 50% $AgCl$ + 10% Ag_2SO_4

- (wt%: Ag 96.5, Cu 3.5).
- (wt%: Ag 98.5, Cu 1.5).
- (wt%: Ag 92.5, Cu 7.5).
- (wt%: Ag 80, Cu 20)

The dimension of all samples are $\varnothing 20 \text{ mm} \times 2 \text{ mm}$. All samples were mirror polished and cleaned with ethanol in an ultrasonic bath for 15 min [148]. The samples were placed on a ceramic disc inside a desiccator with 0.01 M of Na_2S at room temperature and the time was 56 hours for the first three samples and 104 hours.3.10.

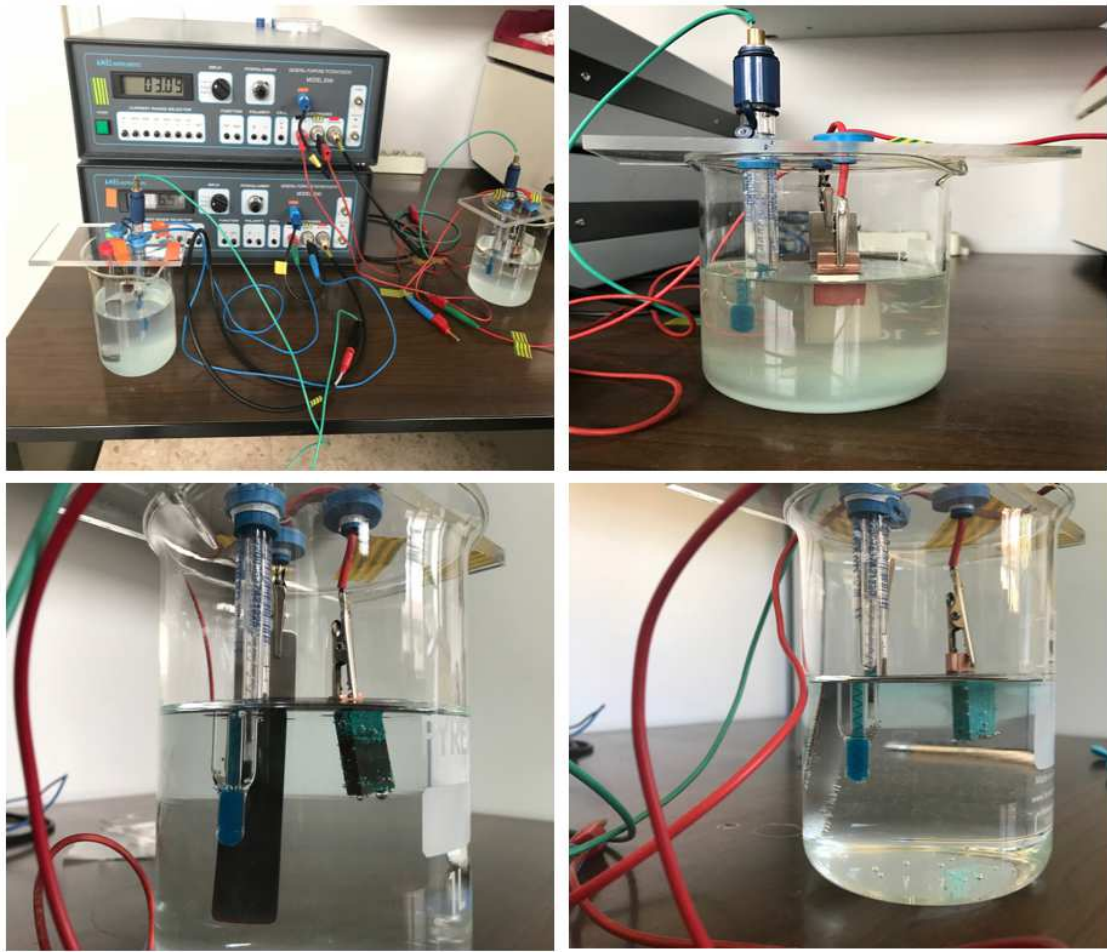


Figure 3.9: Artificial corrosion of copper samples

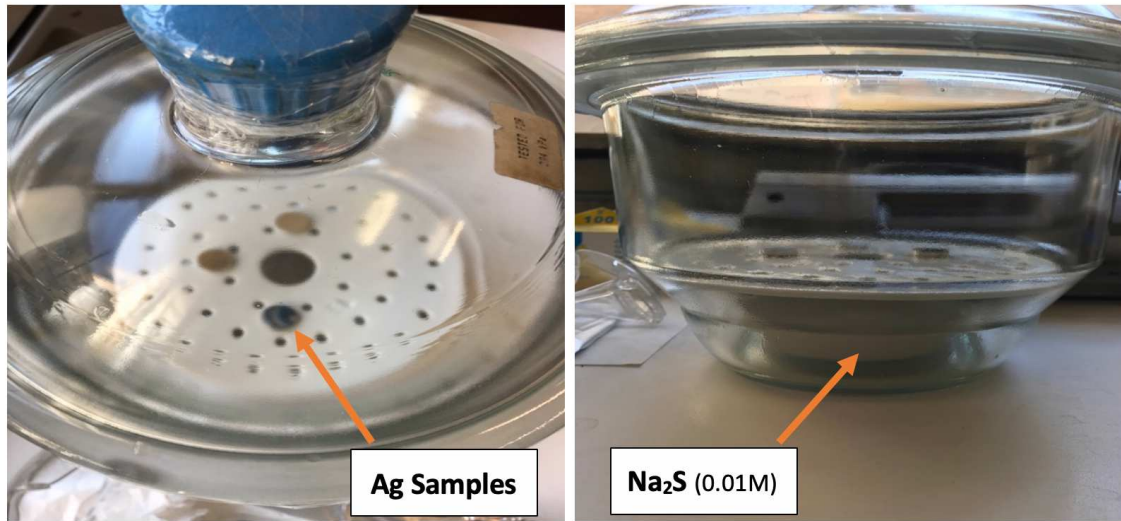


Figure 3.10: Artificial tarnishing of silver alloy samples

Plasma cleaning conditions

The cleaning parameters were carried out in two the first one was pre-treatment test to evaluate the conditions and compare with different parameters like the gas pressure, the Rf power, and the used target. The second performed as the best chosen condition from the point of the researcher. In the pre-treatment step the used target was copper but there were some sputtering from it on the samples surface at low power. To avoid this sputtering the only solution to decrease the rf power to 10-20W which means increase the treatment time to have good cleaning results. On the other hand when we changed the target to Aluminium the sputtering wasn't exists which gives us the ability to increase the power to 100 W. With this high power the efficiency of the plasma cleaning was higher with less cleaning time than before. The temperature were between 20-55°C during the treatment. The long term treatment as the 3 hours not performed directly but 30 minutes after 30 minutes to avoid the increase of the temperature and the overload for the the plasma reactor. Before perform the cleaning process we masked the half of each sample with Aluminum foil to avoid the bombardment and cleaning of half of the sample and easily compare the result before and after cleaning but some times the musk not completely avoid the bombardment as we can see in the photos3.12.

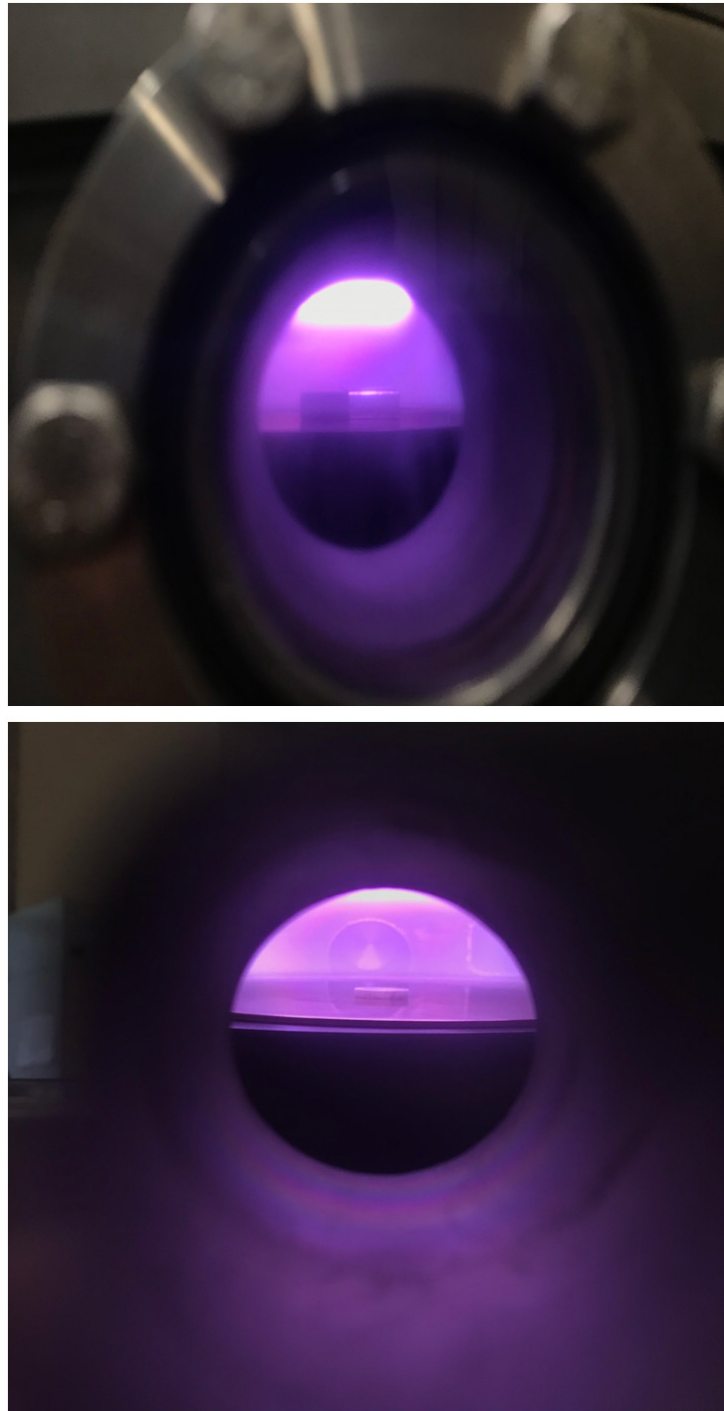


Figure 3.11: Photo of the copper and silver samples inside the chamber at the treatment time

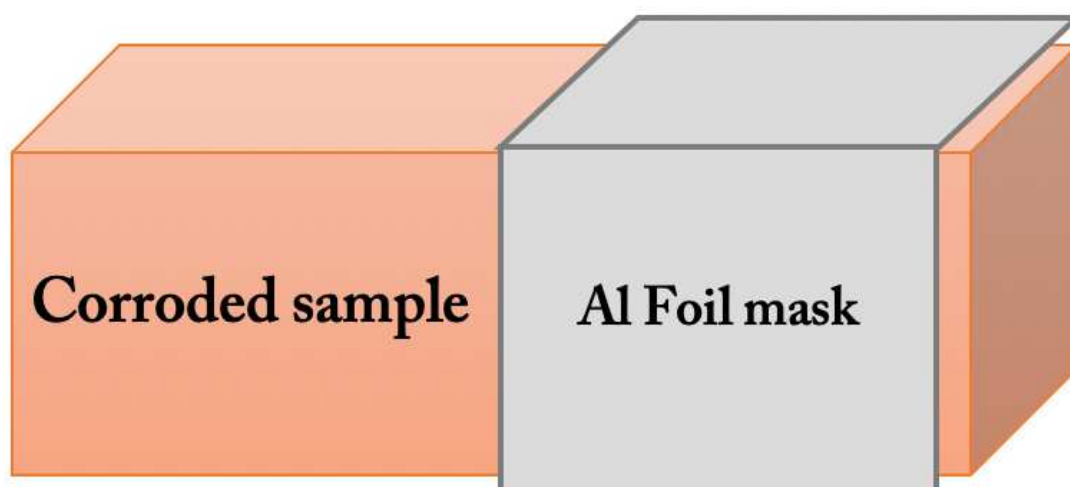


Figure 3.12: Schematic of the Aluminium foil mask on the half of the sample

Table 3.2: Pre test for plasma cleaning parameters

Code	Type	Corrosion	H ₂ / Ar _{scm}	RF power _W	Pres. _{mbar}	Time _{Min}	Target
C1	Cu	Cu ₂ O	40-60	20	1.1 x 10 ⁻¹	30	Cu
C2	Cu	Cu ₂ O	70-30	30	2.6 x 10 ⁻¹	30	Cu
C3	Cu	Cu ₂ O	80-80	40	1.9 x 10 ⁻¹	30	Cu
C4	Cu	Cu ₂ O	95-95	40	1.9 x 10 ⁻¹	60	Al
M1	Cu	Mix	80-80	20	1.6 x 10 ⁻¹	30	Cu
M2	Cu	Mix	95-95	20	1.9 x 10 ⁻¹	60	Cu
M3	Cu	Mix	95-95	20	2.0 x 10 ⁻¹	60	Al
Ag 1	Ag alloy	Ag ₂ S	95-95	20	1.9 x 10 ⁻¹	30	Al
Ag 2	Ag alloy	Ag ₂ S	80-80	20	1.9 x 10 ⁻¹	30	Al
Ag 3	Ag alloy	Ag ₂ S	95-95	20	1.9 x 10 ⁻¹	30	Al

3.2 Results and discussion

In the first test there were different changes in the Rf power, time of cleaning, the ratio between hydrogen and argon, the used target for cleaning. All these parameters were tested to evaluate the best condition between them. Through these tests we observed that using Cu target cause little sputtering of Cu-nano particles on the samples surface in the high Rf power such as 30 - 50 W and sputtering from 10-20 W power. In

Table 3.3: Plasma cleaning parameters

Code	Type	Corrosion	H ₂ / Ar _{sccm}	RF power _W	Pres. _{mbar}	Time _{Min}	Target
Cup 1	Cu	Cu ₂ O	95-95	100	180	Al
Cup 2	Cu	Cu ₂ O	95-95	100	150	Al
Cup 3	Cu	Cu ₂ O	95-95	100	120	Al
Cup 4	Cu	Cu ₂ O	95-95	100	90	Al
Cup 5	Cu	Cu ₂ O	95-95	100	60	Al
Oxy 1	Cu	Mix	95-95	100	180	Al
Oxy 2	Cu	Mix	95-95	100	150	Al
Oxy 3	Cu	Mix	95-95	100	120	A
Oxy 4	Cu	Mix	95-95	100	90	Al
Oxy 5	Cu	Mix	95-95	100	60	Al
Ag 1	Ag alloy	Ag ₂ S	95-95	20	30	Al
Ag 2	Ag alloy	Ag ₂ S	80-80	20	30	Al
Ag 3	Ag alloy	Ag ₂ S	95-95	20	30	Al

addition, the changes in the gas ratio and time also affects the cleaning process. On the other hand the uses of Al target allowed to clean the samples without any sputtering on the surface even though the use of 100 W of power. The samples were characterized by different methods high resolution camera photos (Canon EOS 1200 D CMOS and Nikon D5600), FESEM, EDS and XRD to evaluate the efficiency of the plasma cleaning. The idea for using mixture of argon and hydrogen was good and efficient. With argon we can avoid the possibility of metal oxidation in the glow discharge in addition The existence of metastable states in ionized argon can contribute significantly to the activation of other gasses. On the other hand Plasma hydrogen can reduce certain products of corrosion back to metal[28, 29].

3.2.1 High resolution photos

In the pre-treatment we used camera (digital reflex Canon EOS 1200 D CMOS (complementary metal-oxide semiconductor) 18 megapixels. EF-S lens 18-55mm f / 3.5-5.6 IS STM) to capture some photos in high resolution scale to have little information about the samples before and after cleaning due to the colour changes. The Photos gives an indication about the efficiency of the cleaning test, moreover, if there is any sputtering on the samples surface. It was clear that there are some copper nano particles on the samples surface C1, C2, C3 figures 3.13, 3.14, 3.15 due to using the cu target(Cathode) for cleaning the samples but the amount of sputtering are difference due to the RF power in each sample. Sample C1 is less sputtering and less nano particles on the surface due to use rf 20w, whereas, C2 and C3 more sputtering and nano particles on the surface due to increasing the rf power to 30 and 40 w . On the other hand when the target changed

to Aluminium target (Cathode), it was clear that there isn't any sputtering on the C4 sample surface 3.17, even if using high rf power. After the pre-treatment step the best conditions were used for the final treatment test are:

- RF power of 100 W.
- 95 sccm of H₂ + 95 sccm of Ar .
- The used target was Aluminium.
- Finally to compare the treatment efficiency changing *time* was the factor of evaluation.

For the final treatment test we used Nikon D5600 DSLR Auto focus with AF-S, AF-P and AF-I lenses and manual focus MF. 24.2 megapixel of resolution with lens AF-S DX NIKKOR 18-55mm f/3.5-5.6G VR II. The images resolution were 300 × 300 ppi.

* **Statistical evaluation of plasma treatment of samples images**

Before putting the samples inside the chamber, all the samples captured with the camera and masked have of the sample using aluminum foil to avoid the plasma cleaning to all the sample. In this case we can compare the efficiency of the treatment easy. The idea of this evaluation method is to use different statistical parameters of the images before and after and have a clear view about plasma cleaning. This method is low-cost quantitative evaluation to test the efficiency of the plasma treatment. The statistical evaluation depending on two main factors, the rigor and the visual accuracy of the observer. It is based on analysis of the color histogram (mean, standard deviation, skewness) of the processed images before and after cleaning. The first aspect relates to the type of color space used to acquire or display images. In our work, RGB (Red, Green and Blue) was adopted. To processing images the following parameters have been considered:

1. The *Mean* which is related to the object's brightness degree ; a lower/higher mean reflects a higher degree of dirtiness / cleanliness.
2. The *Standard deviation* is a measurement of the pixel values in an image, high/low values coincides with higher/ lower contrast.
3. The *skewness* is a measurement of the pixel level distribution symmetry, the symmetrical distribution has zero skewness, negative / positive values show that the data is skewed right / left "tail" is longer. Images have many pixels with high values are usually skewed right, suggesting a tendency to saturate the bright pixels. This inclination to the highest values corresponds to clean and shiny surfaces. To do this type of statistical analysis the conditions of the image capture should following some procedures which are:

- The **white balance** of the camera has been manually adjusted and kept without any changes during the images acquisition.
- Identical **shutter time** and **aperture** have been used for every pair of images (before and after cleaning).
- The **appropriate** settings for image acquisition were cross-checked by digitally comparing identical areas from the background. [68, 67, 149, 150, 151, 152, 153, 154]

The Statistical parameters illustrated some data about the plasma cleaning efficiency by using the mean, the standard deviation (Std) and skewness (Skew). This statistical processing of photographic images showed increases of the histograms mean in all cases except one copper sample (C3) due to the sputtering of copper nano particles on the sample surface. In addition the pre-treatment samples C1, C2 and C3 have a nano copper thin film due to the uses of copper target in the first cleaning test as seen in figures 3.13, 3.14, 3.15. After changing the copper target to Aluminum target to avoid the sputtering and increasing the rf power the result were very good at all. The Cuprite samples group (Cup1, Cup2, Cup3), it was clear that the cleaning efficiency in the first 30m was very fast (cup3) and the mean increases in brightness and it became more brightness than the other samples Cup1, Cup2. The meaning of these two samples were less than the first one which means the cleaning efficiency became slow with increasing the time of cleaning. The Oxychlorides samples shows complete removal of green patina as seen in figures 3.23, 3.22, 3.21 due to the effect of plasma cleaning. The mean of sample Oxy1 increased with high value of 24.56 from 29.771 to 54.331 due to the increasing of the cleaning time. On the other hand in Samples Cup3, Cup2 the mean value changed lower. It can be seen the change of color and completely transformed of green patina to red and dark-brown patina after only 30 min of treatment. The silver alloy samples also shows increases of the mean of the histograms before and after cleaning on a scale of 256 gray levels. Samples Ag2, Ag3, Ag4 and Ag 5 became shiny again after cleaning except sample Ag1, but it was difficult to capture the images with this shiny surface because it reflects the light to the camera lens and it is not possible to change any setup or settings through shooting because in this case all the statistical parameters will be changed. Moreover, the overall trend of standard deviation increase reflects the idea that a small range of pixel values has become a wider range, so we can observe that the plasma cleaning is homogeneous and the tarnishing layers were removed and the silver alloys samples became bright and shiny. The cleaning efficiency were confirmed also by skewness values. A high degree of cleaning reflects an asymmetrical tendency of the histogram towards brightness. In some cases also the cleaning were not completely done in this case the skewness value decreases or becomes negative, which can reflecting the asymmetry of histograms for plateau part, with a left oblique distortion, which means a low selection of exceptional values, the area being a homogeneous plateau as regards the degree of contamination. Finally we can conclude that the statistical evaluation

and build an assumption to describe the efficiency of the plasma cleaning degree over skewness:

- The plasma cleaning is uniform and safe.
- The increasing of the cleaning time affects the process.

It could be considered the purity of silver alloy which means when the amount of silver increases the plasma cleaning becomes faster. sample Ag1 contains.

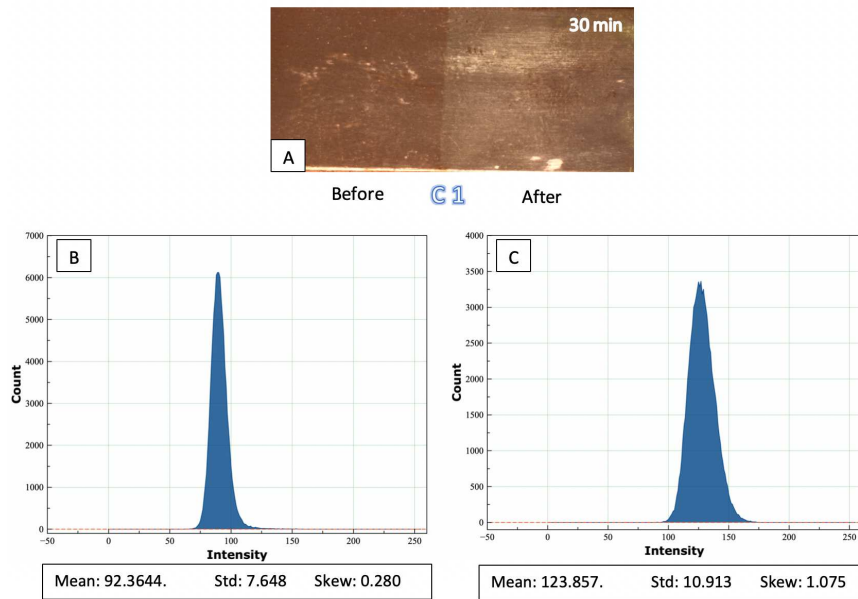


Figure 3.13: Sample C1, (A) before and after treatment, (B) histogram of patches before treatment and (C) histogram of patches after treatment. It shows the sputtering of copper nanoparticles from the target on the surface

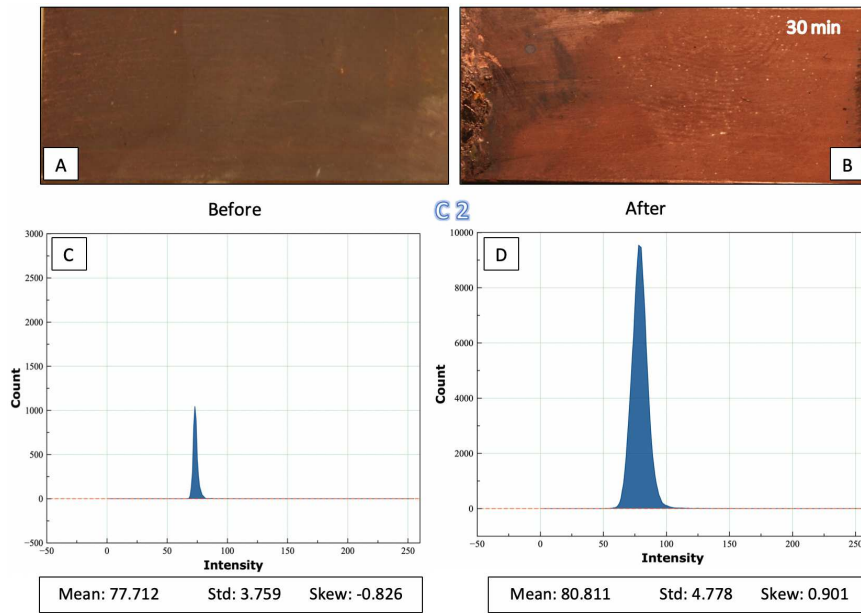


Figure 3.14: Sample C2, (A, B) before and after treatment, (C, D) histogram of patches before and after treatment. It shows the sputtering of copper nanoparticles from the target on the surface

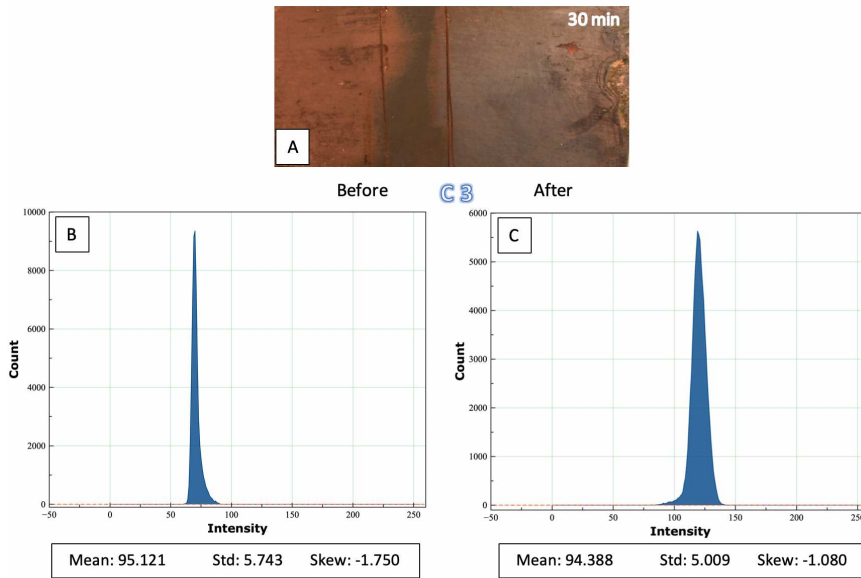


Figure 3.15: Sample C3, (A) before and after treatment, (B, C) histogram of patches before and after treatment. It shows the sputtering of copper nanoparticles from the target on the surface.

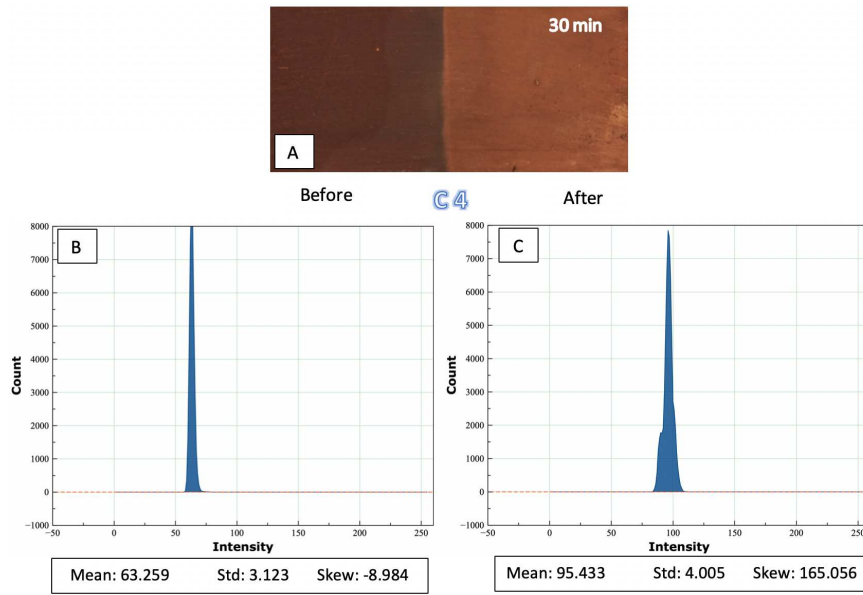


Figure 3.16: Sample C4, (A) before and after 30 minutes of treatment, (B, C) histogram of patches before and after treatment.

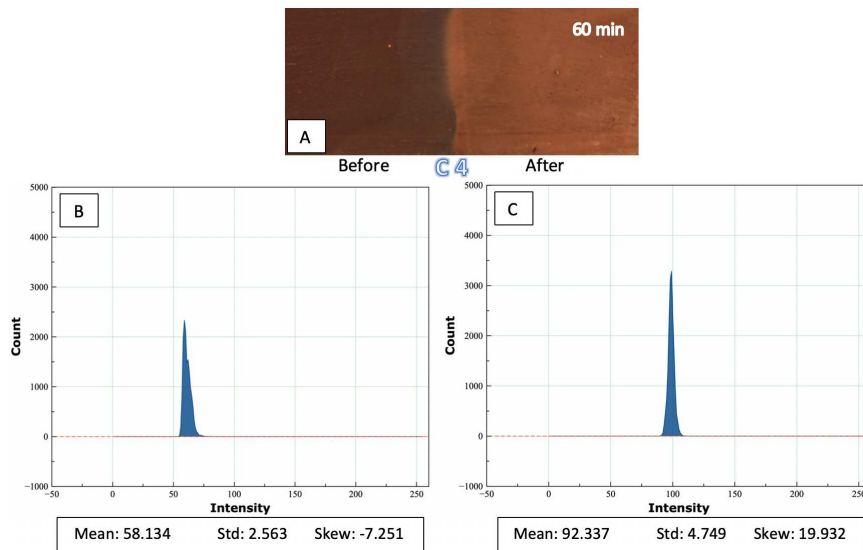


Figure 3.17: Sample C4, (A) before and after 60 minutes of treatment, (B, C) histogram of patches before and after treatment.

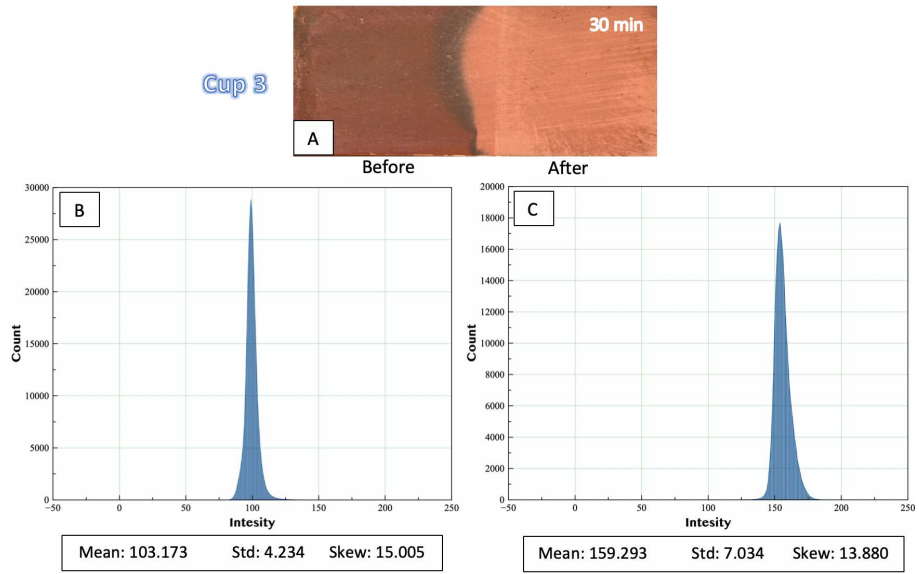


Figure 3.18: Sample Cup3, (A) before and after 30 minutes of treatment, (B, C) histogram of patches before and after treatment.

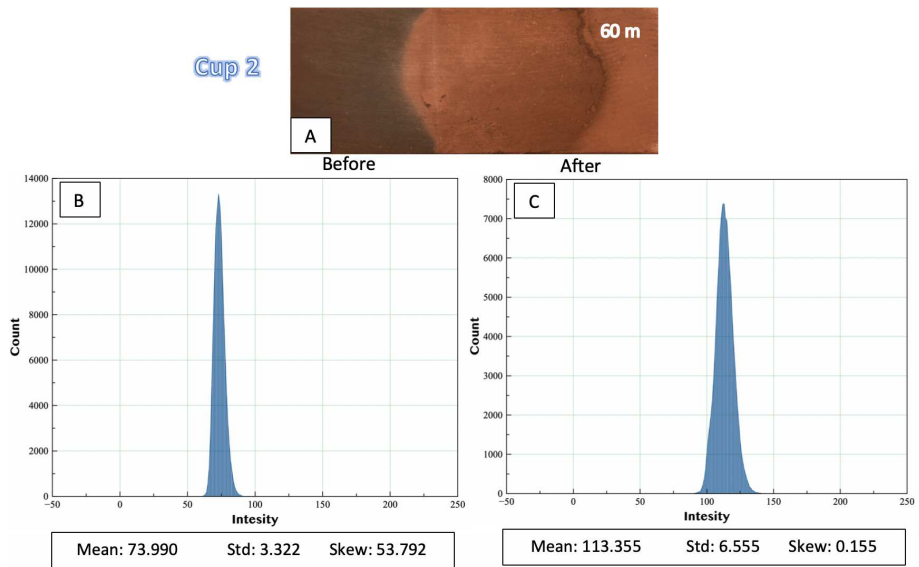


Figure 3.19: Sample Cup2, (A) before and after 1 hours of treatment, (B, C) histogram of patches before and after treatment.

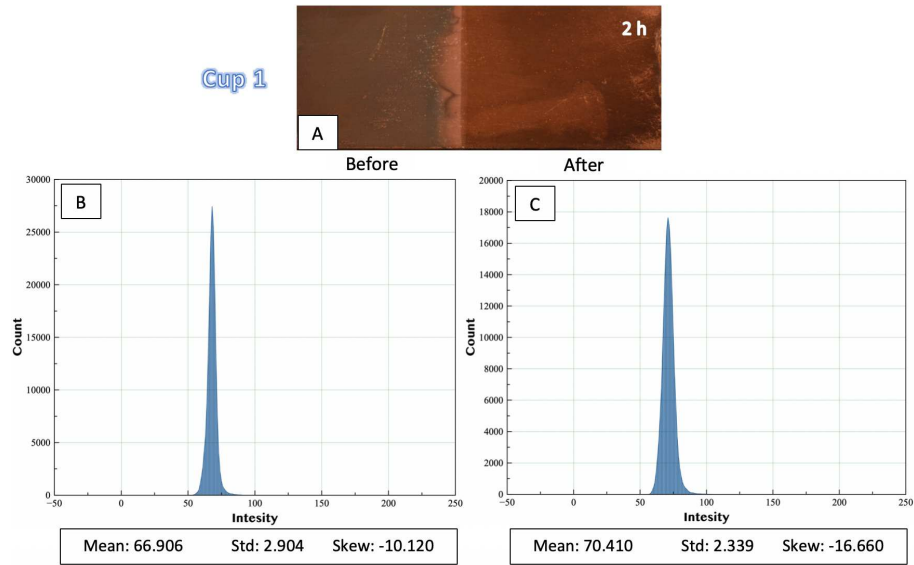


Figure 3.20: Sample Cup1, (A) before and after 2 hours of treatment, (B, C) histogram of patches before and after treatment.

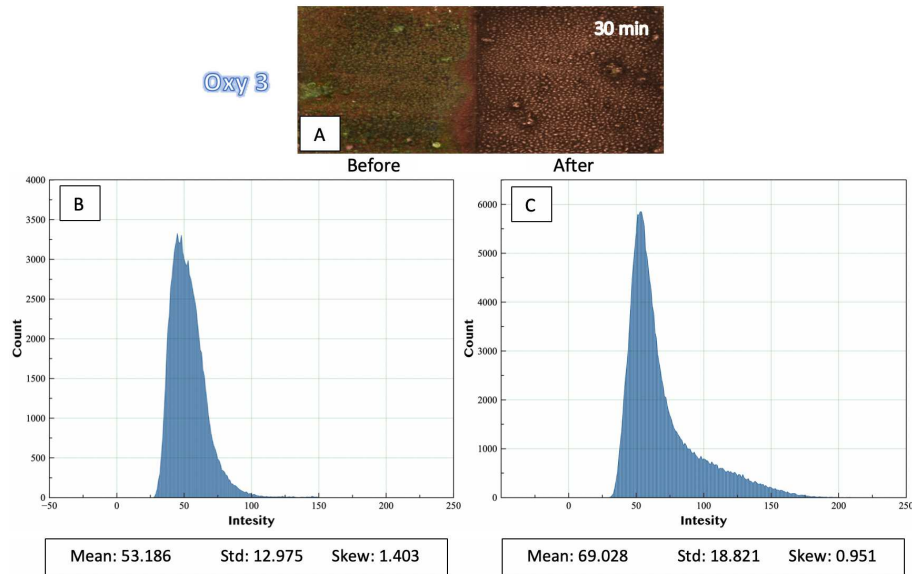


Figure 3.21: Sample Oxy3, (A) before and after 30 min of treatment, (B, C) histogram of patches before and after treatment.

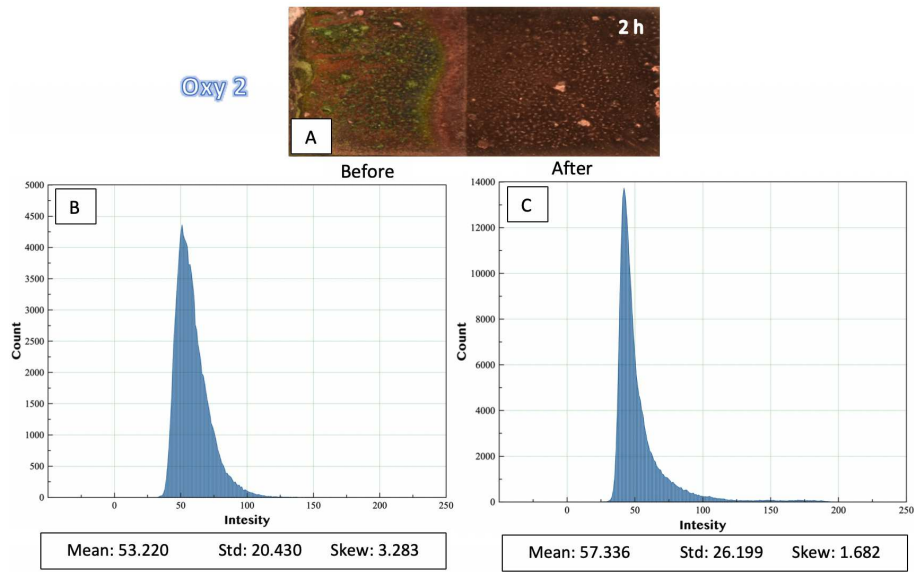


Figure 3.22: Sample Oxy2, (A) before and after 2 hours of treatment, (B, C) histogram of patches before and after treatment.

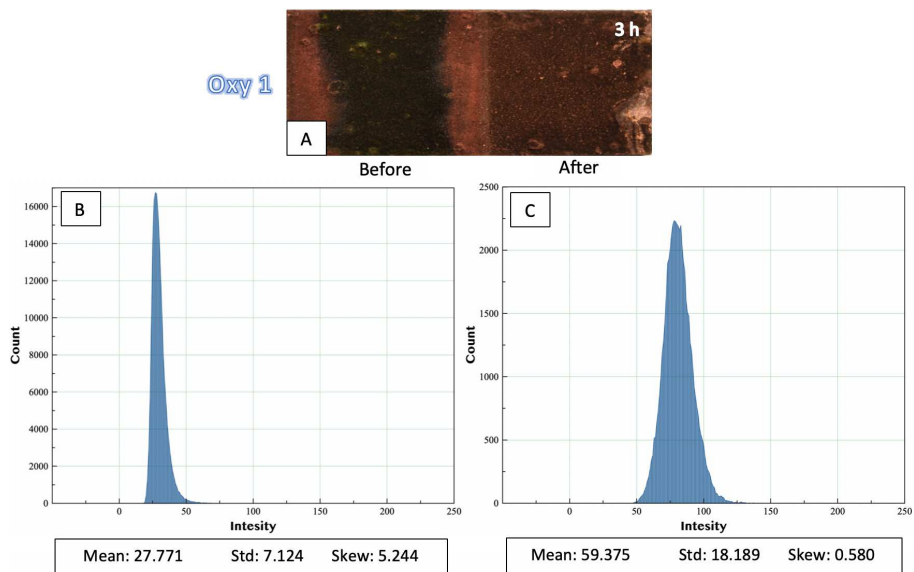


Figure 3.23: Sample Oxy1, (A) before and after 3 hours of treatment, (B, C) histogram of patches before and after treatment.

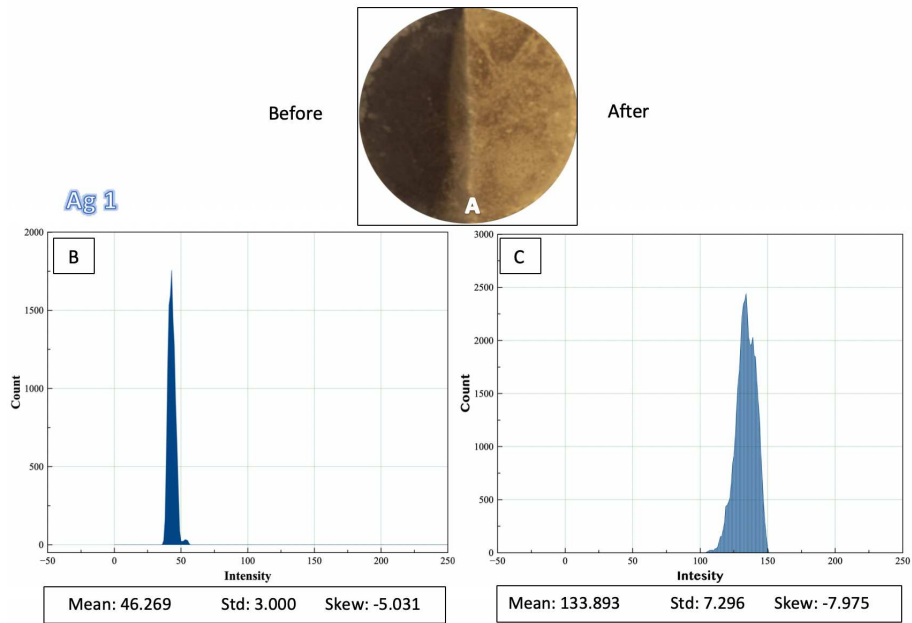


Figure 3.24: Sample Ag1, (A) before and after 30 minutes of treatment, (B, C) histogram of patches before and after treatment.

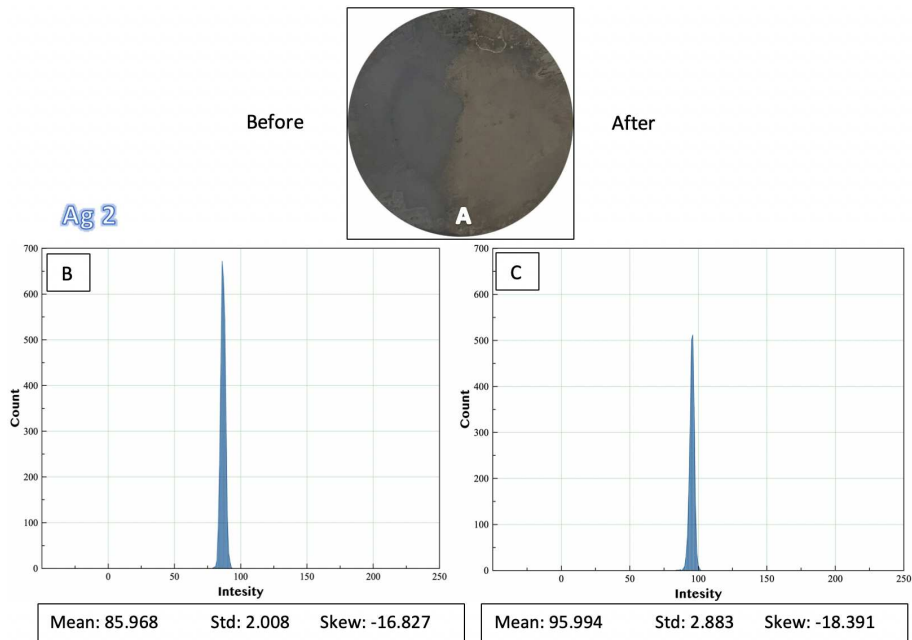


Figure 3.25: Sample Ag2, (A) before and after 30 minutes of treatment, (B, C) histogram of patches before and after treatment.

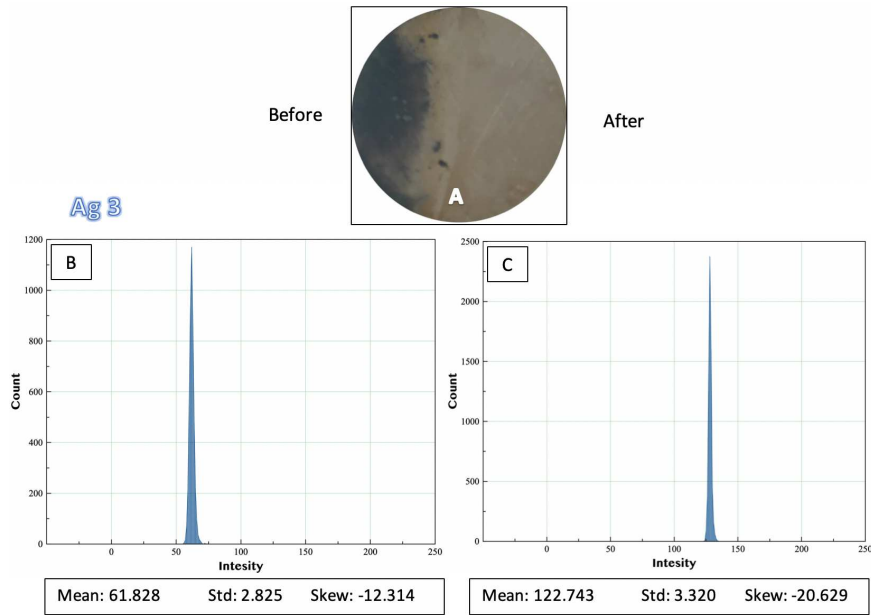


Figure 3.26: Sample Ag2, (A) before and after 30 minutes of treatment, (B, C) histogram of patches before and after treatment.

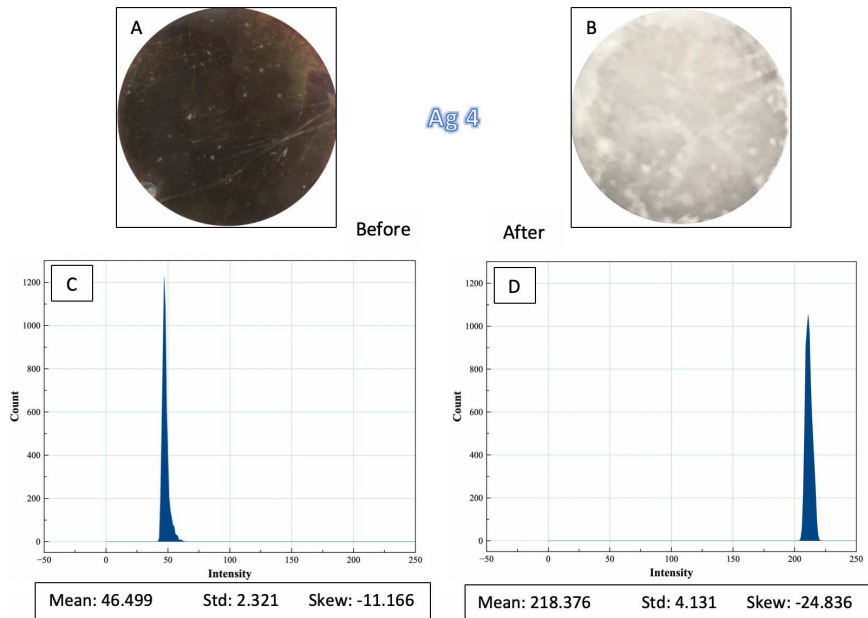


Figure 3.27: Sample Ag4, (A) before cleaning, (B) after 30 minutes of treatment, (C, D) histogram of patches before and after treatment.

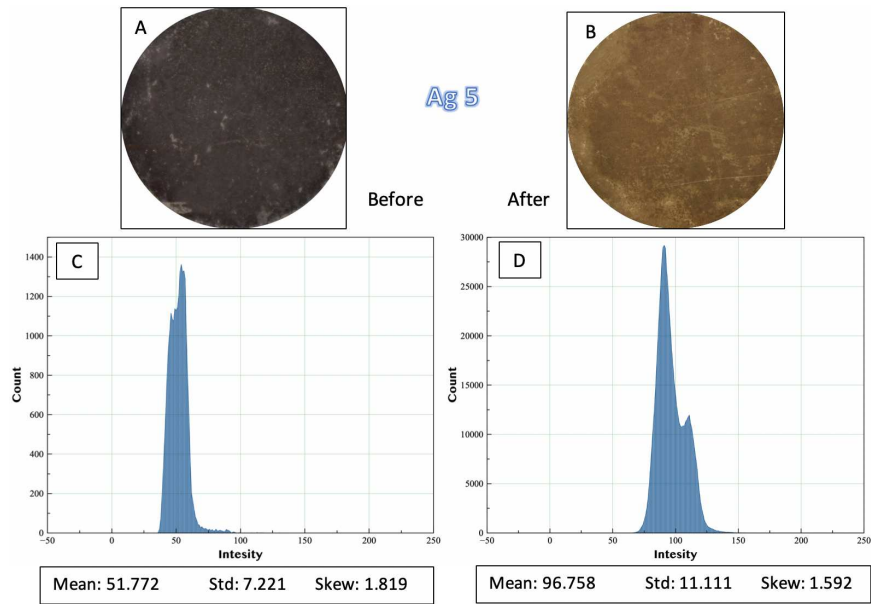


Figure 3.28: Sample Ag5, (A) before cleaning, (B) after 30 minutes of treatment, (C, D) histogram of patches before and after treatment.

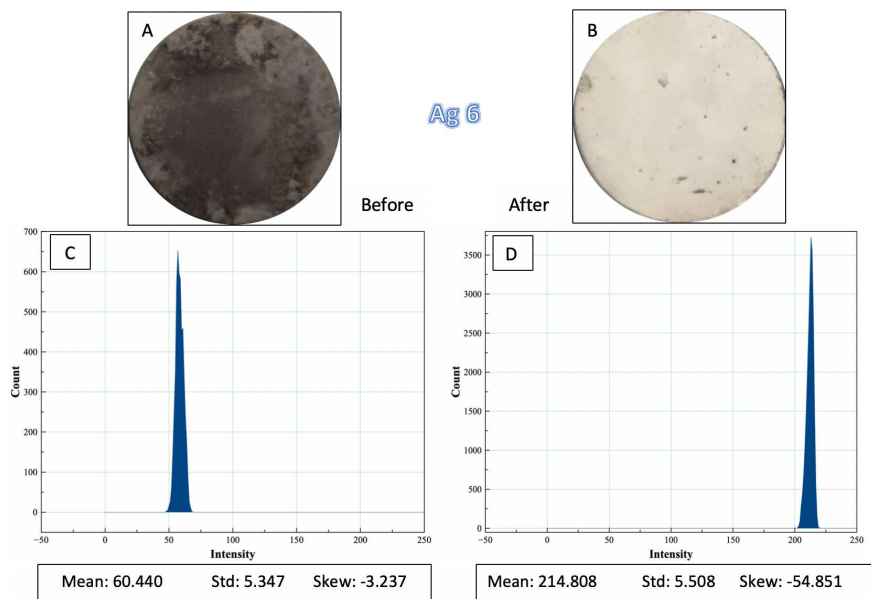


Figure 3.29: Sample Ag6, (A) before cleaning, (B) after 30 minutes of treatment, (C, D) histogram of patches before and after treatment.

3.2.2 FSEM and EDS

The samples were analysed by using FESEM SUPRA™ 40 (ZEISS) equipped with EDAX 9900 (Energy Dispersive X-ray Analysis) detector, Si(Li) detection technology that allows the analysis of light elements below beryllium. There are two classes of emission sources: thermionic or field-effect. The main difference between the scanning electron microscope (SEM) and the field emission scanning electron microscope (FESEM) is the source type. The thermionic emission sources use the electric current to heat a filament; the two most common materials used for filament are tungsten (W) and lanthanum esaboride (LaB6). When the heat is sufficient to overcome the working function of the filament material, the electrons can escape from the material itself. The sample and the electron beam interact in an elastic and inelastic way, from the obtained signals specific information is obtained on topography, crystallography, surface characteristics and sample composition.

The efficiency of the plasma cleaning was investigated by means of FESEM and EDS spectrum. The samples patinated with the cuprite layer (Cup2 and Cup3) were analysed to compare the results of the plasma cleaning performed with different treatment time. Figure 3.30 illustrates the morphology of the surface before and after cleaning. It can be observed that after one hour of treatment the surface morphology changed the crystals of the sample is more clear and shaped after treatment than before. In addition, the morphology of the samples after treatment seems more homogeneity. Figure 3.34 shows sample Cup2 before treatment and the oxygen peaks is high intensity due to the existence of copper oxide so oxygen and copper illustrated as major elements with traces of sulfur which can be due to the uses of Na₂SO₄ solution for the artificial ageing of the samples. Figure 3.35 shows the EDS patterns after one hour of treatment and it is clear that the amount of the oxygen (copper oxide) decreased 80% and the copper amount increased and became 94.69% which means the sample is almost clean. Moreover, Al traces can be seen which created from using Aluminum foil as a mask of half of the sample. Figure 3.31 illustrated the FESEM image of the morphology of the surface before and after 2 hours of cleaning. It can be observed that after 2 hours of treatment the surface morphology changed much than before due to the long time treatment The down right photo shows the broken of cuprite crystals due to the effect of the ion bombardment. Figure 3.36 shows EDS spectrum of sample Cup3 before cleaning and figure 3.37 shows the EDS spectrum after 2 hours of cleaning. We can see that the cuprite layer completely removed due to increasing the treatment time with trace of Al from the foil mask.

Samples (Oxy1 and Oxy3) which patinated with the mixture of carbonates, chlorides and sulphides. Figure 3.32 FESEM images before and after 30 minutes of treatment . The crystals shapes changed after the treatment due to the ion-bombardment and the cleaning is more efficiency. Figure 3.42 Oxy3 after 30 minutes of treatment. The chlorine and carbonate also completely removed form the first time and the amount of oxygen decreased to more than 60% copper increased more than 96% with trace of Al from the

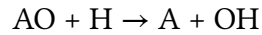
aluminium foil mask as usual.

Figure 3.33 FESEM images before and after 3h hours of treatment . It is clear that the crystals shaped changed more and seems melted after the long time of treatment due to the ion-bombardment and the cleaning is more efficiency. Figure 3.38, 3.39 confirmed the existence of oxygen, chlorine, carbon as mixture of copper oxide, copper chloride and copper carbonate. Figure 3.40 confirmed the cleaning of the sample Oxy1 after 3 hours of treatment. The chlorine and carbonate completely removed and the oxygen decreased to more than 90% due to increasing the treatment time.

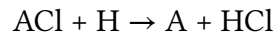
In the case of the Silver alloy samples it is clear that the cleaning efficiency is higher than cleaning of copper samples. The efficiency were between 98- 100% at only 30 minutes of cleaning time. The EDS spectrum confirmed the removing of 100% of silver sulfide from the surface of samples Ag3, Ag4 and Ag6 after 30 min of treatment 3.46, 3.47, 3.49. On the other hand the efficiency of cleaning of samples Ag2 and Ag5 were 99% and 97% 3.44, 3.48.

The possible explanation for the difference of the cleaning effectiveness on the silver alloy samples can be found in the different amount of copper in the alloy. In the case of samples Ag2 and Ag5, with copper content of 7.5- 20 wt% , 30 min of cleaning are not enough to have a complete cleaning but in the case of samples Ag3, Ag4 and Ag6 when the copper amounts are between 1.5- 5.5 wt% , 30 min of cleaning are enough to clean the sample 100%. Moreover, there is not a big difference between the effectiveness of the silver alloy cleaning in case of increasing the power and we can see that in the case of use 20w of power for cleaning Ag1, Ag2, and Ag3 than the use of 100W for cleaning Samples Ag4, Ag5, and Ag6. The difference were only depends on the copper amount in the alloy and the treatment time. According to the high resolution photos sample Ag1 and Ag5 were not glossy as before ageing because the treatment time was not enough to have full cleaning but other samples were glossy as before and maybe the photos were not clear to seen due to the the reflection of the light in the camera lens. In the case of copper cleaning The decreasing of oxygen and chlorine are due to the formation of OH radicals and HCl molecules by the reaction with the atomic hydrogen and argon. wherefore, the oxygen remove by reactions with neutral species whereas, chlorine remove by the interactions with hydrogen charged particles. This volatile HCl removed from the chamber with the gas flow. On the other hand, some scientists consider that the use of hydrogen plasma is better for cleaning silver alloys artefacts because it is a less invasive process, the artefact temperature remains low (50-80°C) and the radicals density increase more than in case of hydrogen/argon treatment. In addition, the use of pure hydrogen plasma with less hydrogen and low pressure also generates a high amount of ionized hydrogen and is therefore more efficient in reducing corrosion products than the hydrogen / argon mixture [58, 65, 54, 34].

The main reaction of creation of OH and HCl in the glow discharge can be described as follow:



Where AO means a metals-based compound which contains an oxygen atom, and A is the same compound with one less oxygen atom. This reaction can be performed several times until the metal surface is completely cleaned from oxygen. Then in the second step, the OH is transformed into water by another hydrogen atom. In one step, a similar reaction is also possible if highly excited molecular hydrogen reacts instead of two hydrogen atoms.



Where ACl is a compound containing an atom of chlorine and where A is the same compound with one less atom of chlorine. This reaction is much more effective with atomic hydrogen ions because of the strong electronegativity of chlorine atom[155]

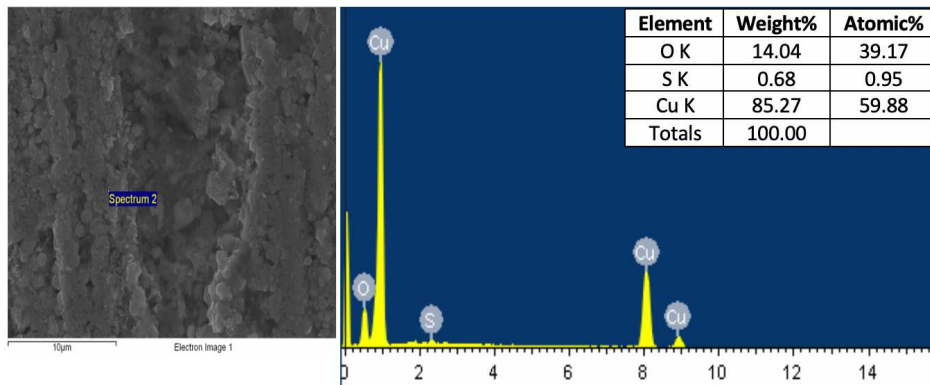


Figure 3.34: FESEM image and EDS analysis of sample Cup2 before treatment.

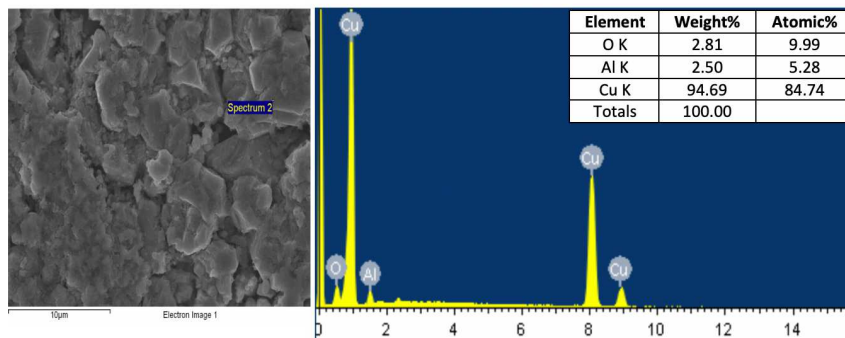


Figure 3.35: FESEM image and EDS analysis of sample Cup2 after 1 hour of treatment.

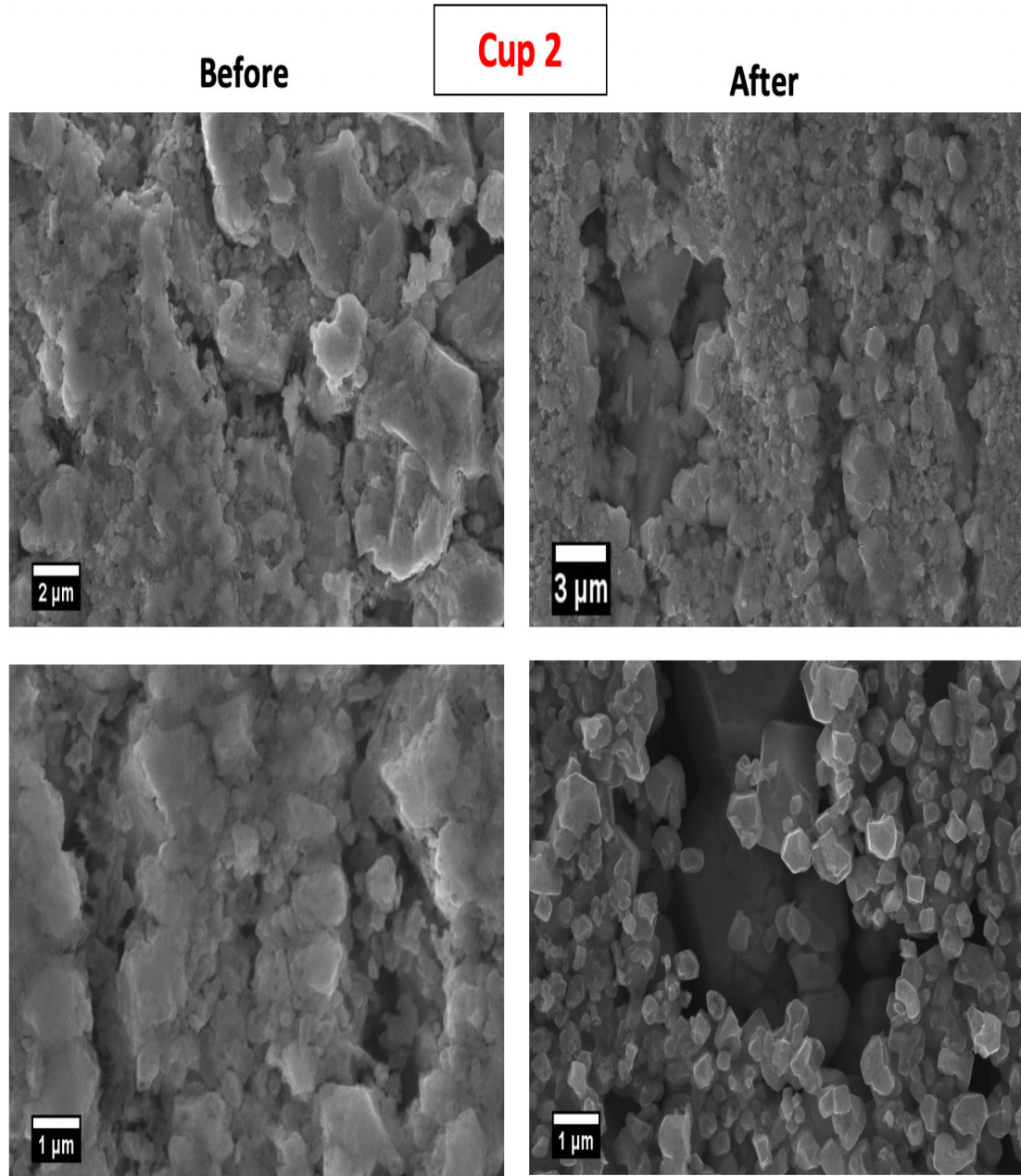


Figure 3.30: FESEM image of sample Cup2 before and after 1 hour of treatment.

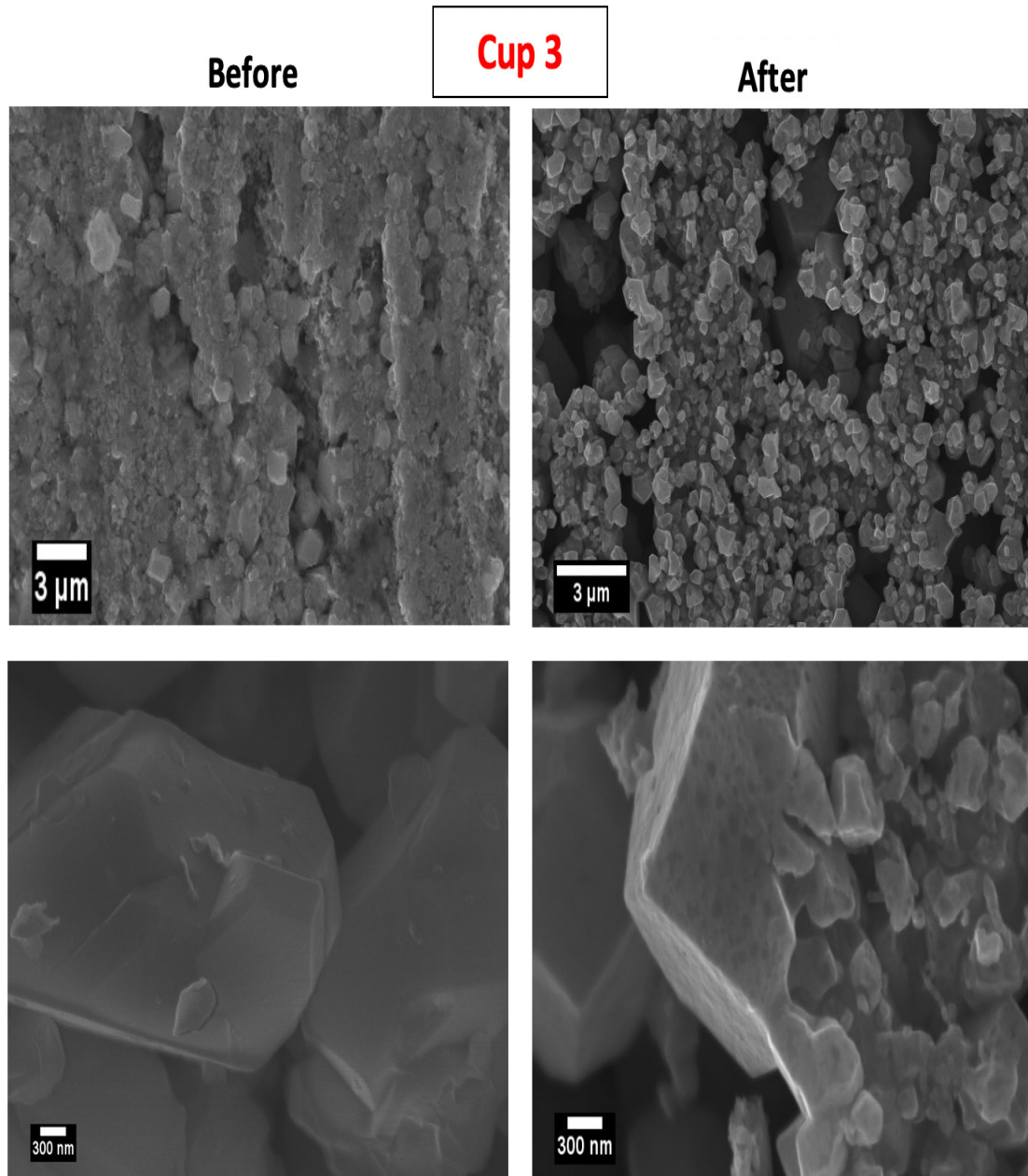


Figure 3.31: FESEM image of sample Cup3 before and after 2 hours of treatment.

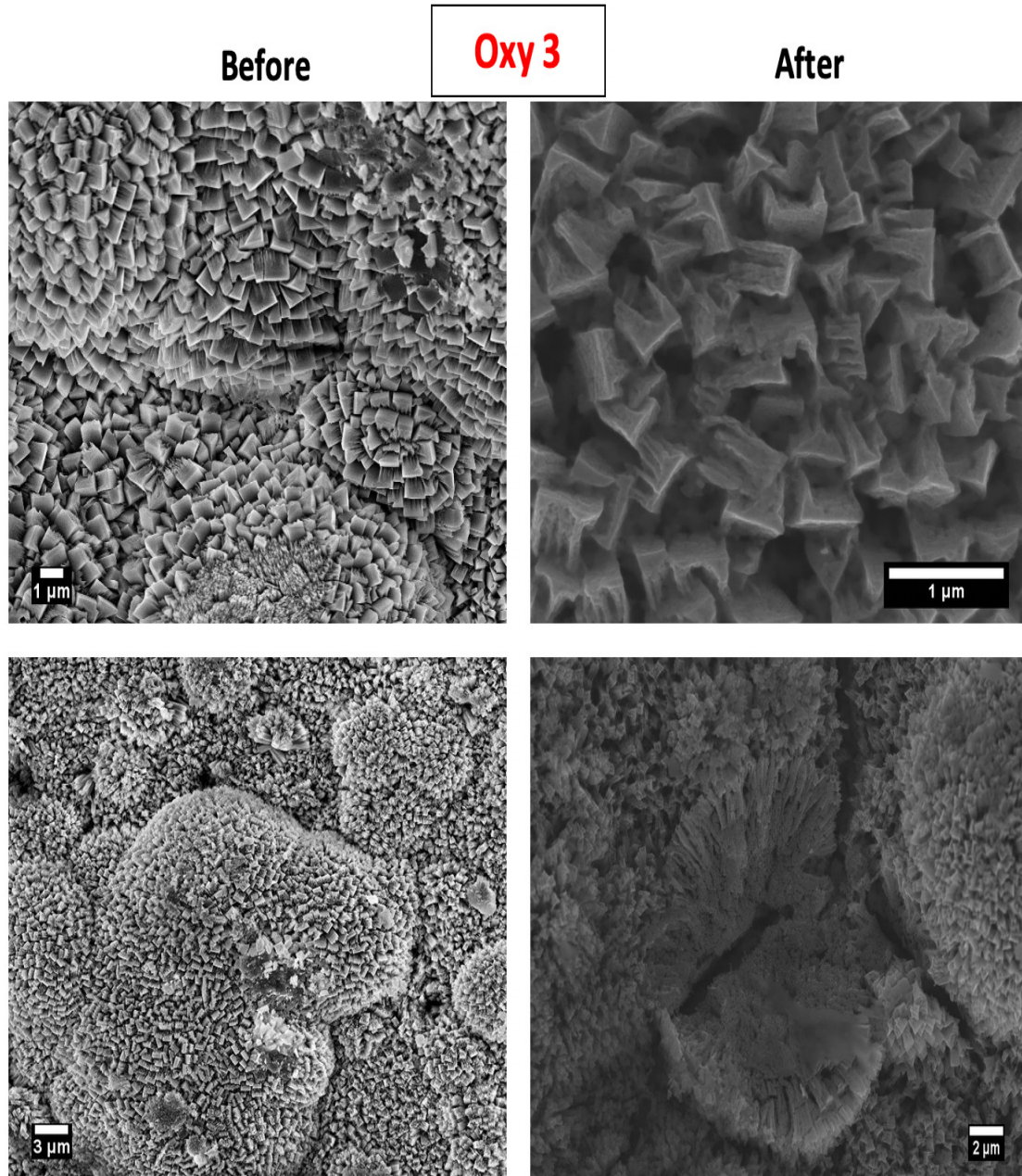


Figure 3.32: FESEM image of sample Oxy3 before and after 30 minutes of treatment.

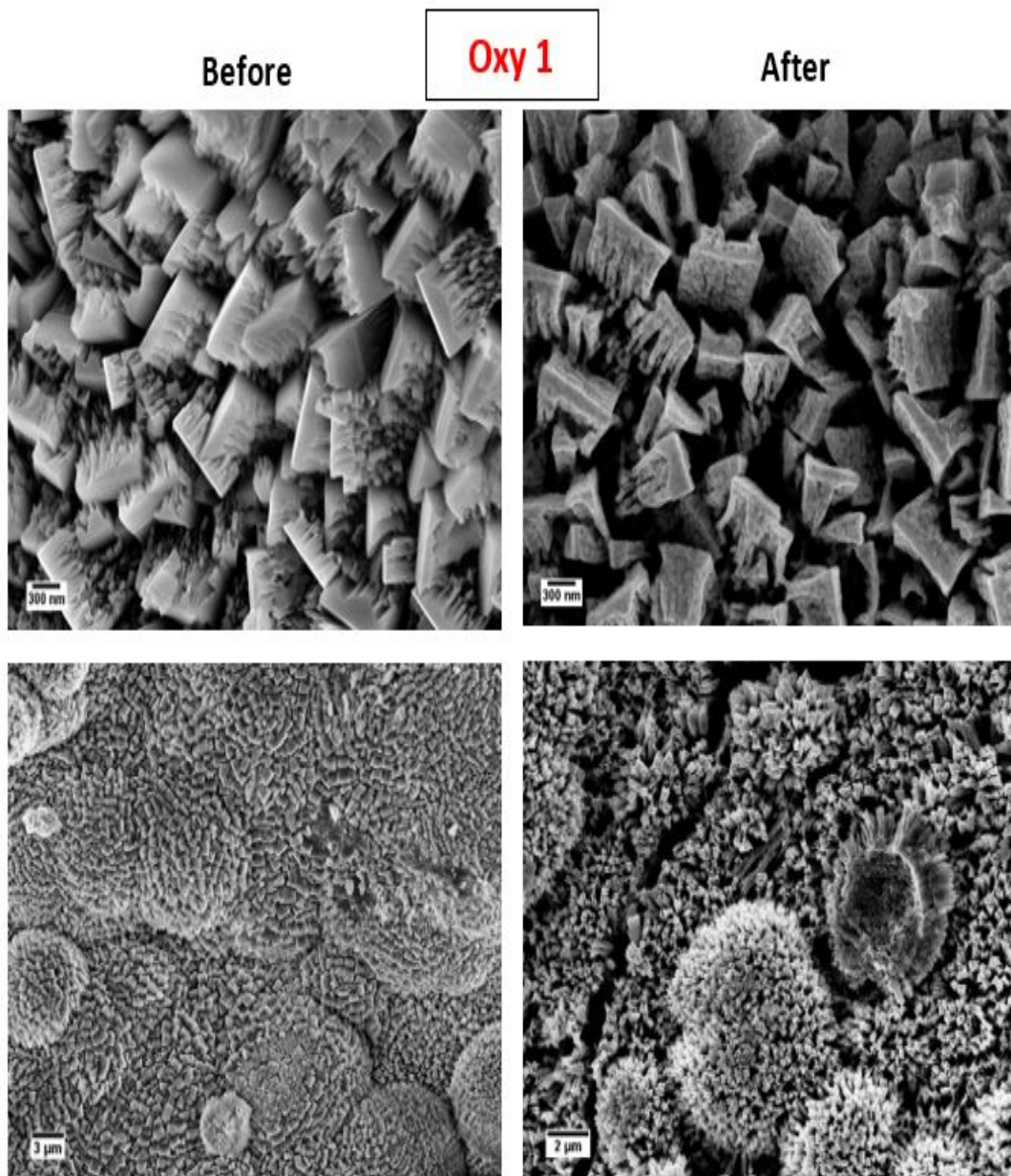


Figure 3.33: FESEM image of sample Oxy1 before and after 3 hours of treatment.

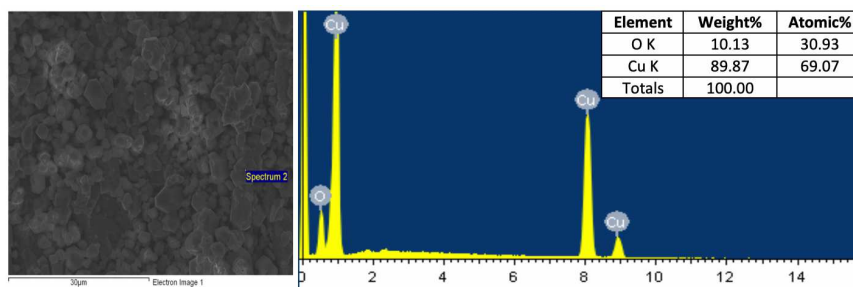


Figure 3.36: FESEM image and EDS analysis of sample Cup3 before treatment.

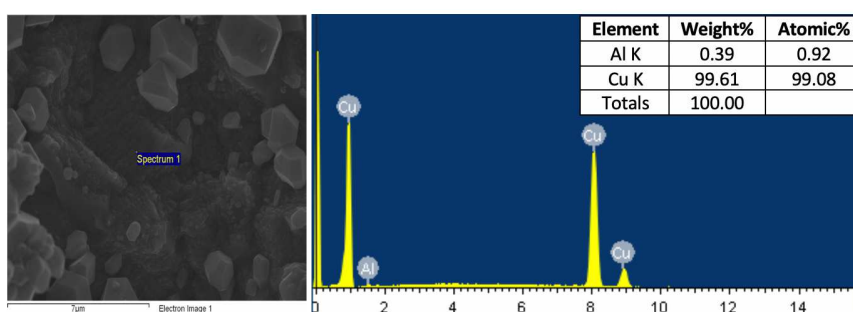


Figure 3.37: FESEM image and EDS analysis of sample Cup3, after 2 hours of treatment.

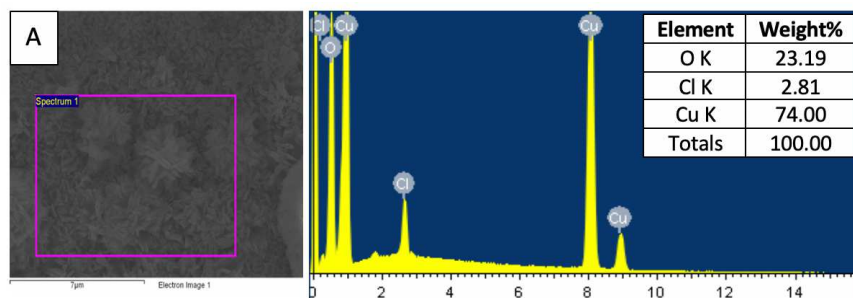


Figure 3.38: FESEM image and EDS analysis of sample Oxy1 (A) before treatment.

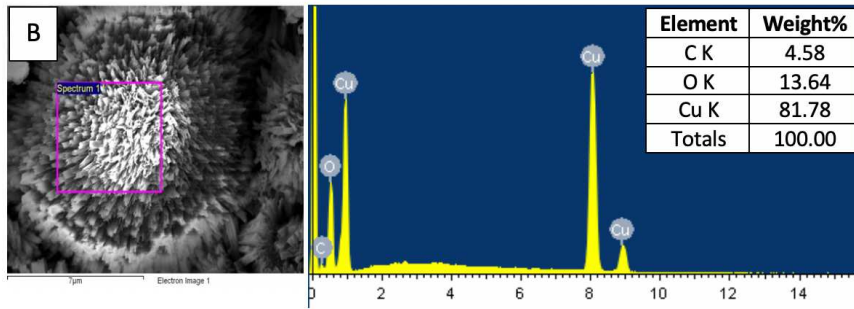


Figure 3.39: FESEM image and EDS analysis of sample Oxy1 (B) before treatment.

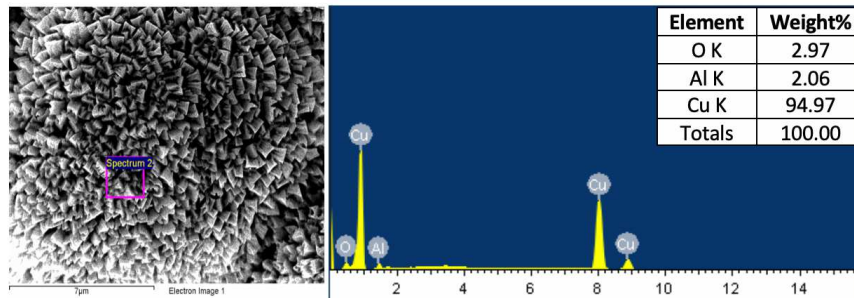


Figure 3.40: FESEM image and EDS analysis of sample Oxy1, after 3 hours of treatment.

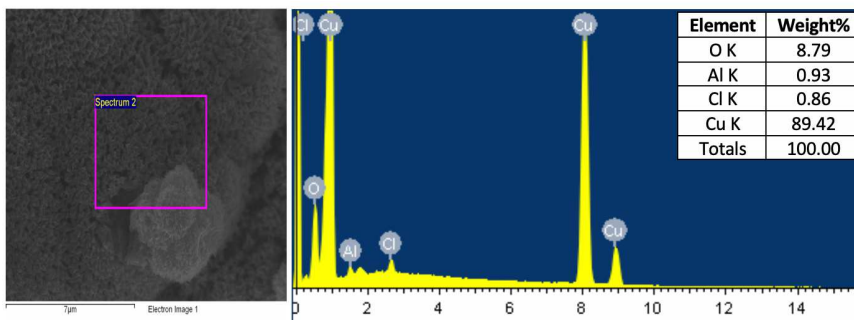


Figure 3.41: FESEM image and EDS analysis of sample Oxy3 before treatment.

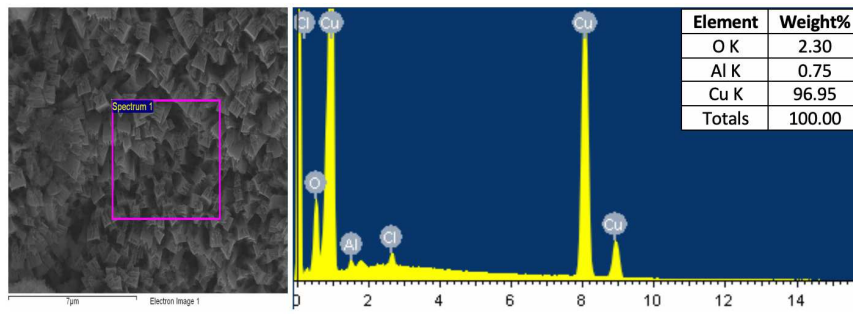


Figure 3.42: FESEM image and EDS analysis of sample Oxy3, after 30 minutes of treatment.

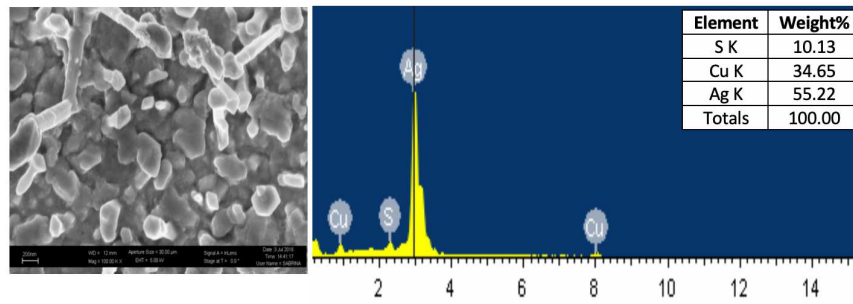


Figure 3.43: FESEM image and EDS analysis of sample Ag2 before treatment.

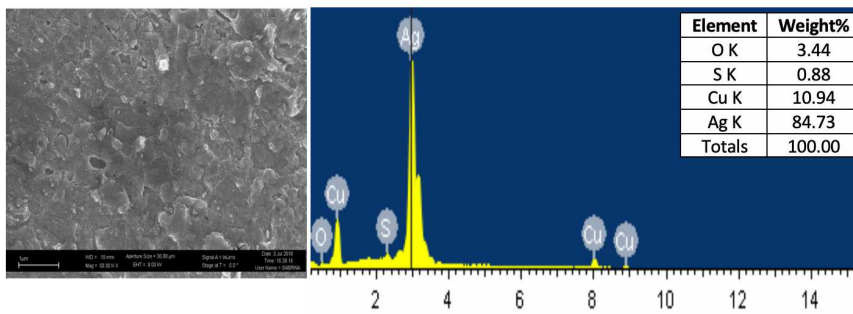


Figure 3.44: FESEM image and EDS analysis of sample Ag2, after 30 min of treatment.

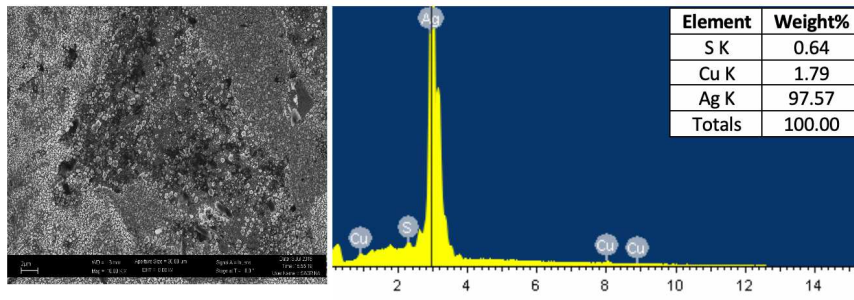


Figure 3.45: FESEM image and EDS analysis of sample Ag3 before treatment.

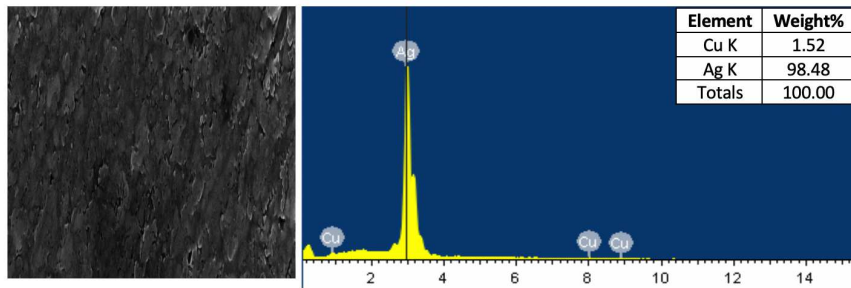


Figure 3.46: FESEM image and EDS analysis of sample Ag3, after 30 min of treatment.

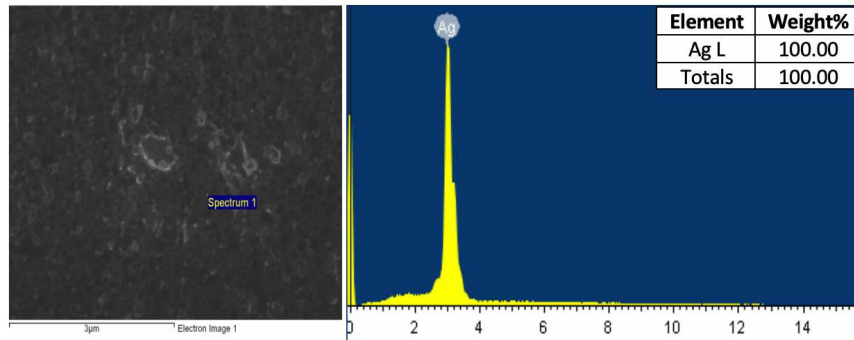


Figure 3.47: FESEM image and EDS analysis of sample Ag4, after 30 min of treatment.

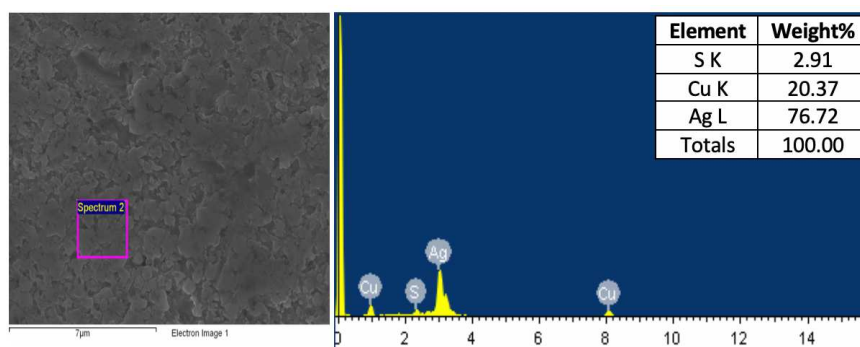


Figure 3.48: FESEM image and EDS analysis of sample Ag5, after 30 min of treatment.

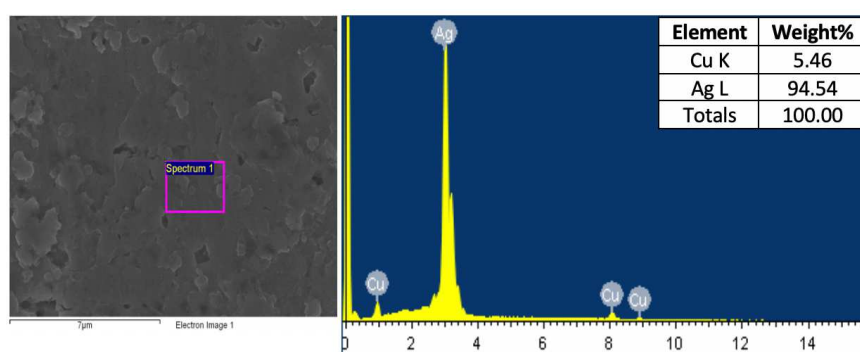


Figure 3.49: FESEM image and EDS analysis of sample Ag6, after 30 min of treatment.

3.2.3 XRD

The XRD analysis was performed to compare the corrosion products before and after plasma treatment. XRD is semi-quantitative analysis so we can monitor the reduction of the corrosion products after plasma treatment[64]. The result was sufficient for all the analysed samples Figure 3.50 shows the XRD patterns of sample Cup3 exposed to 30 min of plasma cleaning. Due to the comparison of the peaks intensity before and after cleaning, the cuprite decrease and copper increase may be observed. Moreover, The reduction of the cuprite more than 95% of removal in short time. In the case of cleaning of sample Oxy1 after 3 hours of treatment, the XRD spectrum confirmed the complete removal of the malachite and paratacamite and the increase of copper with some of the cuprite are still not completely removed after three hours. In order to have a complete removal of the cuprite, the cleaning time has to be increased figure 3.51. The reduction of cuprite was confirmed by the reaction of atomic hydrogen with oxygen in the corrosion layer as mentioned before and it can occur due to the following schema:

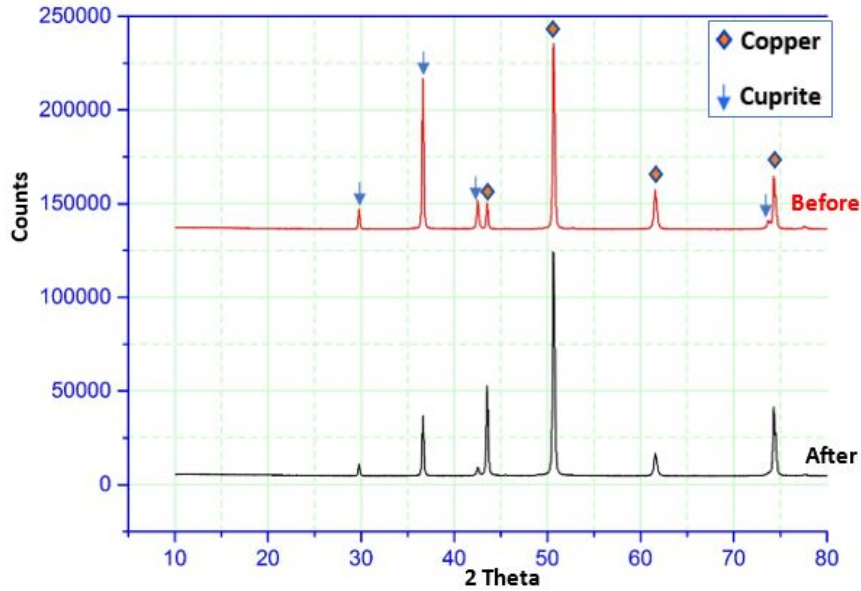
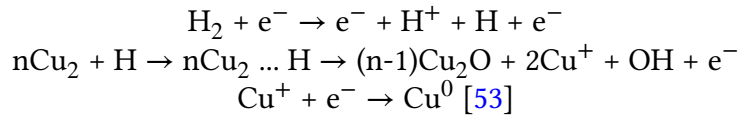


Figure 3.50: XRD spectra of sample Cup3, before and after 30 minutes treatment.

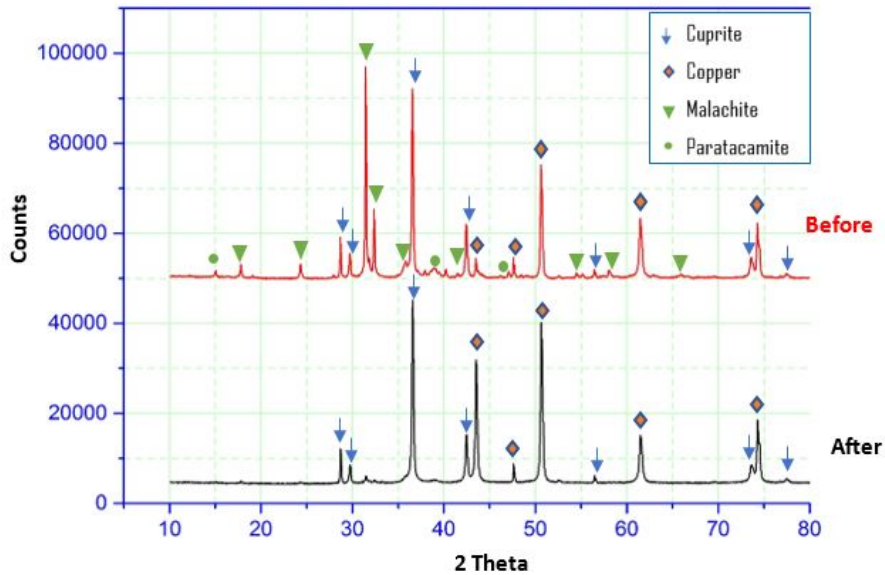
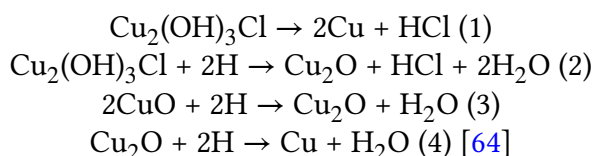


Figure 3.51: XRD spectra of sample OX1, before and after 3 hours of treatment.

The possible interactions which can occur indicate that, according to (Eq.1), hydrogen plasma treatment may thermally destabilize the basic copper chlorides with the consequent release and formation of cupric oxide of hydrochloric acid in the gaseous phase Which can be considered as an intermediate product before it is subsequently reduced to cuprite (Eq. 3) and also to metallic copper (Eq.4). It is possible to directly reduce the basic copper chlorides to cuprite (Eq. 2).



According to the XRD results, with the parameters of low-pressure H₂/Ar plasma used in this work, it is a safe method for cleaning copper and silver artefacts and it provides a total removal of chlorides at low temperature without any morphological changes of the samples[30].

3.3 Conclusions

Low-pressure plasma cleaning reveals to be a good treatment for culture heritage conservation with several advantages as low environmental impacts and low invasiveness [156]. Many parameters should be consider in the optimization of plasma cleaning treatments, such as input power, composition of the gas mixture, pressure and treatment time. The performed experiments on copper and silver based alloys allowed to optimize the plasma treatment parameters. The hydrogen/argon plasma has a good effectiveness for cleaning the metallic artefacts and depending on the treatment time, the Ar/H₂ discharge was able to significantly reduce the thickness of the corrosion products layer and remove the dangerous copper chlorides from the sample surface[122]. In the plasma a combined of the argon ions bombardment of the sample surface and the effect of the hydrogen species (atoms, ions, molecules in the fundamental and excited state) allow to remove the corrosion products and to reduce copper ions to metallic copper[61]. Eventually in the glow discharge Cl⁻ ions are removed as HCl[54, 157]. The etching rate is quite low, however the low input power (100W) and the gas mixture, H₂/Ar 50/50 allow to obtain a good abundance of hydrogen species in the plasma without any thermal effect on the metallic surface [60] On the copper samples the plasma treatment can be optimized in order to preserve the cuprite protective patina and remove the dangerous and reactive corrosion products without affecting the bulk structure. On the silver alloy samples, the tarnishing removal should be faster nd even if the plasma affects the brilliance of the metal, no modification of the alloy metallic features was observed. It is possible to conclude that plasma cleaning can be easily applied on metallic artefacts

and tailored treatments can be performed without irreversible changes of the surfaces. [45].

Chapter 4

Case Studies

This chapter deals with the characterization of some real coins excavated in Al-Fustat city in Egypt and stored in the museum of the Faculty of archaeology of the Sohag University, Sohag, Egypt. The coins were characterized using FESEM, EDS, XRD and optical microscope in order to understand the effect of the Egyptian soil and the production methods of some ancient coins and try to simulate the corrosion products in the artificial ageing of new samples. The second item is with the production of reference samples with nanostructured thin films to investigate their corrosion susceptibility in comparison to bulk copper. Final goal is to evaluate the feasibility of employing Cu nanostructured thin films as reference material to assess the atmosphere aggressiveness in museum indoor environments. Moreover, a new smart monitoring system based on a wireless network composed of small sensors, designed to satisfy the requirements for their employment in the Cultural Heritage field was tested in the same museum, as shown in the following Chapter.

4.1 The Corrosion Mechanism of ancient Coins

This study deals with the characterization of some ancient coins from the excavations in AL-Fustat city in Egypt, with respect to the effect of the Egyptian soil and the manufacturing technique on their conservation conditions. The analytical techniques employed were Field Emission Scanning Electron Microscope (FESEM) coupled with EDS, Optical Microscopy and X-Ray diffraction (XRD). The characterization methods allow to state that all these coins are made of bronze with different amounts of tin in addition to other elements as soil compounds. The production method was hammering into moulds. Moreover, the corrosion products were copper oxides and copper chloride due to long-term burial period in the soil rich in chloride ions. Through the time there are good indications about ancient ages life by the ancient coins, although the production technology and other information about these periods[71].

The investigation was performed on three coins from the excavation site of Al-Fustat, the first capital city of Egypt in the Islamic civilization. The city was built by Amr Ibn Al-As in 641 AD on the east bank of the Nile and replaced ancient Memphis to the west [72, 73].

The coins are an important item for any civilization economy and give a background about the art and metallurgical skills. Copper and bronze were widely used in coins production [74]. Coins are affected at different extents by the corrosion processes in dependence on different parameters such as the nature of the metal, soil composition, coin microstructure, soil pH value, etc. The understanding of the corrosion mechanism is important to find tailored strategies for the conservation process [71, 74, 75, 76, 77, 16]. Some results were presented in the conference of EuroCorr 2017.

The soil typology may affect in a different way the degradation phenomena of the metallic alloys. Some of those effects depend on physical, chemical, biological factors of the environment. Moreover, the composition of the soil and the organic and inorganic components increase the corrosion process, moreover coins can be effected by mechanical actions of natural forces, plant roots, the organic substances which create biological activities. Pure copper shows lower corrosion resistance with respect to its alloy, as bronze because of the tin content in the alloy and the formation of the protective oxide layer on the surface [78]. Oxygen interacts with copper and bronze coins. Copper slowly oxidizes to form cuprite (Cu_2O), which changes to tenorite (CuO) when the oxygen amount increases. According to the Pourbiax diagram 4.1, tenorite can be found on the cuprite surface. It is not kinetically favoured and usually, it can be found in burned burial environment. The presence of chloride ions in the environment leads to the growth of nantokite ($CuCl$), atacamite, paratacamite ($Cu_2(OH)_3Cl$), which induces a cyclic corrosion phenomenon, the bronze disease which attack and destroy the metal morphology and microstructure. In addition other corrosion products as copper carbonates [azurite ($Cu_3(CO_3)_2(OH)_2$ and malachite ($CuCO_3Cu(OH)_2$) may form due to the soil environment and components. When the soil has other ions such as carbonates, the copper-based alloys interact with these ions to form copper carbonates as a corrosion product [79, 80, 81, 82] [83, 84] [85, 86, 87].

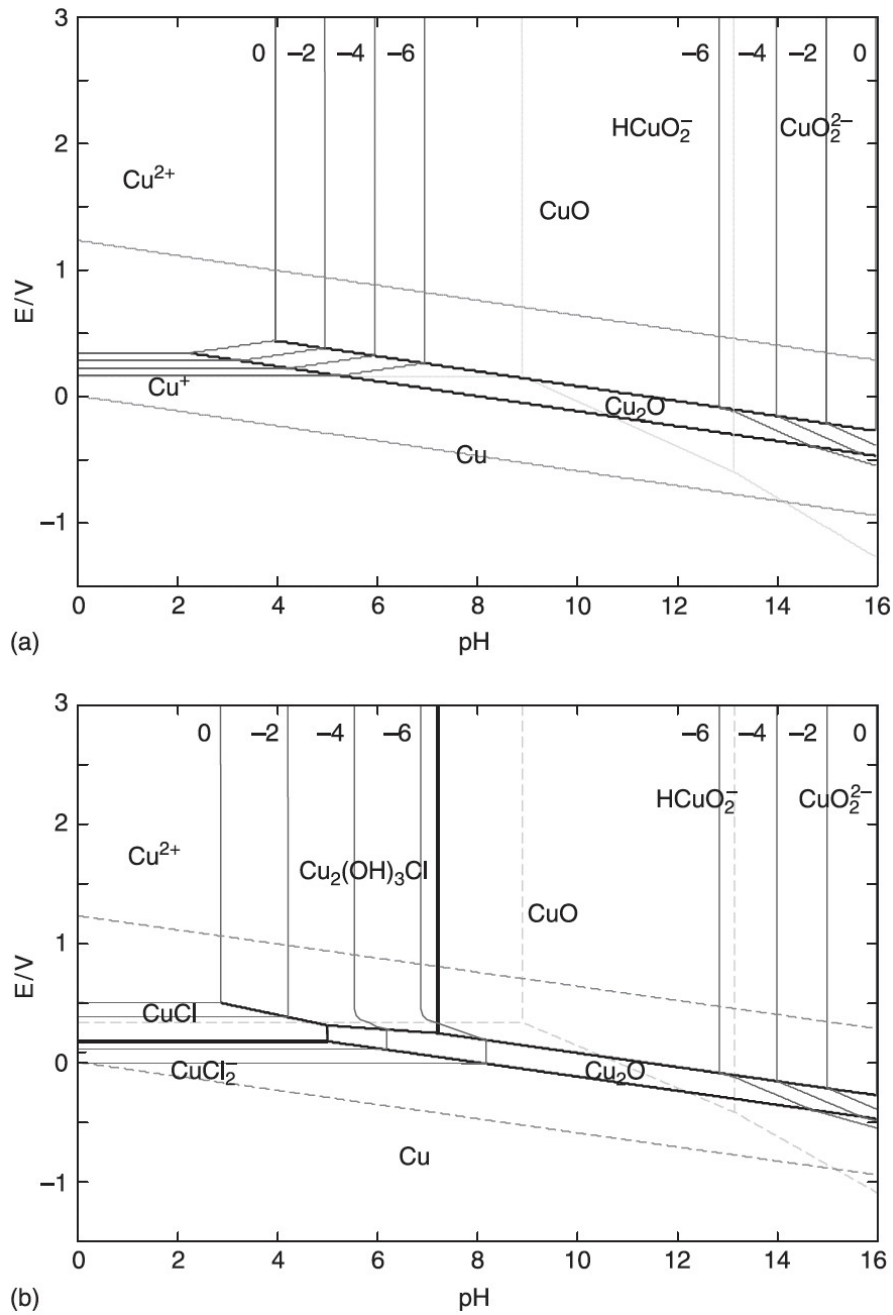


Figure 4.1: (a) Copper–water and (b) copper–chloride–water Pourbaix diagrams. The diagrams show the different products that can exist when copper is in contact with water in the absence and presence of chloride. The regions where solid products exist are marked with bold and dissolved products are marked in normal font (reprinted with permission from author)[88]

4.1.1 Materials and Methods

The macroscopic and microscopic investigations were carried out to identify the corrosion products of the coins. The coins morphology, microstructure and composition were investigated by different methods as FESEM with EDS, Metallographic microscope, and XRD.

FESEM and EDS For the micro-analytical investigation of the coins, samples were characterised by field emission scanning electron microscope (FESEM, Zeiss, supra 40) so the micro-chemical studied from (10- 200 μ m). Moreover, the non-destructive analysis of Energy Dispersive X-ray Spectrometry (Philips) which attached with the microscope that used for coins composition.

XRD X-Ray diffraction (μ XRD, Rigaku D/max-Rapid instrument) was used to study the corrosion products of the coins. The condition was 1 Bragg Brenton spectrum, 10°-80° angle(theta-2 theta), step 0.2-1 shave spectrum, detector moving from 10°-80°, tube at 4°degrees (omega-2-theta). Mask: 10 on the tube side 1.5-2.

Metallographic microscope The metallographic microscope was Leica DMI 5000M. The coins were polished with paper from 320- 2000 and then etched in ferric chloride solution, for the study of the microstructure of the coins. The scale of the photos was 10 μ m-100 μ m

4.1.2 Results and Discussion

The coins images were obtained with the high-resolution digital camera (4000 \times 3000 pixels, Panasonic Lumix G2) see figures 4.2, 4.3, 4.4. This camera was modified to capture coins surface at high resolution in order to identify the coins morphology. The coins size ranges between 1.35 cm to 2 cm and the weight ranges from 2.03g to 3.34g. The variation of surface colours is due to different types of the corrosion products of the coins. The images show the real size of the coins affected by the degradation processes.

FESEM and EDS results FESEM images in scale 100 μ m with EDS maps for the elements of the inner and outer layer of coin C1 ??, ?? show the presence of copper as a major element of the alloy, tin as a minor component of the bronze because in Islamic civilization it was normal to use a tin amount between 9 - 10 wt%. As a matter of facts, depending on the tin amount the melting point decrease for example, when they add 10 wt% of tin the melting point is 1005°C also when the tin increase to 15 wt% the melting point decrease to 960°C so the amount of the tin affects on the melting point and helps the workers through the forming and annealing process[89, 90]. Moreover, there are other elements like oxygen as metal oxides, and some traces of elements as carbon, iron, chlorine, calcium, magnesium and aluminum deriving from soil contamination.



Figure 4.2: High resolution image of Coin C1



Figure 4.3: High resolution image of Coin C2

In addition, to the high amount of iron which perhaps the worker added to the alloy because of the lower cost or due to an insufficient purification of the alloy. Another possibility is that this coin was in contact with the soil with iron artefacts[91].

The FESEM images of the samples surface indicated that all of them have almost the same corrosion products. Fig. 3.5, 3.6, 3.7 shows the corrosion layers of the coin C1, identified with XRD as cuprite, tenorite, atacamite and paratacamite. It can be seen the sponge shape of the corrosion layer. Moreover, Fig. 3.8 and 3.9 show for coin C2 that



Figure 4.4: High resolution image of Coin C3

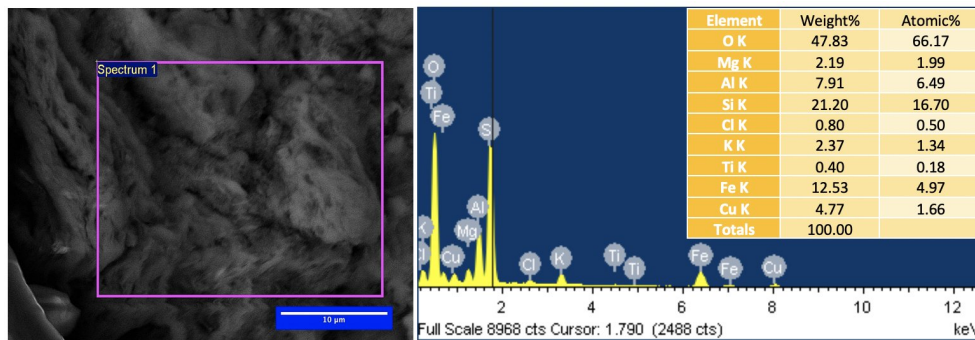


Figure 4.5: FESEM and EDS analysis of the outer layer of Coin C1

presence of copper and chlorides, the corrosion products of the coin identified by XRD are cuprite, atacamite and paratacamite around the core of the coin. Fig. 3.10, 3.11 show for coin C3 copper and chloride, and by XRD it was identified a thick layer of atacamite and cuprite. Furthermore, the image shows that there is no metal core because the coin completely corroded and mineralized due to the effects of cyclic corrosion.

Metallographic results The microstructure of the coins 4.12 shows some details about the coins as the recrystallisation, annealing and cold-working formation process. Usually, in ancient Egypt, the coins were produced by hammering in the mould, for preparing the two printed faces moulds with the ornamentation in both sides and then put the metal between the two pieces then start hammering. After etching coins with ferric

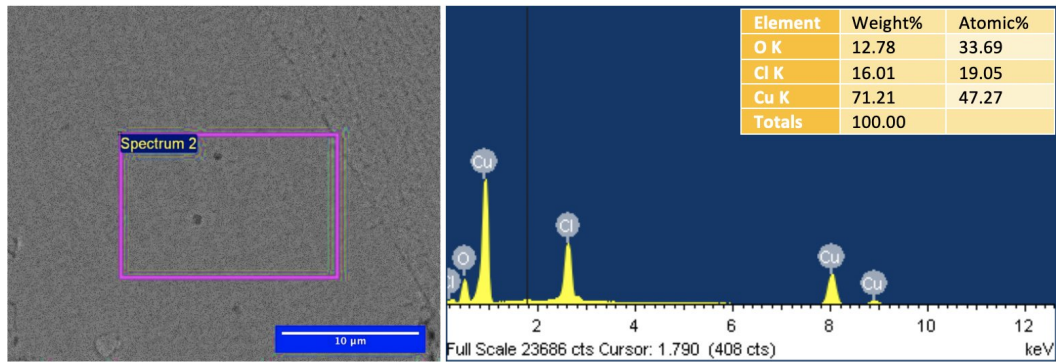


Figure 4.6: FESEM and EDS analysis of the inner layer of Coin C1

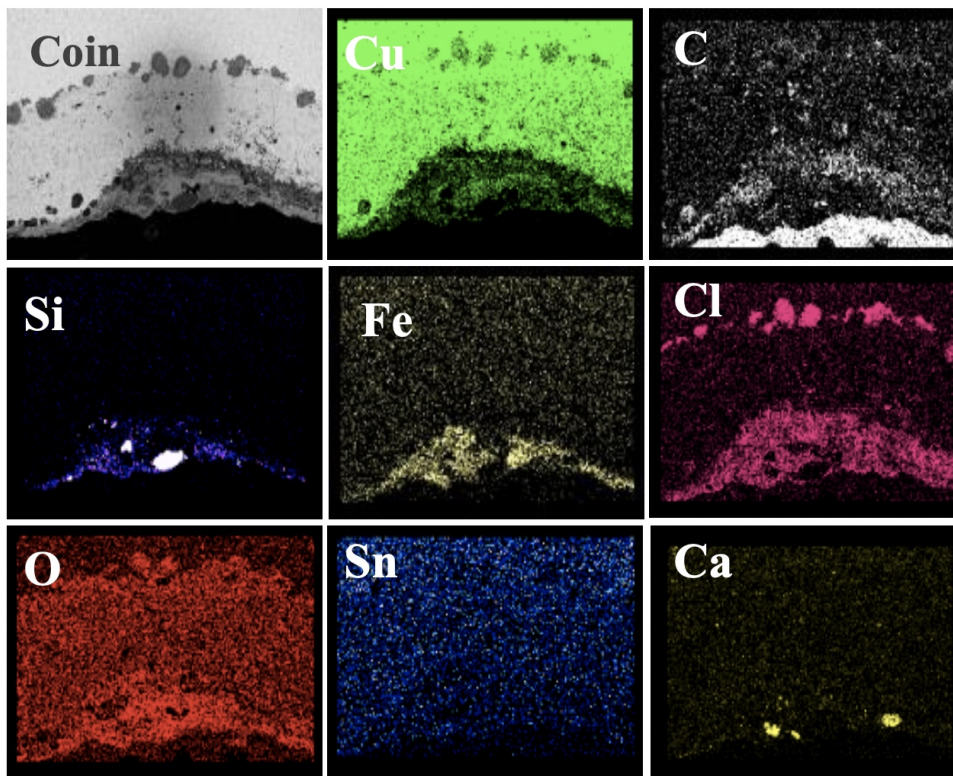


Figure 4.7: EDS map of Coin C1

chloride the surfaces were examined by means of the metallographic microscope figure ?? Fig. 3.12 (A) is the metallography of coin C1 and shows the twinning grains in some areas and α phase in gold (bright) colour due to the annealing after cold-working which

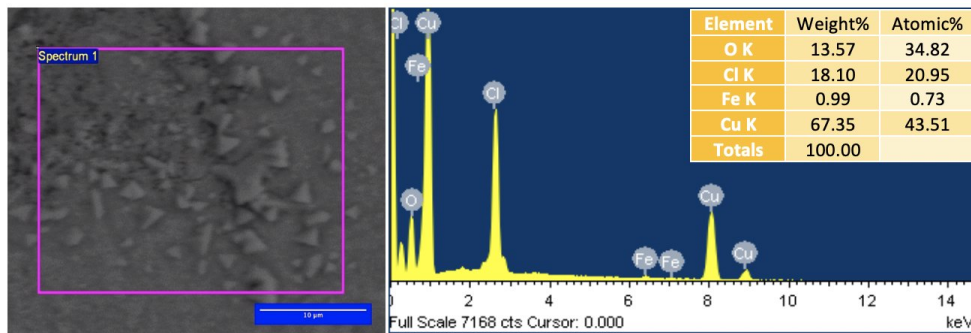


Figure 4.8: FESEM and EDS analysis of the inner layer of Coin C2

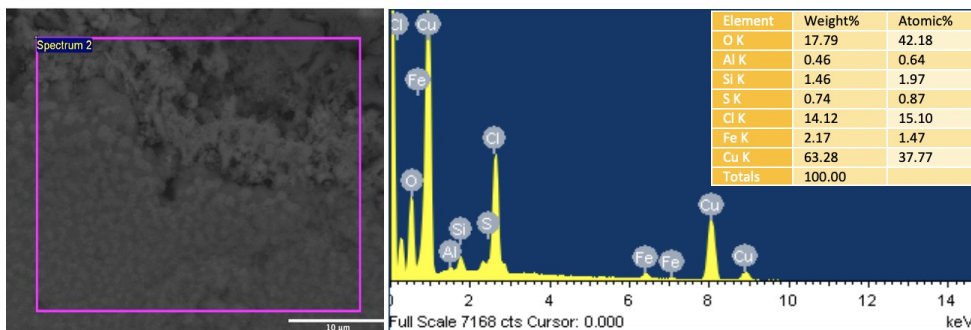


Figure 4.9: FESEM and EDS analysis of the outer layer of Coin C2

destroys dendrites, so the metal recrystallized and twinned grains with straight lines appears and the grain size is smaller. Furthermore, the primary α -Cu phase and $(\alpha + Cu_2O)$ eutectic appears. Moreover, the Cu-O binary phase diagram evidenced that this eutectic reaction occurs around 1066°C due to the oxygen content during the melting process. The cuprite in the metal core forms typically in normal oxidizing condition in the melting of copper. The twinning in the phase appears related to the recrystallization of the heat treatment. Figure ?? 3.12 (B) is the metallography of coin C2, it illustrates cold-working annealed with flattened and long grains due to the hammering process. Moreover, the shape is altered by slip and dislocation in the metal microstructure. Corrosion products in grey and dark green colour are present. The selective corrosion appears as a result of the segregation through the alloy working.

Figure?? 3.12(C) is the metallography of coin C3 and shows copper. The metallographic images show that the three coins have been made by hammering. Related to the grain size is the tin amount because if the alloy has less than 17% of the tin it will be easy to form with cold-working and annealing. According to the cold-working amount on the alloy, each metal will be able to recrystallize successively at lower temperature [92,

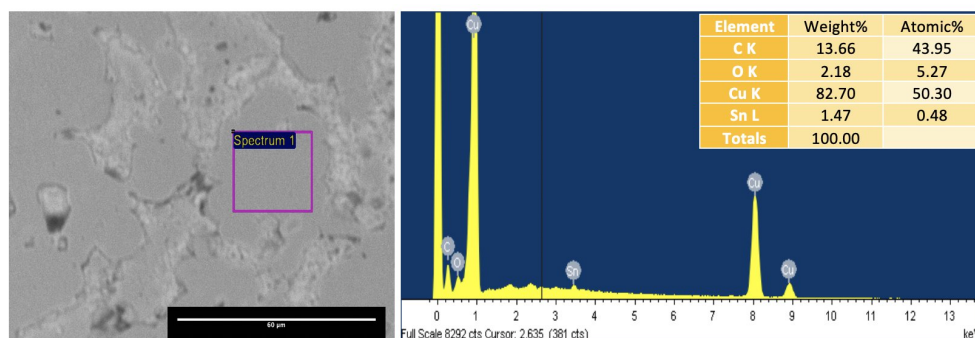


Figure 4.10: FESEM and EDS analysis of the inner layer of Coin C3

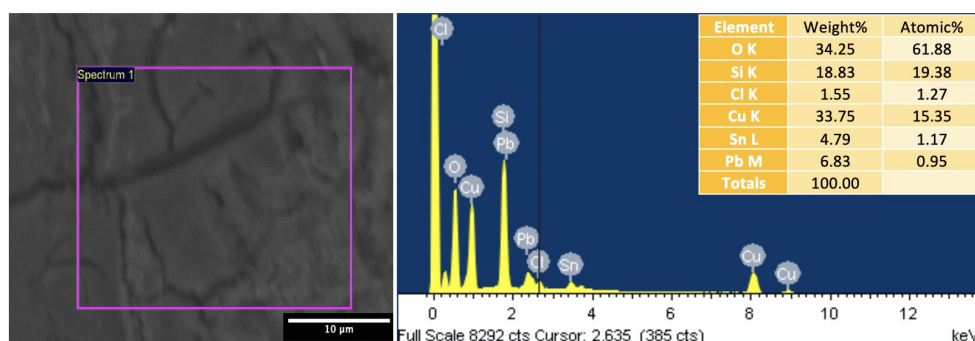


Figure 4.11: FESEM and EDS analysis of the outer layer of Coin C3

93]

XRD results X-Ray diffraction analysis (XRD) shows that all the coins are bronze. The corrosion products are related to the burial soil. The copper chlorides, atacamite and paratacamite, derive from the high amount of chlorine ions in the Egyptian soil. Moreover, the copper oxides which result from the interaction between copper and oxygen, when the soil has a high concentration of the soluble oxygen and reach of (Cl^-) , the oxygen starts to interact with the copper and bronze alloy to form a thin layer of cuprite (Cu_2O) in red color that transforms to a dark brown or black layer, tenorite (CuO), with time. Additionally, the (Cl^-) ions interact to form atacamite and paratacamite [91]. Figure 4.14 XRD pattern of coin C1 and the major compound is basic copper chloride [atacamite] $Cu_2(OH)_3Cl$; copper chloride [paratacamite] $Cu_2(OH)_3Cl$, and some traces of cuprous oxide [cuprite Cu_2O] are also present. Figure 4.15 the pattern of coin C2 shows that the major compound is cuprous oxide [cuprite Cu_2O], then the presence of copper chloride [atacamite] $Cu_2(OH)_3Cl$, and small amounts of cupric oxide [tenorite CuO], and copper chloride [paratacamite] $Cu_2(OH)_3Cl$, are detected. Figure 4.16 XRD pattern

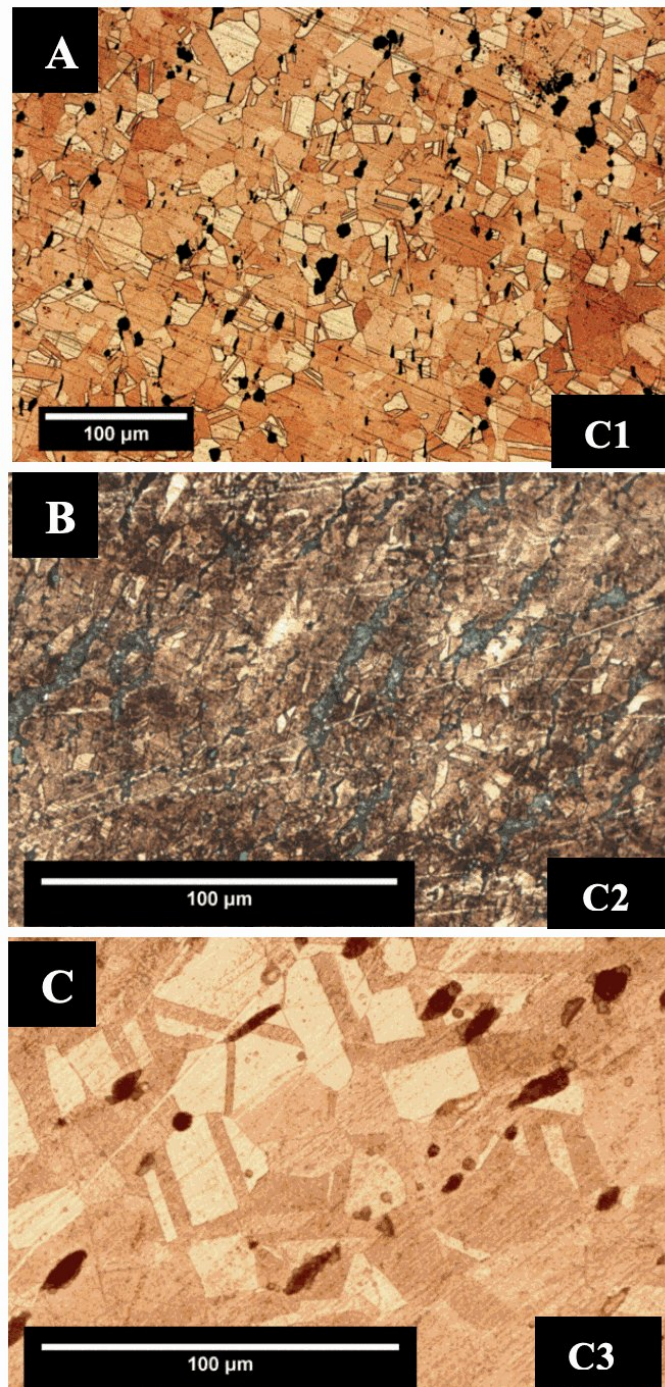


Figure 4.12: Metallographic microscope images for the microstructure of the coins

of coin C3 and it shows that the major compound is basic copper chloride [atacamite] $Cu_2(OH)_3Cl$; copper chloride [paratacamite] $Cu_2(OH)_3Cl$ and cuprous oxide [cuprite]

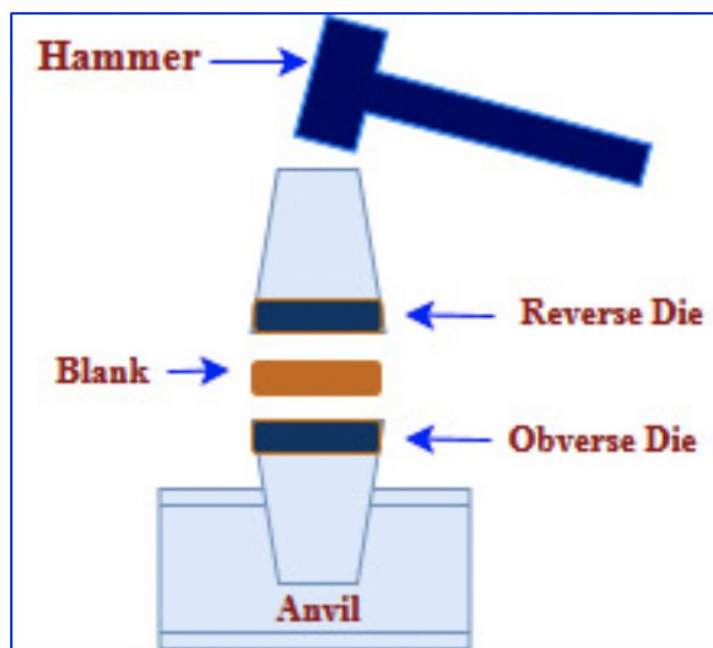


Figure 4.13: schematic show the coin production in ancient ages

Cu_2O] are also present.

Table 4.1: XRD results of the coins corrosion products

Compounds	Coin C1	Coin C2	Coin C3
Cuprite 00-001-1142	Minor	Major	Trace
Tenorite 00-048-1548	0	Trace	0
Atacamite 00-023-0948	Major	Minor	Major
Paratacamite 00-023-0947	Major	Trace	Minor

All the coins show the same corrosion products because the copper oxides (cuprite) are the first patina formed on the surface of the coins due to the interaction between coins and dissolved oxygen in the soil. Through the increase of the oxygen ions in the

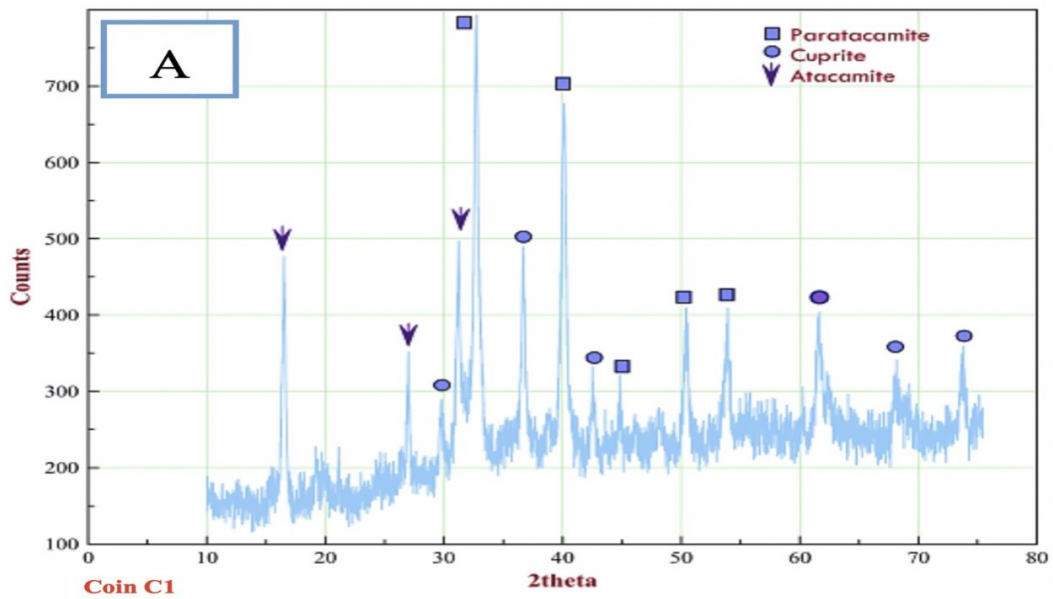


Figure 4.14: XRD pattern of coin C1

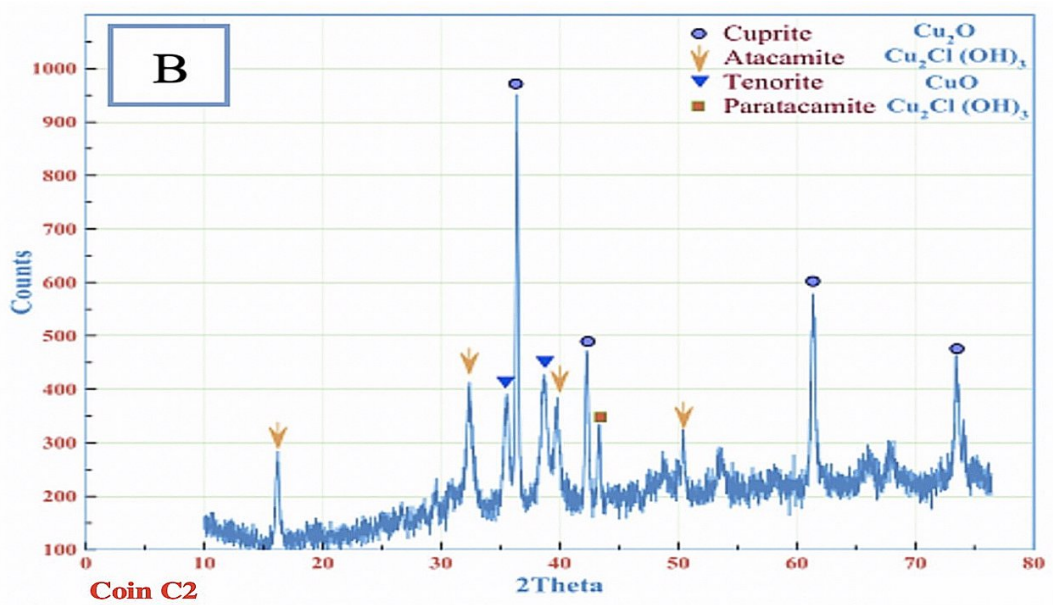


Figure 4.15: XRD pattern of coin C2

soil, cuprite transforms to tenorite. Moreover, the cuprite has a high electrical conductivity and allow the copper ions to migrate through the cuprite layer so the copper ions dissolve in soil water. Then the copper ions interact with chloride to form botallackite

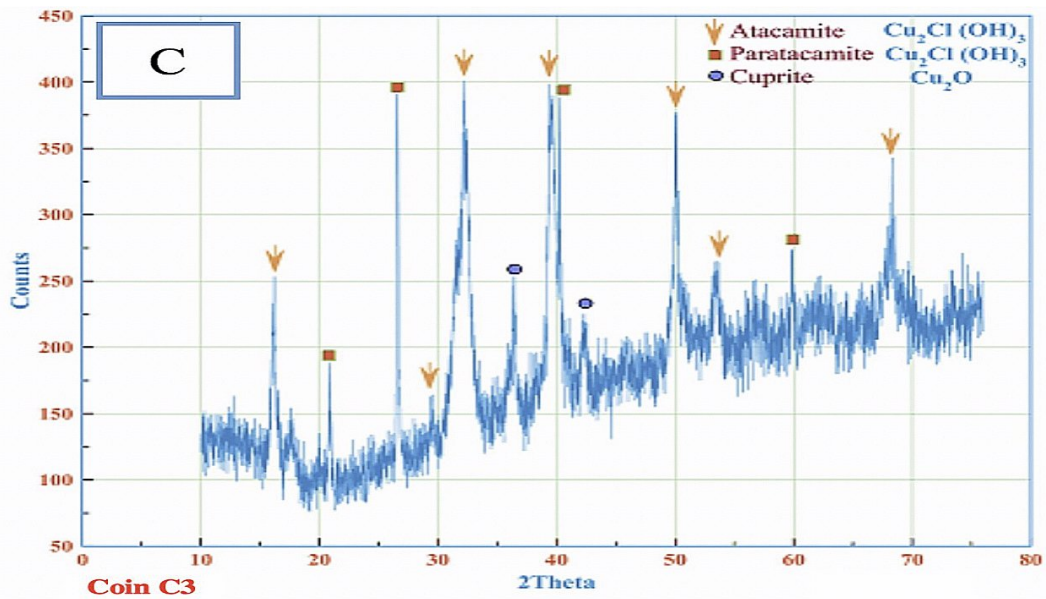


Figure 4.16: XRD pattern of coin C3

($\text{Cu}_2(\text{OH})_3\text{Cl}$) which transforms to atacamite and paratacamite[94].

4.1.3 Conclusions

The microstructural investigations evidenced that the three coins have been produced by hammering in mould as confirmed by grain size and shape 4.13.

The investigated coins suffered from different types of deterioration which corroded and destroyed them. Moreover, the aggressivity of the Egyptian soil, rich in sodium chloride, interacted with the coins to form copper (II) chloride hydroxide [atacamite and paratacamite] with formula $\text{Cu}_2(\text{OH})_3\text{Cl}$.

These investigations allowed to evaluate the coins degree of conservation and to define the proper strategies for restoration and conservation of these ancient artefacts. The workers add little amount of tin for the coin alloy to have a good alloy for production through the annealing and hammering process. In addition to the grains elongation and flatted grains, it is not very flattened because the coins not hammered a lot and it doesn't need more hammering power to print the shape on the coin face. Another possibility the workers used impure copper for the alloy so that there are some other elements in the chemical analysis of the coin. The recrystallization temperature effects by the impurities and alloying elements.

Chapter 5

Assessment of atmospheric corrosion effects

One of the main problems for the artefacts inside the museums is the micro-climate parameters and aggressiveness of the atmosphere that could seriously affects the conservation state of the artefacts, in museum rooms and showcases. The evaluation of the atmospheric corrosion effects on the metallic artefacts inside the museums was performed by using a smart monitoring system and reference samples, in particular copper samples coated with a nanostructured thin films. The employment of nanomaterials means the use the materials at very small scale (atom by atom) whose sensitivity to atmopspheric corrosion is very high[95]. The environmental monitoring, of one year, was performed as a case study in the Museum of the Faculty of Archaeology of the Sohag University, Egypt. Some results of this work were presented in the conference of MetroArchaeo 2018.

5.1 The environmental monitoring campaign in the Museum of the Faculty of Archaeology of the Sohag University (Egypt)

The preventive conservation of materials in museums is very important to keep the artefacts in safe displaying and storage conditions[96]. There are four parameters that could affect the interior climate of the museums [97]:

1. Temperature.
2. Relative Humidity.
3. Light.
4. Air pollutants.

Otherwise, to control the museum microclimate there are three main primary and linked steps[96]:

1. Determine the effects of the environment on materials and objects.
2. Set specifications based on the results of Step 1, taking into consideration the type of collection, the building and the local climate and economics.
3. Maintain and monitor the environment based on the results of Step 2.

The aim of the study based on two procedure:

1. Evaluation of the feasibility of employing Cu nanostructured thin films as reference material to assess the atmosphere aggressiveness in museum indoor environments
2. Employment of a smart monitoring system and correlation of the environmental monitoring data of the museum temperature and relative humidity with the exposed nanostructured specimens.

But two important questions should be considered before the work.

- Why it is better to use a reference material not sensors for measure the museum pollutants?
- Why it is better to use copper nanostructured thin films not use bulk copper?

The answer are: for the first question it is better to use reference material not sensors because the cost of the sensors is very high especially for high quality sensors. In this case the study needs many types of sensors for collect all the pollutants in the museum microclimate. Moreover, it is better to use Cu nanostructured thin film samples because of the high sensitivity of this film due to the atmospheric corrosion and environmental conditions.

Sohag is a city in the south of Egypt. It is located at 26°33'N, 31°41'E, 69 m (226 ft) figure ?? . Sohag has a subtropical desert / low-latitude arid hot climate (Köppen-Geiger classification: BWh). According to the Holdridge life zones system of bioclimatic classification Sohag is situated in or near the subtropical desert biome. The average annual relative humidity is 43.7% and average monthly relative humidity ranges from 30% in May to 57% in January. The temperature is hot in summer specially August (40- 43°C) and cold in winter (5-10°C)[98, 99]. For this reason it is important to assess the climatic changes especially for this museum as the second museum in Sohag city after the national museum of Sohag governorate. The museum collection was a private collection of Dr Henry Amin Awad. He is a dermatologist and he donated all these collections to the faculty in 1979 to open an educational museum for students. In 2005 the museum opened officially for the public. The museum is one single big room (8,50 × 13,25 meters) figure 5.2.

The total number of the showcases inside the museum are 26 made of wood and glass. 9 of them are wall showcases and the 17 are ground showcases see figures 5.3, 5.4. In addition some artefacts displayed in open air show without showcases such as some gravestones and one big Kilim 5.5. The sizes of the showcases classified in five categories. The size of the first category is 75 × 75 × 50 cm. The second category size is 75 × 75 × 65 cm. the third is 80 × 80 × 80 cm. The fourth is 150 × 80 × 25 cm and the last group is 145 × 80 × 30 cm. The museum contains 674 pieces from different eras, 15 pieces from ancient Egyptian period, 90 Greek-Roman pieces, 30 pieces from the Christian period and 539 pieces from the Islamic period. The artefacts of the museum made of different materials as metals and alloys (Silver, Copper, bronze and brass), pottery, stones, glass. further, some organic materials as textiles, paper, leather, wood and ethnographic materials.

The museum has some problems because it is located in the last floor of the building and there are only two air conditions in the Room. These air-conditions switched on only in the work time from 8.30 AM to 2 PM. The museum use the normal Thermo-hygrometer to measure the temperature and relative humidity. Moreover, they use silica gel to reduce the RH inside the showcase figure 5.6.



Figure 5.1: Sohag location at the map of Egypt

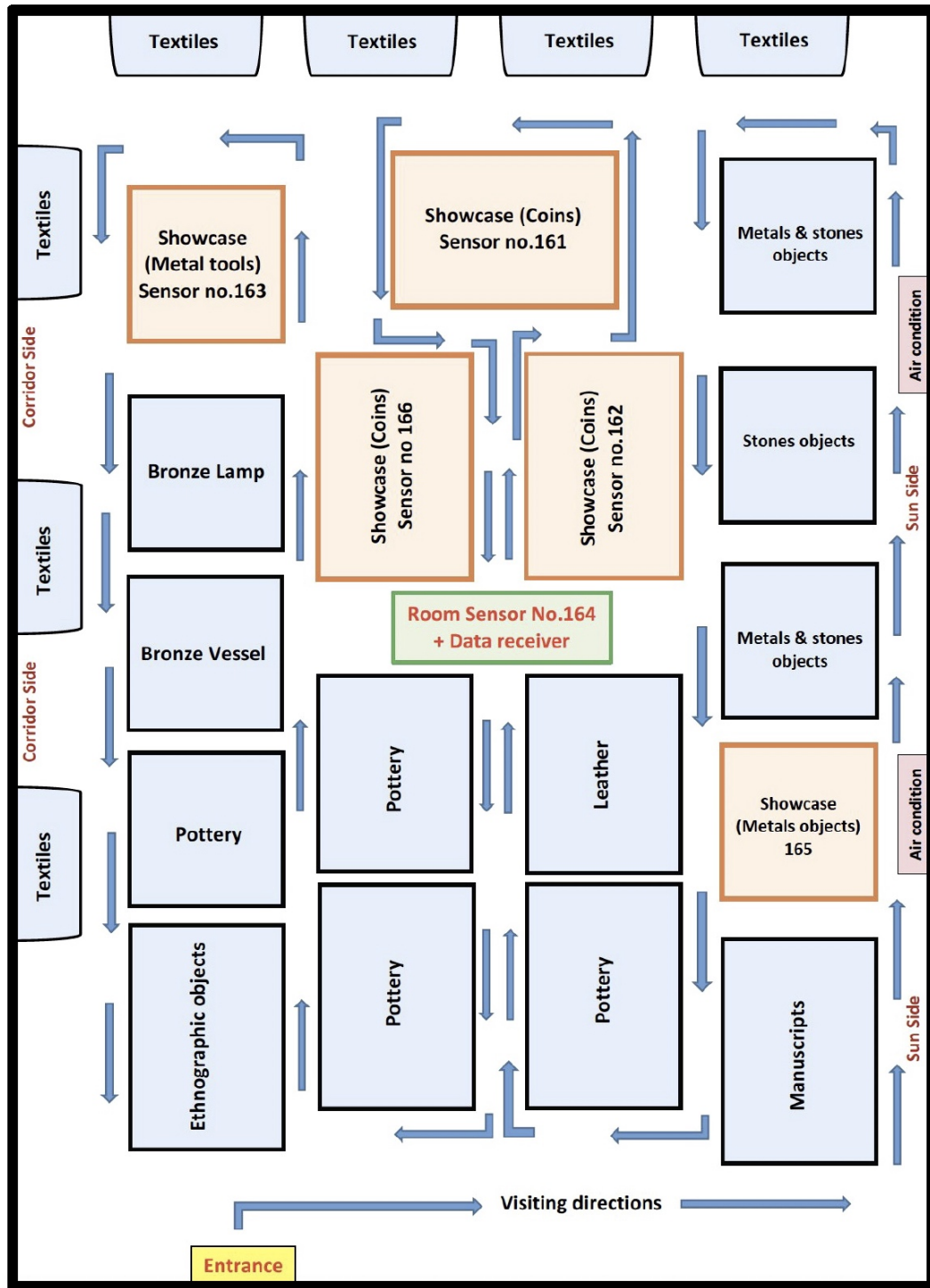


Figure 5.2: The museum structure



Figure 5.3: The Faculty museum



Figure 5.4: The Faculty museum



Figure 5.5: Some artefacts in the museum



Figure 5.6: Thermo-hygrometer to measure T and RH in the museum and silica gel for reduce the RH inside the showcases

5.1.1 Materials and Methods

For many years the scientists tried to develop new devices and strategies to control the museums environment. The best condition of the museum related to the different materials and the best temperature and RH degree to keep the artefacts in safe condition have to be defined for every museum. Many organisations and companies developed different platforms and technologies for monitoring system. [100, 101, 102, 103]. Metallic materials and organic materials are more sensitive to the microclimate condition and significantly affected due the the changes in the museum conditions. According to ISO 11844-3:2006 the indoor corrosivity toward metals and alloys can be assessed by measuring from one side, temperature (T) and relative humidity (RH), and from the other, airborne contaminants, such as gases and particles[104]. Hence in the ISO 11844-1:2006 indoor atmospheres are classified into 5 corrosivity categories 5.1 as follow[105]:

According to ISO 11844-1:2006, when the relative humidity increases the atmospheric also increase and the aggressivity increase depends on the type and the level of pollutants. The museum microclimate could contain different types of indoor and outdoor components such as SO_2 , NO_2 , O_3 , H_2S , Cl_2 , NH_3 , HCl , HNO_3 , Cl^- , NH_4^+ , organic acids, aldehydes and particles. On the other hand, each metal has a specific corrosion behaviour in indoor atmosphere such as silver an copper.

Table 5.1: Corrosivity categories of indoor atmospheres

Indoor corrosivity category	
IC 1	Very low indoor corrosivity
IC 2	Low indoor corrosivity
IC 3	Medium indoor corrosivity
IC 4	High indoor corrosivity
IC 5	Very high indoor corrosivity

Copper corrosion behaviour:

1. Sensitive to relative humidity.
2. Sensitive to a broad range of pollutants
3. Significant influence of H_2S , sulphur dioxide.
4. Little influence of NO_2 , Cl_2 and NH_3 .
5. Synergistic effect of SO_2 , NO_2 and O_3 .
6. The most severe contaminant is hydrogen sulfide, especially in combination with chlorine.
7. Corrosion rate shows a general decrease with time (particularly for the less corrosive sites).

Silver corrosion behaviour:

1. Corrodes indoors at approximately equivalent rates to outdoors, the reason for this similarity is supposed to be independence of silver corrosion rate on relative humidity.
2. The corrosion rate is governed by the reaction with H_2S , rather than by the acidity of the pollutants.
3. Corrosion rate is dependent on the reduced sulphur pollutant concentration.
4. Gaseous hydrogen peroxide, which is sometimes present, strongly accelerates corrosion.
5. Quite sensitive to molecular chlorine.
6. Insensitive to organic acids and has not been reported to be reactive towards most other common indoor organic molecules and radicals.

7. Corrosion rate decreases with time.

Further, The important characteristic of temperature and RH can be described as follow:

Temperature:

- The average of temperature (monthly, seasonal, annual).
- Minimum and maximum temperature (monthly, seasonal, annual).
- Character of temperature changes (fluent, abrupt, accidental).

The measurement period is preferably one year, or one month for each yearly season. Shorter periods should cover typical seasonal or operational situations. **Relative Humidity**

- The average of Relative Humidity (monthly, seasonal, annual).
- Minimum and maximum humidity (monthly, seasonal, annual).
- Time with relative humidity in a given interval.
- Level for average of relative humidity.

Table 5.2: Levels for average of relative humidity

Level	Relative humidity average%
1	RH < 40
2	40 ≤RH < 50
3	50 ≤RH < 70
4	RH ≥70

The measurement period is preferably one year, or one month for each yearly season. Shorter periods should cover typical seasonal or operational situations [105].

For all these reasons it is very important to develop new smart monitoring system which fits to all the requirements of the museums with high accuracy. Our monitoring campaign in the Faculty of archaeology museum employed for one year of measurement according to ISO 11844-1-2006. The system based on two actions:

- The deployment of a cloud-based sensors network capable of recording T and RH close to the artefacts.
- The deployment of some reference specimens coated with Cu nanostructured thin films for assessing the atmosphere aggressiveness.

The campaign started in August 2016. We developed a new real-time monitoring system to allow the curators to have all the information about the T and RH in the museum anytime and everywhere using Mobile application and website. Moreover, The curators can compare the night/day and seasonal measurement to have a clear view about the museum condition. Due to the existence of many devices and monitoring systems the value of the work is developing a new smart system, so our system has some advantages in the comparison with the commercial devices which are:

- Full fit all the requirements to use in the field of culture heritage conservation.
- Low Cost.
- No cabling.
- Small dimensions $\varnothing 35 \text{ mm} \times 15 \text{ mm}$.
- Long life battery (3 years).
- Easy time setup for measuring and upload the data to the cloud.
- Uncertainty of $\pm 3 \text{ }^\circ\text{C}$ and $\pm 2\% \text{ RH}$.
- Wireless range $> 10 \text{ m}$

Five sensors were distributed inside the showcases (codes, S161, S162, S163, S165, S166) and one in the room (code S164) 5.7. The sensors positioned near the Cu nano-structured reference specimens allows to monitor the effects of the environmental parameters and assess the aggressiveness and degradation effects of the atmosphere on the metallic artefacts in short time [106].

5.1 – *The environmental monitoring campaign in the Museum of the Faculty of Archaeology of the Sohag University (Egypt)*

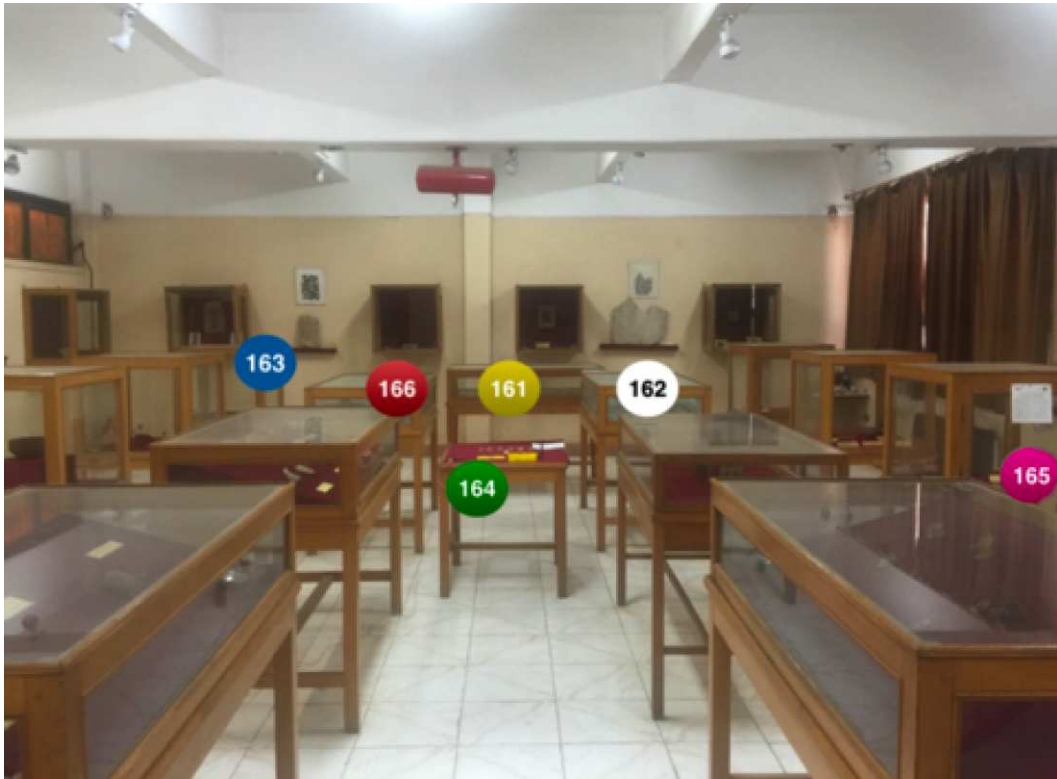


Figure 5.7: Sensors distribution inside and outside the showcases



Figure 5.8: Sensors and Cu nanostructured specimens distribution inside and outside the showcases

5.1.2 Sensors description

The monitoring system is a multi-point, based on a network of small autonomous sensors, was employed. The sensors linked with cloud-based system and it was designed and developed by the researchers of the Department of Electronics and Telecommunications of Politecnico di Torino, to satisfy the requirements of the museum curators [107, 108]. The sensors connected with a small wireless data receiver and the setup for measure the Temperature and relative humidity was every 15 minutes 5.9 and to send the measurements to a receiver for routing the data to a cloud system. Once the measured data are stored in the cloud the curators can access to the data and download for data analysis. In addition, the real-time monitoring by their phones everywhere.

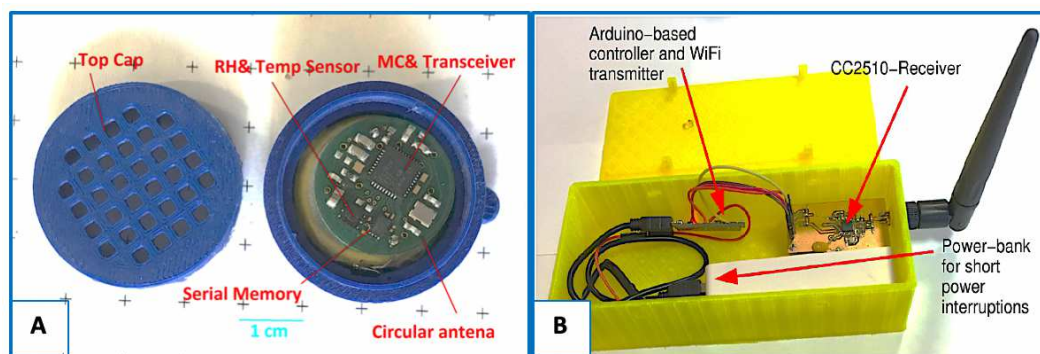


Figure 5.9: (A) small sensor, (B) WiFi data receiver

5.1.3 Cu nanostructured reference specimens

The references samples were copper coated with Cu nanostructured thin film sensitive toward the atmospheric corrosion and useful to assess the aggressiveness of indoor atmospheres inside the museum. The film has a high reactivity to the atmosphere pollutants. The samples surface can react very fast and at the nanoscale level with air pollutants.

Materials with morphological features on the nanoscale (usually smaller than 100 nm) so the nanomaterials can be classified as nano-sized and nanostructured materials [88].

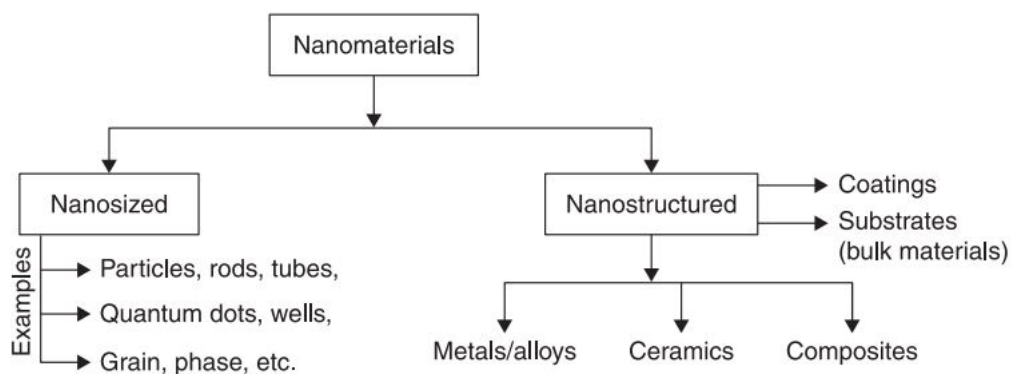


Figure 5.10: Schematic showing nanomaterials

The specimens made of pure copper (99.96 %) in size of 30 × 30 × 0.45 mm, were polished with abrasive paper (320- 1000 grit) followed by cleaning with ethyl alcohol in ultrasonic bath for five minutes then dried with acetone [5.11].

The reference samples were coated with about 200 nm of Cu nanostructured thin films using plasma sputtering deposition. DC glow discharge involves the ionization of gas atoms by electrons emitted from a heated filament. The gas ions in the plasma are then accelerated to produce a directed ion beam. If the gas is a reactive precursor, this ion beam is used to deposit directly onto a substrate; alternatively an inert gas may be used and the ion beam allowed to strike a target material which sputters neutral atoms onto a neighbouring substrate 5.12 [109]. The deposition was performed in a plasma reactor at the Department of Applied science and Technology (DISAT), Politecnico di Torino, using a Cu target (99.99% purity) connected as a cathode electrode with Ar (99.99% purity) as the discharge gas. The target was connected with a RF power supply (13.56 MHz) by an impedance matching unit. Before performing the deposition, the chamber was evacuated at a pressure of 1.5×10^{-7} mbar to avoid any surface contamination. The target cleaned by pre-sputtering process for 15 min at 50 W. All the depositions were performed at the room temperature ($T_f < 70$ °C) and the Ar pressure was 1.3×10^{-2} mbar using 300 W input power.

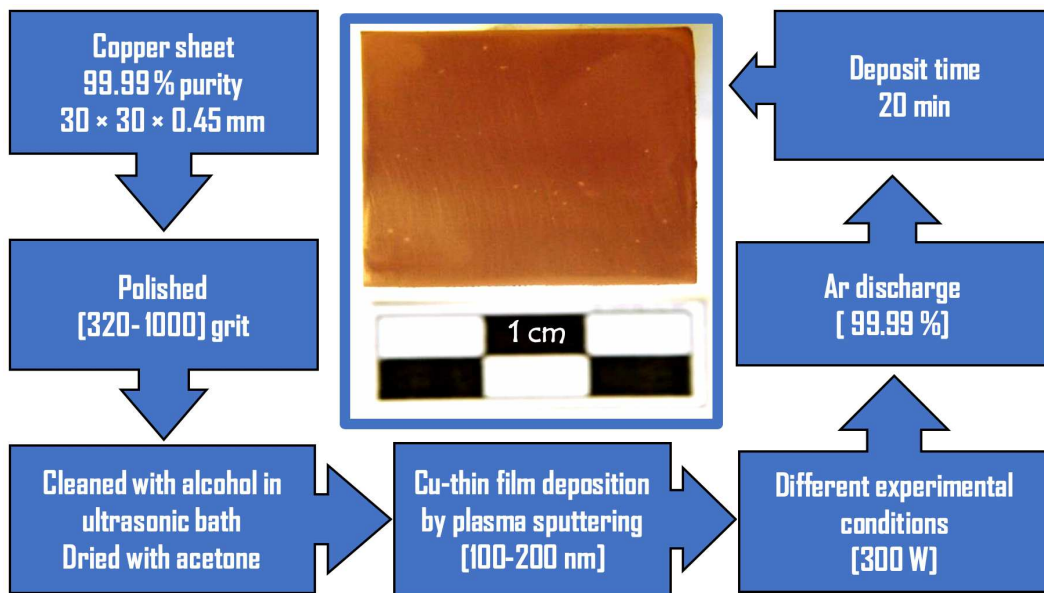


Figure 5.11: scheme of the preparation of Cu nanostructured thin film specimens

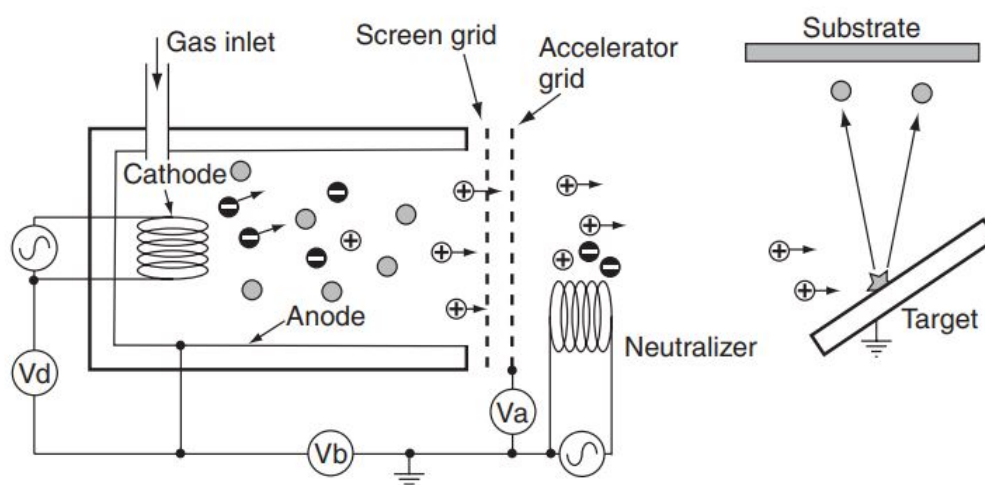


Figure 5.12: Scheme of a DC glow discharge apparatus in which gas atoms are ionized by an electron filament and either deposit on a substrate or cause sputtering of a target [109].

The reference samples were collected at increasing exposure times to the museum indoor atmosphere, after 2 months, 6 months and one year. The specimens were characterized chemically and morphologically using FESEM microscope (field emission scanning electron microscope) (Merlin Zeiss) equipped with a quantitative SSD probe (Oxford xact).

5.2 Result and discussion

Temperature and Relative humidity are outstanding parameters to be considered when developing tailored strategies for metallic Heritage safeguard. They directly affect the metallic artefacts surface and may cause corrosion attacks of different entity. Considering the indoor mmuseum atmosphere, when the relative humidity increases, the amount of water increases in the air, the environment becomes more aggressive for the metallic materials. Generally the accepted values of temperature and relative humidity for indoor museum environment are 20 ± 2 °C, and 50 ± 3 % RH. Furthermore, the climatic condition of the museum's country should be consider. According to the guideline of the Australian Heritage Collections Council for the environmental controls in cultural heritage institutions, they emphasize the need of the evaluation of the local climate conditions and of the adoption of showcases, which might minimize the reliance on full air-conditioning, in order to develop appropriate conservation procedures. The requested climatic conditions are divided in three categories as a function of T and RH values on daily basis:

- Hot humid climates: 22-28 °C, 55-70% RH.
- Hot dry climates: 22-28 °C, 40-60% RH.
- Temperate climates: 18-24°C, 45-65% RH.

Following this classification, Egypt can be considered a hot dry climate country, consequently the environmental conditions inside the Faculty of archaeology Museum are in the proper range, with lower relative humidity values.

The monitoring of the museum environmental condition has to be done by analysing the sensors data day/night, seasonally and in one year. The result can be described as follow:

5.2.1 Day/ night measurement

Temperature and relative humidity values collected in two days in summer and two days in winter have been compared to compare the day/night condition and the effects of the atmospheric corrosion. Figure 5.13 shows the collected data for two days in 20126 summer. The temperature inside and outside the showcases is stable and the values ranges from $\pm 1^{\circ}\text{C}$ so from 34°C to 34.9°C . The RH values are stable too inside the showcases but high frequency in the room sensors. The temperature inside the showcases ranges between 34 : 36 % RH, so the variations may be considered negligible, due to the good sealing of the showcases which avoids the air circulation to change the conditions inside the showcases. Meanwhile the variation in exhibition room evaluated with the sensor S134 was $\pm 5\%$ which may result from the work time of air conditions system.

Figure 5.14 shows the recorded data for two days in winter. Temperature is lower than in summer and the day/night changes ranges between $\pm 2^{\circ}\text{C}$ from 16.75 to 18.75 °C inside and outside the showcases also the changes were slight and stable. While the relative humidity changes were also stable inside the showcases about 45: 48 % and fast changes the the exhibition room between 41.5 : 45.6 % about $\pm 4\%$ RH. The night and day recorded can confirm that even in summer and winter the condition inside the showcases are more or less stable in the exhibition room due to the well-sealed showcases and the variation in the room due to the air condition system in summer and the city climate in summer and winter.

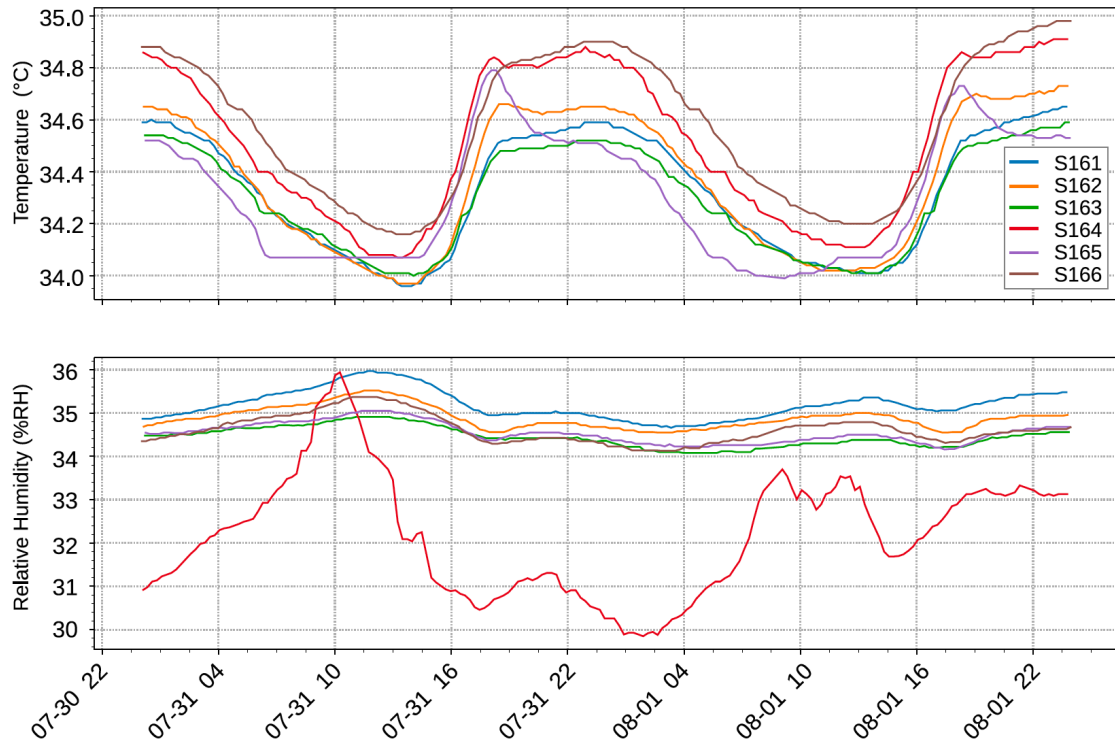


Figure 5.13: T and RH measurements collected for about two days in summer from the smart sensors inside (S161, S162, S163, S165, S166) and outside (S164) the showcases.

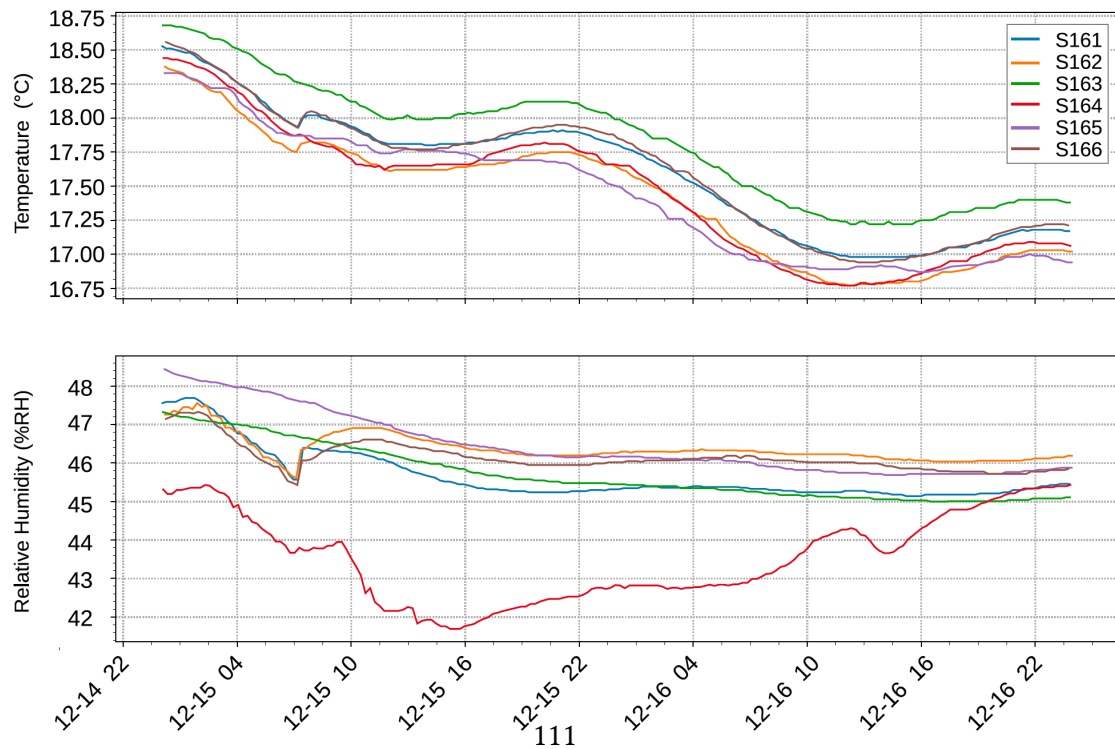


Figure 5.14: T and RH measurements collected for about two days in Winter from the smart sensors inside (S161, S162, S163, S165, S166) and outside (S164) the showcases.

5.2.2 One year environmental monitoring data

The environmental monitoring campaign has been extended for one year. The microclimate conditions over one year are more or less stable inside the Sohag museum. T decreases from the average value 35°C in summer to a minimum average value 15°C in winter. In the meantime, RH increases from 35% in summer to 50% in winter as shown in figure 5.15. According to the previous classification of the Australian Heritage Collections Council guidelines and ISO 11844-1:2006, the microclimate of the Faculty of archaeology museum may be considered stable inside the showcases and good for a long term preservation of the artefacts.



Figure 5.15: T and RH measurements collected for one year of measurement with the smart sensors inside (S161, S162, S163, S165, S166) and outside (S164) the showcases.

5.2.3 Surface characterization of Cu reference specimens

The surface characterization of the Cu reference specimens confirms that the microclimate condition of the Sohag museum are good for the artefacts conservation. After two months the first group of samples was collected from the museum to study the effect of the atmospheric corrosion on the nanostructured specimens. Figure 5.16 shows

that the surfaces of the reference samples are slightly affected by the atmospheric corrosion after 2 months exposure in the museum. The samples inside (S162, S165) near the air conditioning system and outside (S164) shows a slight corrosion products on the samples surfaces. On sample (S163) there is no corrosion on the surface due to the position of the showcase in the left part of the museum and far from the air conditioning or the right side of the museum so the showcase are more safe with higher temperature and less relative humidity in comparison with the other samples as shown in figure 5.14, 5.13. Moreover, the samples in the room are more corroded than the others in the showcases due to the variation and fast changes of T and RH in the exhibition room.

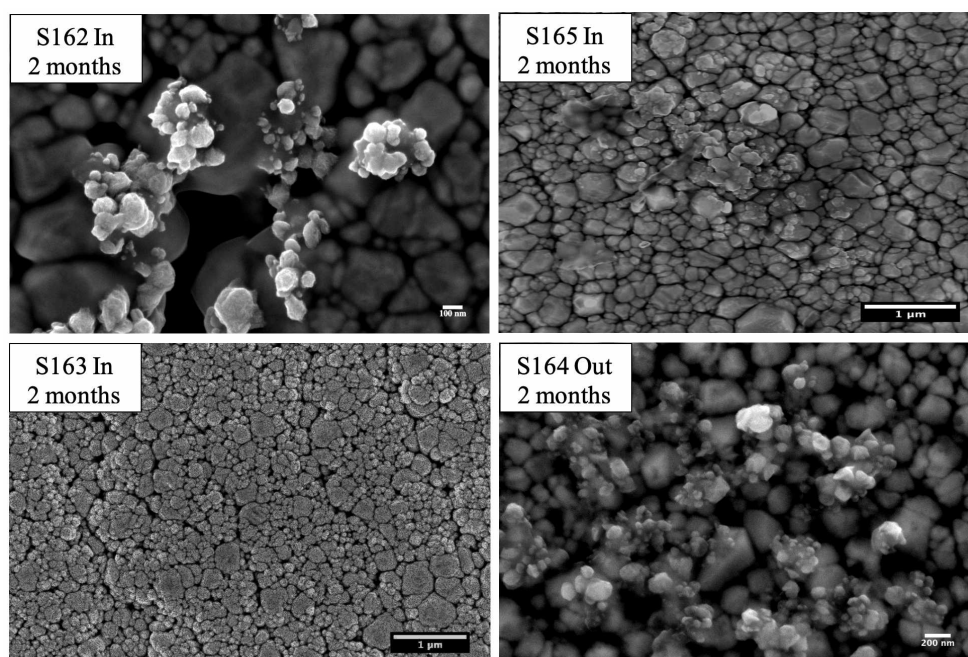


Figure 5.16: FESEM images of the Cu nanostructured reference specimens exposed for 2 months inside showcases (S162, S163, S165) and outside in the room exhibition (S164)

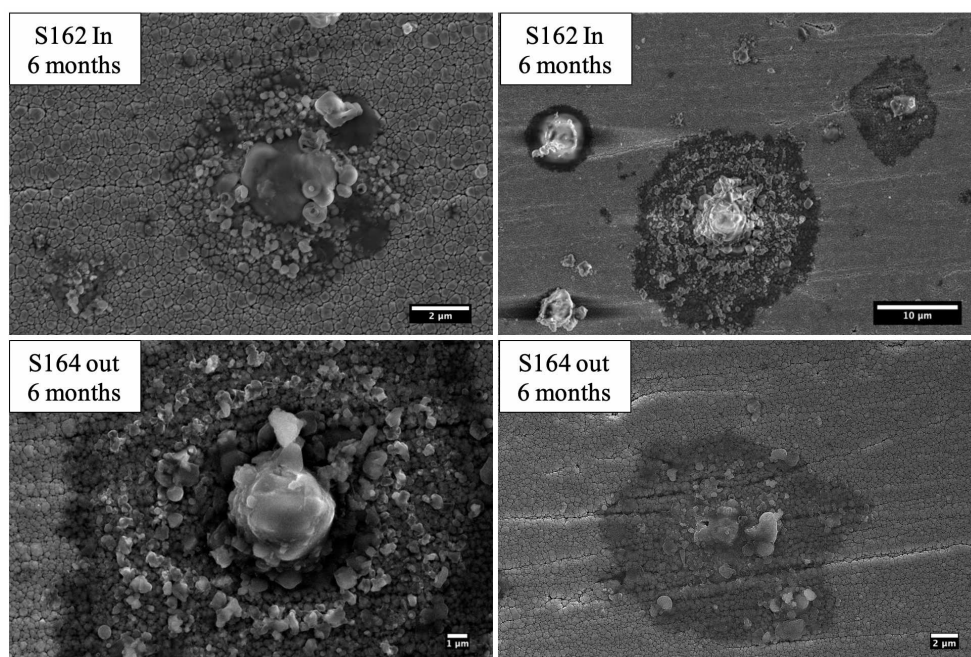


Figure 5.17: FESEM images of the Cu nanostructured reference specimens exposed for 6 months inside showcases (S162) as an example and outside in room exhibition (S164)

Figure 5.17 shows the increase of the corrosion products on the surface of the reference samples after 6 months of exposure to the indoor atmosphere. The chemical composition of the corrosion products found on the Cu nanostructured specimens of sample (S162) after 2 and 6 months of exposure 5.18 revealed the presence of copper oxide, copper sulphide and copper chloride. In addition, the amount of oxygen, sulfur and chlorine increased due to the time as a result of the long-term exposure. The high amount of sulfur could be due to the use of the velvet textile in the showcases. In addition, some other elements which can be part of the pollutants inside the museum.

Fig. 5.19 shows the effects of the atmosphere on the nanostructured film inside (S165) and outside (S164) the showcases. The increase of the exposure time increases the degradation extent of the samples. On the surface of sample S165 the presence of localised corrosion attacks is observed in addition to the presence of an amorphous copper oxide. On the other hand samples S164 in the room are more corroded and the spots of the localised corrosion (circle-shape corrosion spots) are bigger due to the effect of high variation changes in the temperature and relative humidity [106]. The chemical analysis shows the presence of high amount of copper oxide and copper chloride. Figure 5.20 (A) shows the elements of sample S165 inside the showcase located near the air-conditioning. The sample S164 confirms higher amount of oxygen than the S165 because the room environment is not controlled as the showcases. The other elements present may be due to different types of pollutants in the museum microclimate.

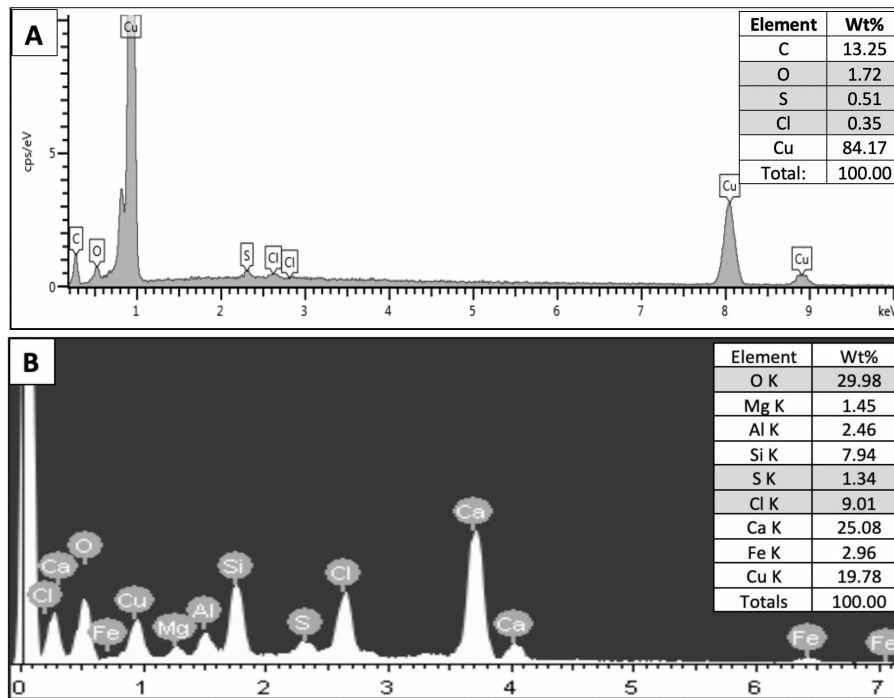


Figure 5.18: EDS analysis of chemical composition of corrosion products for the Cu nanostructured reference specimens exposed for (A) 2 months & (B) 6 months inside showcases (S162)

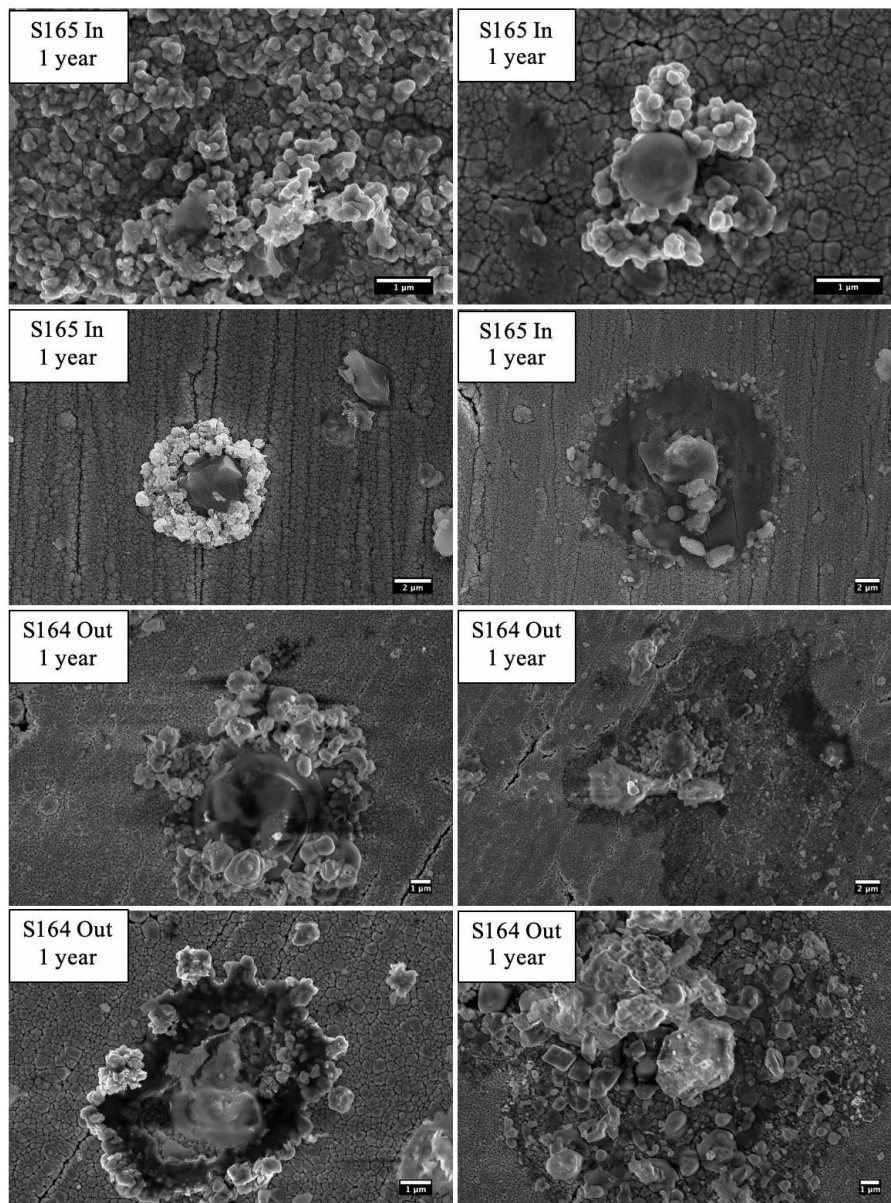


Figure 5.19: FESEM images of the Cu nanostructured reference specimens exposed for year inside showcases (S165) as an example and outside in the room exhibition (S164)

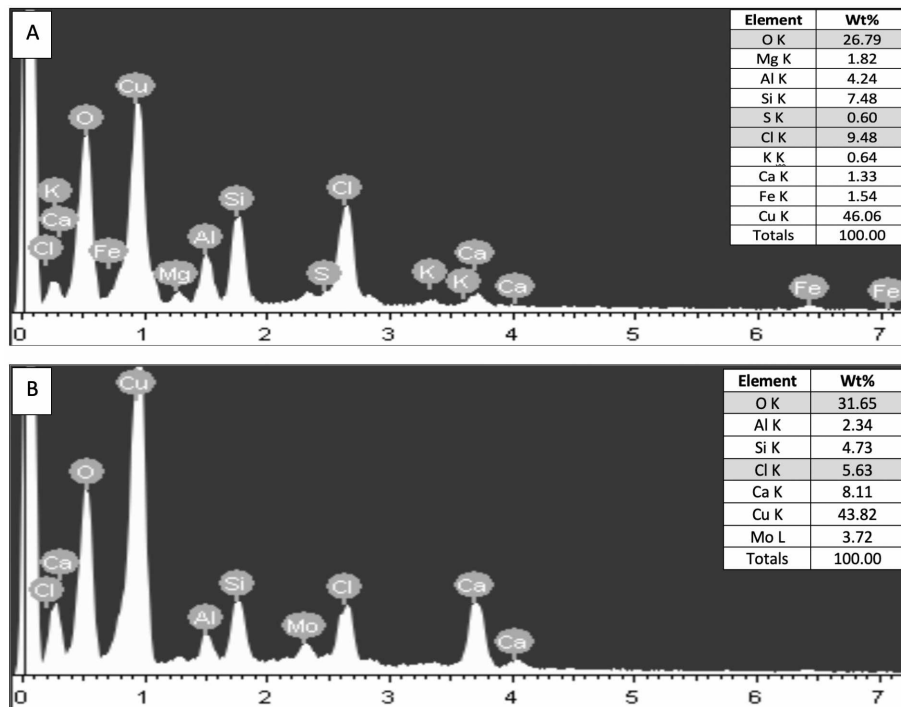


Figure 5.20: EDS analysis of chemical composition of corrosion products for the Cu nanostructured reference specimens exposed for 1 year (A) inside showcase S165 and (B) exhibition room S162

5.3 Conclusions

The preventive conservation strategies are fundamental for safeguarding metallic artefacts and may be applied in the museums microclimate control. The environmental monitoring campaign of the faculty of Archaeology museum in Sohag University, assess the efficacy of the online monitoring system developed in Politecnico di Torino. The smart button network system fits all the requirements for the use in cultural heritage field also from an economic point of view, because of the low cost. The museum microclimate more or less stable for the metals except the presence of the high amount of sulfur which can be decreased by using some filters and change the displaying velvet textiles in the showcases and use better materials for display. Furthermore, the showcases are good sealed so the environment inside the showcases more stable than the exhibition room. The temperature and relative humidity changed due to the seasonal conditions were negligible. Moreover it can be confirmed that the normal system of the monitoring by thermo-hygrometer is not accurate and it could be good solution if they can change the silica gel inside the showcases periodically. The Cu reference samples confirmed the high reactivity of the Cu nanostructured thin film for the atmosphere.

The thin film corrodes faster in comparison with bulk material. For this reason the Cu nanostructured thin films may be used as reference material to assess the atmosphere aggressiveness in museum indoor environments.

5.3.1 Assessment of the atmospheric corrosion of copper at nanoscale

This work was presented in the conference of EuroCorr 2018, Poland. All properties of materials changes at nanoscale such as, chemical, physical properties including magnetic properties, optical properties, melting point, crystal morphologies, sensitivity of the materials to corrosion, and surface reactivity [95, 110]. This part is the second part of the assessment of the atmospheric corrosion effect and test the sensitivity of the Cu nanostructured thin film. This experiment was an artificial ageing of a copper nanostructured thin film following the ISO 3231-1993 standard method which is a determination of resistance to humid atmospheres containing sulfur dioxide.

5.3.2 Materials and methods

Accelerated aging can be used to simulate the natural corrosion process. Copper behavior in atmospheric corrosion is little complicated because of this it was important to do an artificial aging to evaluate the effect of atmospheric corrosion on the nanostructure thin film.

Copper exposed to the atmosphere is superficially oxidized and covers with a layer of Cu_2O copper oxide that for longer exposures further oxidizes CuO formed. In dependence of the ions present in the atmosphere it may form a green patina of copper sulphides brochantite $\text{Cu}_4(\text{SO}_4)(\text{OH})_6$, antlerite $\text{Cu}_3(\text{SO}_4)(\text{OH})_4$ is not uncommon and traces of posnjakite $\text{Cu}_4(\text{SO}_4)(\text{OH})_6 \cdot 2\text{H}_2\text{O}$, and copper chlorides as $\text{Cu}_2\text{Cl}(\text{OH})_3$ atacamite are also commonly found [77, 111, 112].

This accelerated aging was carried out to determine the resistance to sulfur dioxide gas SO_2 in humid atmospheres [113]. Cu nanostructured thin films have been deposited on pure Cu sheets (30x30 mm, 0.45 mm thick) by plasma sputtering. The deposition was performed in high vacuum conditions at the pressure of 1.3×10^{-2} mbar using Ar (purity 99.99%) as discharge gas and by applying an input power in the range of 100W to 500W for 20 min. The Cu film thickness was in the range of 100 nm to 500 nm. The samples were divided into two groups. The first group consisted of three samples sputtered with 100w input plasma and the second group consisted of three samples sputtered with 500w input power for 20 min due to different layer thickness and grain size in order to correlate grain size with corrosion effects. A set of Cu nanostructured films have been submitted to accelerated ageing test according to the ISO 3231:1993 standard method, in order to assess the resistance to a humid atmosphere containing SO_2 . Samples have been maintained at 40°C for 8 hours in a humid condensing atmosphere in the presence

of SO_2 ; then, they have been dried at $23 \pm 2^\circ C$ and $50 \pm 5\%$ RH for 16 hours. The ageing cycle has been repeated for 3 days.

Different analytical techniques can be utilize to characterize nanoparticles :

- Morphology
- Crystal structure
- Chemistry
- Electronic structure

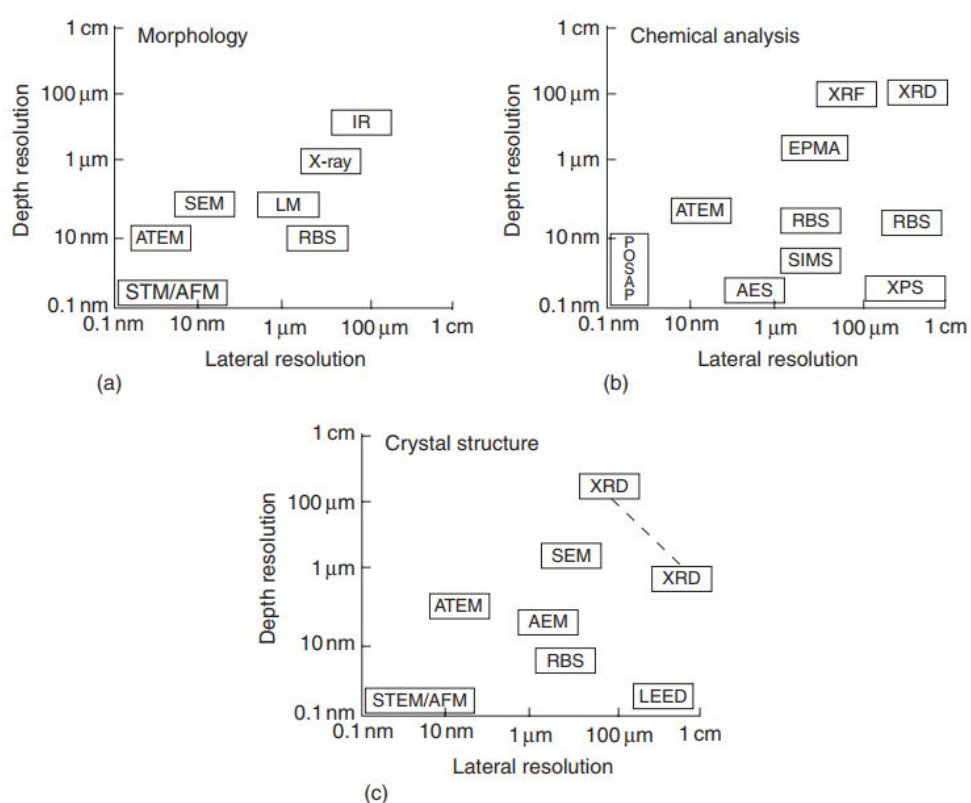


Figure 5.21: Schematic classification of the information content of different imaging and analytical techniques in terms of their lateral and depth resolutions

[109].

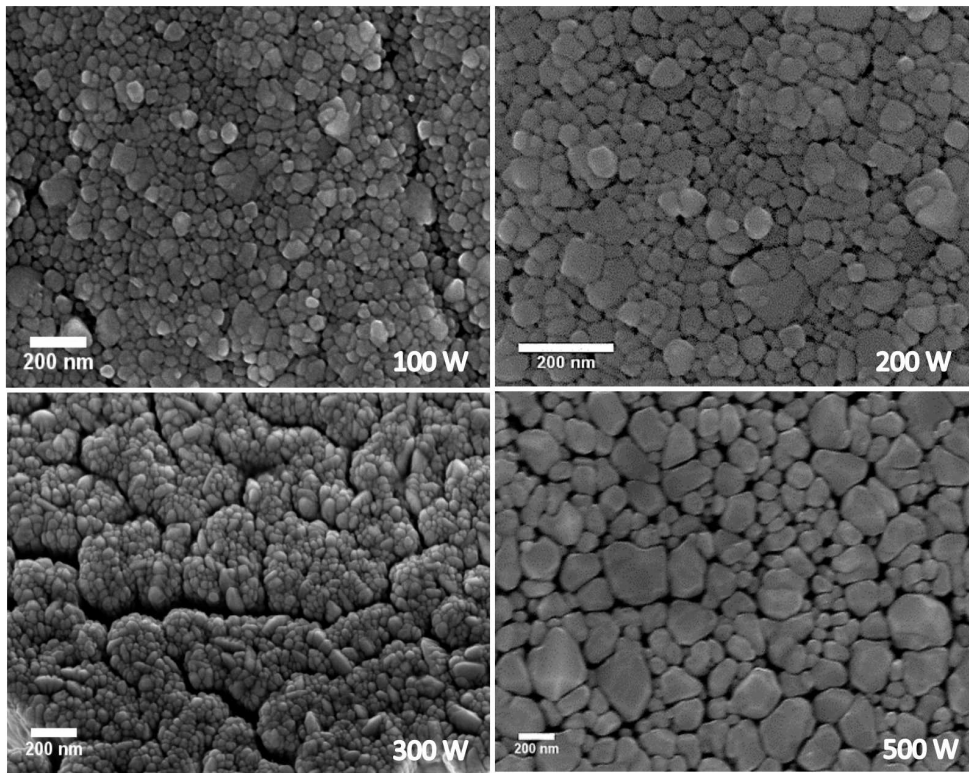


Figure 5.22: FESEM image of the Cu nanostructured thin film with different nano particles size with different power

It is important to develop nanomaterials because they allow to study the correlation between nanolayers and corrosion as seen in figure 5.23 [88].

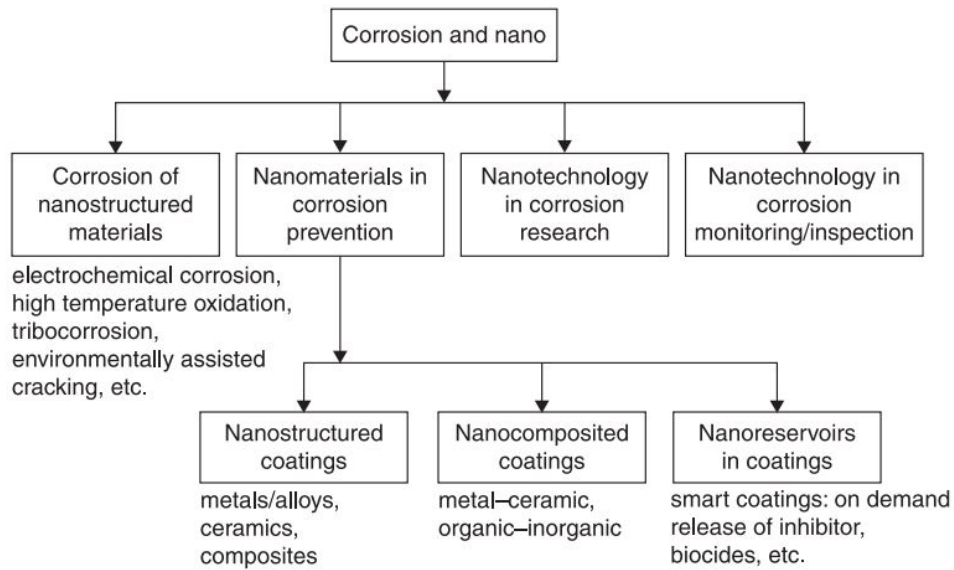


Figure 5.23: Diagram showing correlation between nanotechnology with corrosion , nanostructure mainly refers to (nanograin) and nano-composite materials are mentioned separately.

Results and discussion

- Mass changes

The first two samples (Group 1) show a mass increase after the first cycle but with minor changes so in the sample (100w-1) the amount was 0.0006 g and in the second cycle the mass increases to 0.0059 g then decreased to 0.0018 g due to the protection of the copper oxide film. The line chart provides a clear view of the increase in sample mass 100w-1 and 500w-1 due to the SO₂ gas exposure time. In the second pairs (group 2) the same behaviour occurred, the mass increased by 0.0043 g in sample 100w-2 after 24h, then after 48h increased by 0.003 g after 48h with a small amount. The sample weight of 500w-2 increased by 0.0052 g after 24h, then by 0.0019 g. The mass changes in the second group show very small differences, that may be due to the different thickness of the cuprite layer as the first group. On the other hand, the third group has different behaviour in sample 500w-3 due to weight loss of 0.0848 g after 24h and increased by 0.0047 g in sample 100w-3 due to grain size and grain boundaries so the weight increased [5.24](#)

The behaviour of the third group (Group3) was slightly different because the mass of sample 100w-3 increased as usual, but the sample 500w-3 decreased [5.25](#) may result in a mass loss due to the grain size or some defects in the nanostructured so it was not good that it may also be related to the substratum polishing. Thus the major cause of nanostructure corrosion is the layer defects due to the layer's high sensitivity. In

general, however, the rate of copper corrosion decreases with exposure time in outdoor conditions regardless of the type of atmosphere [114, 115].

While the corrosion rate increases significantly with time under indoor conditions [116]. In addition, the rate of atmospheric corrosion and corrosion depends primarily as a direct proportion on relative humidity[117]. According to ISO 11844-1:2006 very low indoor mass increase rate for copper and silver is $r_{mi} \leq 25 \text{ mg}/(\text{m}^2 \cdot \text{a})$

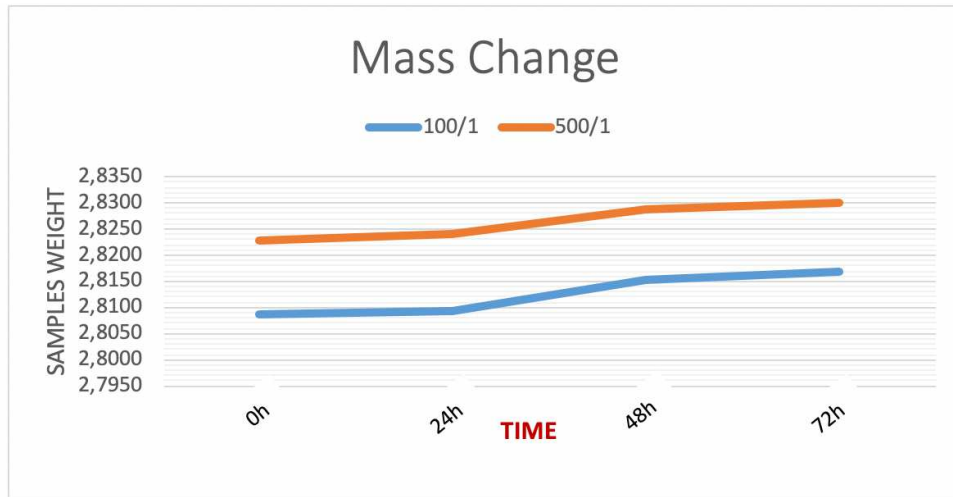


Figure 5.24: Difference in the mass increase between the two samples related to the time of the test

Sample code	Group	Initial mass [g]	Mass after 1st cycle [g]	Mass after 2nd cycle [g]	Mass after 3rd cycle [g]	Mass Sum	Mass Average	Mass increase	Mass Loss	No of cycles
100w-1	1	2.8087	2.8093	2.8152	2.8170	8.4415	2.8138	0.0051	-	3
500w-1		2.8229	2.8242	2.8287	2.8299	8.4828	2.8276	0.0047	-	3
100w-2	2	2.6807	2.6850	2.6880	-	5.3730	2.6865	0.0058	-	2
500w-2		2.8851	2.8903	2.8922	-	5.7825	2.8913	0.0061	-	2
100w-3	3	2.8032	2.8079	-	-	-	-	0.0047	-	1
500w-3		2.8689	2.7841	-	-	-	-	-	0.0848	1

Figure 5.25: Mass changes of the samples due to the accelerated ageing test

- Optical microscope results

The optical microscope images of the sample show that due to the high sensitivity of the nanostructured thin film, the entire nanostructured layer was rapidly affected 5.26 a, b). The results of the first two samples (100w-1, 500w-1) after three cycles over three days showed that the surface corrosion is different, so that the 100w-1 sample is more corroded than the 500w-1 sample 5.26. Because of the grain size of both samples as shown in the morphology of the samples 5.26 a, b. Moreover, when the input power of plasma sputtering increases the grain size increase while the grain boundaries decrease, and this is why sample 100w-1 increases more mass than sample 500w-1 due to the increasing mass of corrosion products.

The atmospheric corrosion of the copper nanostructured layer showed that the cuprite patina acts as a protective layer for the pure copper substrate and causes a continuous decrease in copper corrosion rate when exposure time increases, but the increase in time also leads to the oxidization of the copper sulfate (brochantite) to produce various types of corrosion products such as posnjakite [$\text{Cu}_4\text{SO}_4(\text{OH})_6\cdot\text{H}_2\text{O}$], and antlerite $\text{Cu}_3\text{SO}_4(\text{OH})_4$ in a humid air as one of the main corrosion products forms in humid air due to the atmospheric corrosion [77, 111, 112].

Moreover, the sample 500w-3 is fully covered with cuprite compared to other samples that protect the samples from continuing the corrosion process as it works as a barrier layer to anodic reactions[118]. The sensitivity of the layer also depends on the nano size and the thickness of the layer so in this case the thickness of the samples nanostructure layer between 50 to 100nm which means high sensitivity in the indoor environment and more susceptible to atmospheric corrosion.

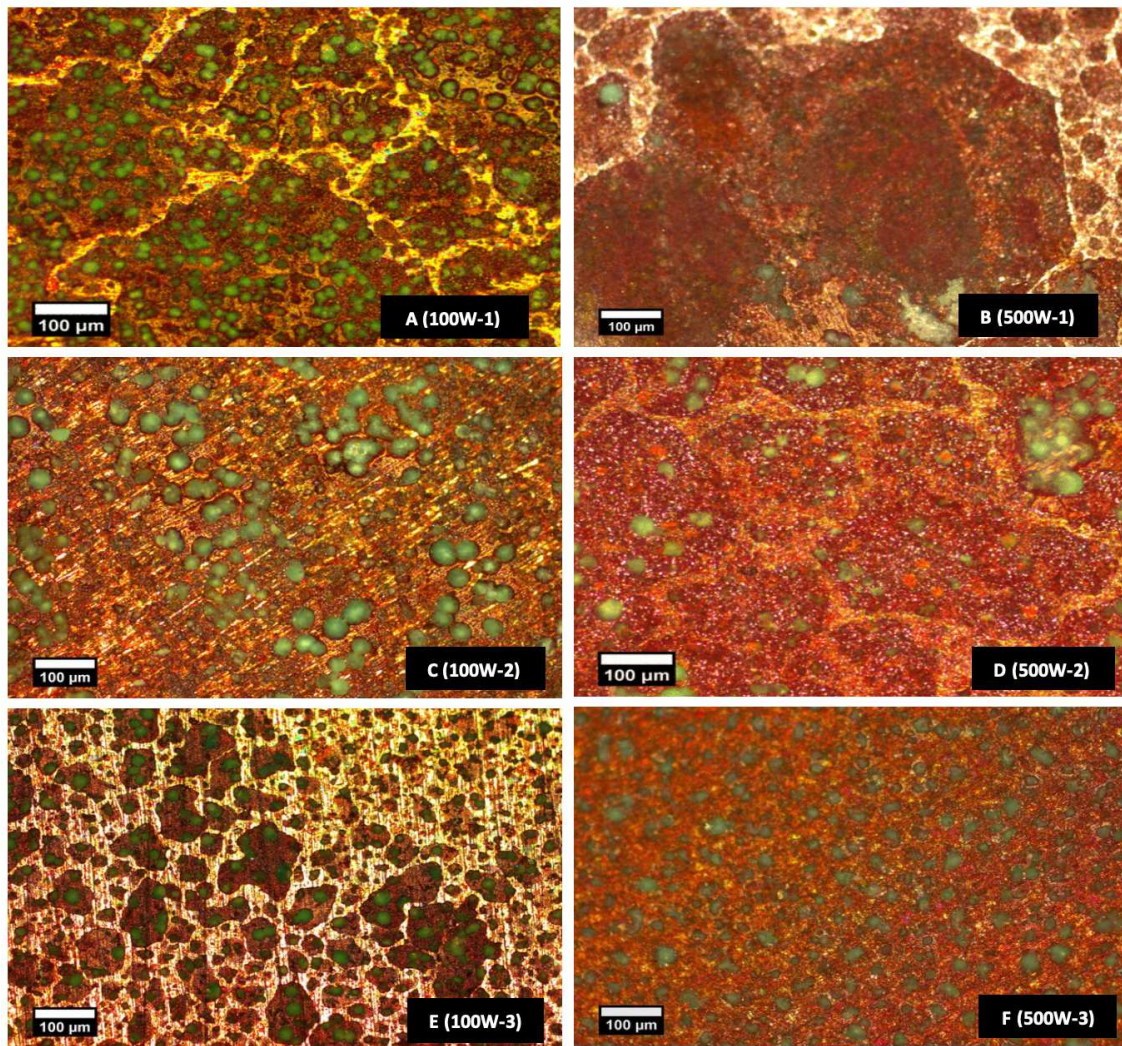
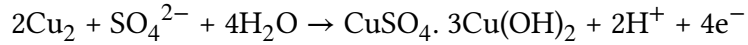


Figure 5.26: Optical microscope images, shows the morphology of the three groups (samples 100w and 500w) after the accelerating ageing test

- FESEM and EDS

The FESEM images shows the effects of artificial ageing on the morphology of the nanostructured thin film. Due to the degradation time, polycrystalline copper sulfate grew in different amounts on the cuprite surface of all samples. Because of the three degradation cycles for 72 hours, samples (100w-1, 500w-1) are more corroded. At some point in the surface, the brochantite $\text{Cu}_4\text{SO}_4(\text{OH})_6$ monoclinical nanocrystals were grown and the octahedral cuprite nanocrystals (Cu_2O) were grown throughout the surface 5.27, 5.28 [119, 77, 111, 112, 120, 114]. Moreover, the FESEM Photos indicated that cuprite was subsequently the first corrosion products to form brochantite as

isolated crystals on the cuprite surface. Therefore, it is common that brochantite is usually the form in the cuprite's outer patina layer as atmospheric exposure time increases. Patina forms in the aqueous layer by the oxidation of cuprite and the incorporation of trace impurities, namely sulphates, by the following overall reaction 5.29 [77, 121].



According to ISA-71.04-1985 standard, in high relative humidity, the corrosion accelerated and the effect of sulfur dioxide (SO_2) became more dangerous for the metals due to the high chemical reactivity with metals. In addition, SO_2 combines with water to form sulfuric acid and thus destroy the metals [118]

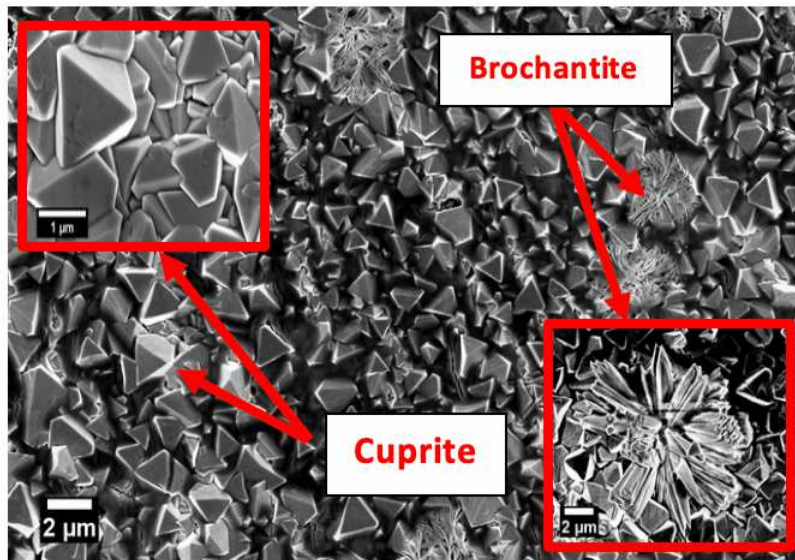


Figure 5.27: FESEM image of sample 100w-1, showing the brochantite and cuprite on the sample surface

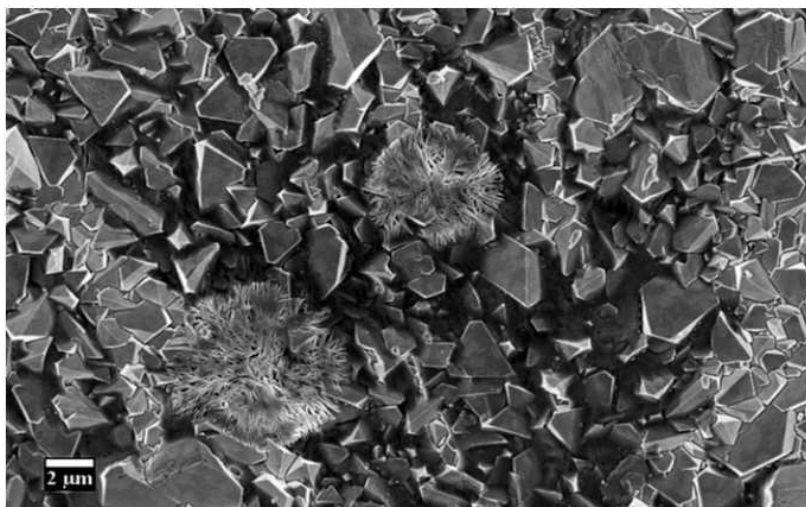


Figure 5.28: FESEM image for sample 500w-1, it shows the brochantite and cuprite on the sample surface

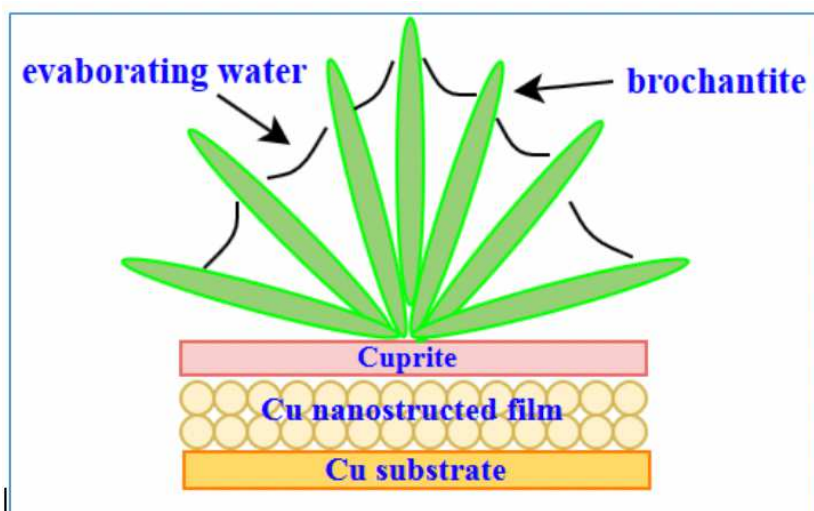


Figure 5.29: schematic of cuprite layer on the nanostructured thin film and the form of brochantite with evaporating water on the cuprite layer due to the humid air through the test

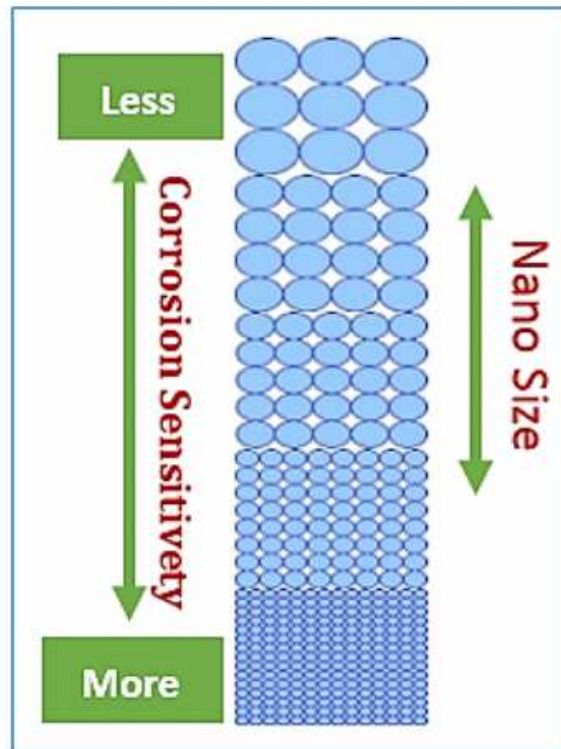


Figure 5.30: Schematic of the relation between the nanoparticles size and sensitivity to corrosion

Conclusions

The increased grain boundary fraction in a nanostructured material can make more anodic sites for corrosion nucleation. High diffusivity and higher electrical resistivity are associated with grain boundaries. When favoring intergranular diffusion of corrosive species, the grain boundaries turn out to be more susceptible to corrosion attack. Meanwhile, a positive effect is that the grain boundaries favor the faster diffusion of passive ions from the bulk to the surface, which can promote the formation of a more effective protective layer. In the case of materials that are highly resistant to degradation due to their passive film, this effect has greatest implication. The proven enhancement of the nanostructured materials bulk electrical resistivity increases the corrosion resistance. [88]. Accelerated ageing with SO_2 shows that when metal grain size decrease the percentage of surface atoms increases. Furthermore, the metals surface begins to affect the metal's properties when particles still 10-50 nm in size so the nanostructured film becomes more sensitive to corrosion. In addition, chemical reactions became faster at lower temperature [95]. There is evidence of increased interatomic spacing with decreasing particle size of metal oxides [109]. Moreover, when the exposure time increases

the corrosion rate decreases due to the formation of a protective cuprite layer which forms faster on the nanostructured Cu thin film. The average of changes between the corrosion of samples 100w and 500w power sputtering is not a big difference in the grain size due to the ageing cycles. The thickness of the layer is one of the main parameters which can affect the corrosion rate. The first corrosion products formed are cuprite and then the brochantite grown as isolated crystals on the cuprite surface.

Bibliography

- [1] UNESCO. *World Heritage*. 2019. URL: <http://whc.unesco.org/en/about/world-heritage> (visited on 04/03/2018).
- [2] Lasse Steiner and Bruno S Frey. “Correcting the imbalance of the world heritage list: did the UNESCO strategy work?” In: *Journal of International Organizations Studies* 3.1 (2012), pp. 25–40.
- [3] Charles Gates. *Ancient cities: The archaeology of urban life in the ancient Near East and Egypt, Greece and Rome*. Routledge, 2011.
- [4] Nissim Amzallag. “From metallurgy to Bronze Age civilizations: the synthetic theory”. In: *American Journal of Archaeology* (2009), pp. 497–519.
- [5] Susan Sherratt, PM Day, and RCP Doonan. “The archaeology of metal use in the Early Bronze Age Aegean: A review”. In: *Metallurgy in the Early Bronze Age Aegean* 7 (2007), p. 245.
- [6] AC Reardon. “Discovering metals—a historical overview”. In: *Metallurgy for the non-metallurgist* (2011), pp. 73–84.
- [7] Loic C Boscher. “Reconstructing the Arsenical Copper Production Process in Early Bronze Age Southwest Asia”. PhD thesis. UCL (University College London), 2016.
- [8] Charles Meyer. “Ore metals through geologic history”. In: *Science* 227.4693 (1985), pp. 1421–1428.
- [9] Andre Desvallees and Francois Mairesse. *Key concepts of museology*. Armand Colin, the ICOM International Committee for Museology, 2010.
- [10] Paola Moscati. “Virtual Museums and Archaeology. The Contribution of the Italian National Research Council”. In: *established by: Mauro Cristofani and Riccardo Francovich* supplemento 1 (2007).
- [11] Alison Heritage & Jennifer Copithorne. *Sharing Conservation Decisions, Current Issues and Future Strategies*. ICCROM, 2018.
- [12] Mohammad M Debajah and Mustafa Al-Naddaf. “Museum Storage Assessment: A Case Study from the Museum of Jordanian Heritage-Yarmouk University”. PhD thesis. 2010.

- [13] O. P. AGRAWAL. "Conservation of Metals in Humid Climate". In: *Proceedings of the Asian Regional Seminar*. ICCROM, 1987.
- [14] Sollen Reguer, P e Dillmann, and F Mirambet. "Buried iron archaeological artefacts: corrosion mechanisms related to the presence of Cl-containing phases". In: *Corrosion Science* 49.6 (2007), pp. 2726–2744.
- [15] Solenn Reguer et al. "Deterioration of iron archaeological artefacts: micro-Raman investigation on Cl-containing corrosion products". In: *Journal of Raman Spectroscopy: An International Journal for Original Work in all Aspects of Raman Spectroscopy, Including Higher Order Processes, and also Brillouin and Rayleigh Scattering* 38.4 (2007), pp. 389–397.
- [16] A Boccia Paterakis. "The formation of acetate corrosion on bronze antiquities: characterisation and conservation". PhD thesis. UCL, University College London, 2011.
- [17] Philippe Dillmann et al. *Corrosion and conservation of cultural heritage metallic artefacts*. Elsevier, 2013.
- [18] Bruno Fabbri. *Science and Conservation for Museum Collection*. Nardini Editore, 2017.
- [19] Nick Merriman. "Museum collections and sustainability". In: *Cultural trends* 17.1 (2008), pp. 3–21.
- [20] Vasilike Argyropoulos et al. "A survey of the types of corrosion inhibitors and protective coatings used for the conservation of metal objects from museum collections in the Mediterranean basin". In: *Strategies for Saving our Cultural Heritage. Proceedings of the International Conference on Conservation Strategies for Saving Indoor Metallic Collections, Cairo (Egypt)*. TEI of Athens, Athens. 2007, pp. 166–170.
- [21] Yang Sook Koh. "Laser cleaning as a conservation technique for corroded metal artifacts". PhD thesis. Luleaa tekniska universitet, 2006.
- [22] Alexander Fridman. *Plasma chemistry*. Cambridge university press, 2008.
- [23] William Dickson Westwood, Stephen M Rossnagel, and JJ Cuomo. *Handbook of Plasma Processing Technology: Fundamentals, Etching, Deposition, and Surface Interactions*. Noyes Publications, 1990.
- [24] Paul K Chu and XinPei Lu. *Low temperature plasma technology: methods and applications*. CRC Press, 2013.
- [25] Andre Anders. "Tracking down the origin of arc plasma science I. Early pulsed and oscillating discharges". In: *IEEE transactions on plasma science* 31.5 (2003), pp. 1052–1059.
- [26] Barry J Setterfield. "A Plasma Universe with Changing Zero Point Energy". In: *energy* 16 (2011), p. 3.

- [27] Michael A Lieberman and Alan J Lichtenberg. *Principles of plasma discharges and materials processing*. John Wiley & Sons, 2005.
- [28] DF O’kane and KL Mittal. “Plasma cleaning of metal surfaces”. In: *Journal of Vacuum Science and Technology* 11.3 (1974), pp. 567–569.
- [29] VD Daniels, L Holland, and MW Pascoe. “Gas plasma reactions for the conservation of antiquities”. In: *Studies in Conservation* 24.2 (1979), pp. 85–92.
- [30] J Pat Scheider and Vepvrek S. “Application of low-pressure hydrogen plasma to the conservation of ancient iron artifacts”. In: *Studies in conservation* 31.1 (1986), pp. 29–37.
- [31] Stanislav Vepvrek, Jorg Patscheider, and Jorg Elmer. “Restoration and conservation of ancient artifacts: A new area of application of plasma chemistry”. In: *Plasma Chemistry and Plasma Processing* 5.2 (1985), pp. 201–209.
- [32] S Veprek, Ch Eckmann, and J Th Elmer. “Recent progress in the restoration of archaeological metallic artifacts by means of low-pressure plasma treatment Plasma Chem”. In: *Plasma process* 8.4 (1988).
- [33] S Keene. “Real Time Survival Rates for Treatments of Archaeological Iron. Ancient and Historic Metals: Conservation and Scientific Research”. In: *Proceedings of a conference held at the Getty Conservation Institute November*. 1991.
- [34] Anker Sjogren and Vagn F Buchwald. “Hydrogen plasma reactions in a DC mode for the conservation of iron meteorites and antiquities”. In: *Studies in Conservation* 36.3 (1991), pp. 161–171.
- [35] Oliver Cummings Farrington. *Meteorites: Their Structure, Composition, and Terrestrial Relations*. The author, 1915.
- [36] Jesus Martinez-Frias. “Meteorites and impacts: research, cataloguing and geoethics”. In: (2004). URL: http://www.ehu.eus/sem/seminario%5C_pdf/SeminSEMv10p75-87.pdf (visited on 12/20/2018).
- [37] EA Deliyanni et al. “Akaganeite under line type beta-FeO (OH) nanocrystals: preparation and characterization”. In: *Microporous and mesoporous materials* 42.1 (2001), pp. 49–57.
- [38] Bull Mineal. “Structural characteristics of hematite and goethite and their relationships with kaolinite in a laterite from Cameroon. A TEM study.” In: *Bull. Mineral* 111 (1988), pp. 149–166.
- [39] Hexiong Yang et al. “Goethite, alpha FeO (OH), from single-crystal data”. In: *Acta Crystallographica Section E: Structure Reports Online* 62.12 (2006), pp. i250–i252.
- [40] Udo Schwertmann and RM Taylor. “Transformation of lepidocrocite to goethite”. In: (1972).

- [41] AU Gehring and AM Hofmeister. "The transformation of lepidocrocite during heating: a magnetic and spectroscopic study". In: *Clays and Clay Minerals* 42.4 (1994), pp. 409–415.
- [42] Donny L Hamilton. "Methods of conserving archaeological material from underwater sites". In: *Texas A&M University* (1999).
- [43] P Arnould-Pernot et al. "Optimisation d'un traitement de dechloruration d'objets ferreux par plasmad'hydrogene". In: *Studies in conservation* 39.4 (1994), pp. 232–240.
- [44] Lyndsie Selwyn. "Overview of archaeological iron: the corrosion problem, key factors affecting treatment, and gaps in current knowledge". In: *Proceedings of metal* (2004), pp. 294–306.
- [45] Herbert Keppner et al. "Process-enhancement of hydrogen-plasma treatment by Argon". In: *Zeitschrift fur schweizerische Archaologie und Kunstgeschichte* 54.PV-LAB-ARTICLE-1997-002 (1997), pp. 25–28.
- [46] R Platz et al. "Comparison of VHF, RF and Dc Plasma Excitation for a-Si: H Deposition with Hydrogen Dilution". In: *MRS Online Proceedings Library Archive* 507 (1998).
- [47] Hannes Schmidt. "Characterization of a high-density, large-area VHF plasma source". In: (2006).
- [48] Alexander Voute. "The Plasma Equipment at the Swiss National Museum: Observations and Improvements". In: *Zeitschrift fur schweizerische Archaologie und Kunstgeschichte* 54.1 (1997), pp. 41–44.
- [49] Katharina Schmidt-Ott. "Applications of low pressure plasma treatment at the Swiss National Museum and assessment of the results". In: *Zeitschrift fur schweizerische Archaologie und Kunstgeschichte* 54.1 (1997), pp. 45–50.
- [50] Pavel Sankot and Alena Havlínová. "The application of low-pressure Hydrogen Plasma in the conservation of metal objects at the Museum of Central Bohemia". In: *Zeitschrift fur schweizerische Archaologie und Kunstgeschichte* 54.1 (1997), pp. 51–53.
- [51] Susan Bradley et al. "Assessment of the plasma treatment for archaeological iron objects in the collections of the British Museum". In: *Zeitschrift fur schweizerische Archaologie und Kunstgeschichte* 54.1 (1997), pp. 54–58.
- [52] Katharina Schmidt-Ott and Valentin Boissonnas. "Low-pressure hydrogen plasma: an assessment of its application on archaeological iron". In: *Studies in conservation* 47.2 (2002), pp. 81–87.
- [53] Zuzana Rávková et al. "Diagnostic of plasmachemical treatment of archaeological artifacts". In: *Czechoslovak Journal of Physics* 52.2002 Suppl D (), p. D927.

- [54] Katharina Schmidt-Ott. "Plasma-reduction: Its potential for use in the conservation of metals". In: *Proceedings of Metal 4* (2004), pp. 235–246.
- [55] CL Xaplanteris and E Filippaki. "Chaotic Behavior of Plasma Surface Interaction: A Table of Plasma Treatment Parameters Useful to the Restoration of Metallic Archaeological Objects". In: *Chaotic Systems: Theory and Applications*. World Scientific, 2010, pp. 377–384.
- [56] Vera Sazavska et al. "Plasmachemical removal of corrosion layers from Iron in pulsed RF discharge". In: *Journal of Physics: Conference Series*. Vol. 207. 1. IOP Publishing, 2010, pp. 012–011.
- [57] Sandra Sif Einarsdttir. "Mass Conservation of Archaeological Iron Artefacts: A Case Study at the National Museum of Iceland". PhD thesis. Goteborgs universitet, Institutionen kulturv, 2012.
- [58] F Krma et al. "Application of low temperature plasmas for restoration/conservation of archaeological objects". In: *Journal of Physics: Conference Series*. Vol. 565. 1. IOP Publishing, 2014, p. 012.
- [59] H. Grossmannová and F. Krcma. "Plasma chemical treatment for metal artefacts: conservation approach". In: International Plasma Chemistry Society, 2015.
- [60] SK Pradhan, M Jeevitha, and SK Singh. "Plasma cleaning of old Indian coin in H₂-Ar atmosphere". In: *Applied Surface Science* 357 (2015), pp. 445–451.
- [61] Vera Sazavska et al. "Plasmachemical Conservation of Corroded Metallic Objects". In: *Journal of Physics: Conference Series*. Vol. 715. 1. IOP Publishing, 2016, p. 120.
- [62] CL Xaplanteris and SC Xaplanteris. "Mechanical and Chemical Results in Plasma-Surface Contact". In: *A Study of Sheath Parameters. Phys Astron Int J* 2.1 (2018), p. 044.
- [63] Frantisek Krcma Radko Tino Katarina Vizarova. *Plasma surface cleaning of cultural heritage objects*. Elsevier, 2018.
- [64] Jelica Novakovic et al. "Plasma reduction of bronze corrosion developed under long-term artificial ageing". In: *Analytical and bioanalytical chemistry* 395.7 (2009), pp. 2235–2244.
- [65] P Fojtikova et al. "Effect of Hydrogen Plasma on Model Corrosion Layers of Bronze". In: *Journal of Physics: Conference Series*. Vol. 715. 1. IOP Publishing, 2016, p. 012006.
- [66] Carla Lucia Soto Quintana. "Development and optimisation of protocols for surface cleaning of cultural heritage metals". MA thesis. Universidade de Evora, 2016.

- [67] BT Goras et al. "Optical evaluation of heritage silver coin plasma cleaning using statistical methods". In: *Optoelectronics and Advanced Materials-Rapid Communications* 4.12 (2010), pp. 2157–2161.
- [68] Emil Ghiocel Ioanid et al. "Assessment of the cleaning effect of HF cold plasma by statistical processing of photographic image". In: *Measurement* 46.8 (2013), pp. 2569–2576.
- [69] Emil Ghiocel Ioanid et al. "Surface investigation of some medieval silver coins cleaned in high-frequency cold plasma". In: *Journal of Cultural Heritage* 12.2 (2011), pp. 220–226.
- [70] E Angelini and S Grassini. "Plasma treatments for the cleaning and protection of metallic heritage artefacts". In: *Corrosion and Conservation of Cultural Heritage Metallic Artefacts*. Elsevier, 2013, pp. 552–569.
- [71] Omar Abdel-Kareem, Awad Al-Zahrani, and Mounir Arbach. "Authentication and conservation of corroded archaeological Qatabanian and Himyarite silver coins". In: *Journal of Archaeological Science: Reports* 9 (2016), pp. 565–576.
- [72] Marta Quaranta. "On the degradation mechanisms under the influence of pedological factors through the study of archeological bronze patina". PhD thesis. alma, 2009.
- [73] MA Emami and M Bigham. "Mechanism of corrosion due to unalloyed copper inclusion in ancient bronzes". In: *Surface Engineering* 29.2 (2013), pp. 128–133.
- [74] Abdunaser Al-Zahrani and Mohamed Ghoniem. "A CHARACTERIZATION OF COINS FROM THE NAJRAN HOARD, SAUDI ARABIA, PRIOR TO CONSERVATION". In: *International Journal of Conservation Science* 3.3 (2012).
- [75] Christopher J Keturakis et al. "Analysis of corrosion layers in ancient Roman silver coins with high resolution surface spectroscopic techniques". In: *Applied Surface Science* 376 (2016), pp. 241–251.
- [76] Ahmed Elsayed. "Investigations methods to study corrosion of some ancient Islamic copper coins at Faculty of arts museum, Sohag university, Egypt". In: *International Conference on Metrology for Archaeology and Cultural Heritage, MetroArchaeo*. IMEKO. 2016, pp. 191–196.
- [77] KP FitzGerald et al. "Atmospheric corrosion of copper and the colour, structure and composition of natural patinas on copper". In: *Corrosion Science* 48.9 (2006), pp. 2480–2509.
- [78] T De Caro et al. "Archaeo-metallurgical studies of tuyeres and smelting slags found at Tharros (north-western Sardinia, Italy)". In: *Applied Physics A* 113.4 (2013), pp. 933–943.

- [79] Cristina Riccucci et al. "Micro-chemical and metallurgical study of Samnite bronze belts from ancient Abruzzo (central Italy, VIII–IV BC)". In: *Applied Physics A* 113.4 (2013), pp. 959–970.
- [80] Gabriel M Ingo et al. "Gold coated copper artifacts from the Royal Tombs of Sipán (Huaca Rajada, Per manufacturing techniques and corrosion phenomena". In: *Applied Physics A* 113.4 (2013), pp. 877–887.
- [81] Ziad Al-Saad and M Bani-Hani. "Corrosion behavior and preservation of Islamic silver alloy coins". In: *Strategies for Saving our Cultural Heritage. Proceedings of International Conference on Strategies for Saving Indoor Metallic Collections. Cairo*. Vol. 25. 2007, pp. 177–183.
- [82] C Soffritti et al. "On the degradation factors of an archaeological bronze bowl belonging to a private collection". In: *Applied Surface Science* 313 (2014), pp. 762–770.
- [83] Elin Maria Soares de Figueiredo. "A study on metallurgy and corrosion of ancient copper-based artefacts from the Portuguese territory". In: (2010).
- [84] Doris E Couture-Rigert, P Jane Sirois, and Elizabeth A Moffatt. "An investigation into the cause of corrosion on indoor bronze sculpture". In: *Studies in conservation* 57.3 (2012), pp. 142–163.
- [85] Wlady saw Kubiak. *Al-Fustat at: Its Foundation and Early Urban Development*. American University in Cairo Press, 1987.
- [86] Khaled Azab. *Al-Fustat, creation, prosperity, receding*. Dar Al-Afaq Al-Arabia, 1998.
- [87] Wladyslaw Kubiak. "Al Fustat: its foundation and early urban development, African Affairs". In: *African Affairs* 85.341 (1986), pp. 626–628.
- [88] Viswanathan S Saji and RM Cook. *Corrosion protection and control using nano-materials*. Elsevier, 2012.
- [89] Alfred Lucas and John Harris. *Ancient Egyptian materials and industries*. Courier Corporation, 2012.
- [90] Ahmed Elsayed. "Restoration and Conservation of two Islamic Metallic antiquities samples from the faculty of arts Museum at Sohag University, Egypt". MA thesis. Conservation department, Faculty of Arts, Sohag University, 2013.
- [91] VK Gouda, GI Youssef, and NA Abdel Ghany. "Characterization of Egyptian bronze archaeological artifacts". In: *Surface and Interface Analysis* 44.10 (2012), pp. 1338–1345.
- [92] Rui Jorge C Silva et al. "Microstructure interpretation of copper and bronze archaeological artefacts from Portugal". In: *Materials Science Forum*. Vol. 587. Trans Tech Publ. 2008, pp. 365–369.

- [93] David A Scott. *Metallography and microstructure in ancient and historic metals*. Getty publications, 1992.
- [94] A Gharib. "A SCIENTIFIC STUDY OF THE PATINA, CORROSION MORPHOLOGY, AND CONSERVATION OF EGYPTIAN BRASS OBJECT". In: *Egyptian Journal of Archaeological & Restoration Studies* 4.1 (2014).
- [95] Kenneth J Klabunde and Ryan M Richards. *Nanoscale materials in chemistry*. John Wiley & Sons, 2009.
- [96] David Erhardt, Charles S Tumosa, and Marion F Mecklenburg. "Applying science to the question of museum climate". In: *Museum Microclimates Conference*. National Museum of Denmark. 2007.
- [97] Pierre R Roberge. *Handbook of corrosion engineering*. McGraw-Hil, 2000.
- [98] Clima temps. *Relative Humidity in Sohag, Egypt*. 2018. URL: <http://www.sohag.climatemps.com/humidity.php> (visited on 12/05/2018).
- [99] CLIMATE-DATA.ORG. *CLIMATE SOHAG*. 2018. URL: <https://en.climate-data.org/africa/egypt/sohag-governorate/sohag-6318/> (visited on 12/05/2018).
- [100] Zhongwen Guo et al. "IMA: An integrated monitoring architecture with sensor networks". In: *IEEE Transactions on Instrumentation and Measurement* 61.5 (2012), pp. 1287–1295.
- [101] John Schmalzel et al. "An architecture for intelligent systems based on smart sensors". In: *IEEE Transactions on Instrumentation and Measurement* 54.4 (2005), pp. 1612–1616.
- [102] Cecily M Grzywacz. *Monitoring for gaseous pollutants in museum environments*. Getty Publications, 2006.
- [103] T Prosek et al. "Real-time monitoring of indoor air corrosivity in cultural heritage institutions with metallic electrical resistance sensors". In: *Studies in conservation* 58.2 (2013), pp. 117–128.
- [104] ISO. "Measurement of environmental parameters affecting indoor corrosivity". In: (2006).
- [105] ISO. "Determination and estimation of indoor corrosivity". In: (2006).
- [106] E Angelini et al. "Innovative monitoring campaign of the environmental conditions of the Stibbert museum in Florence". In: *Applied Physics A* 122.2 (2016), p. 123.
- [107] S Corbellini et al. "Cloud based sensor network for environmental monitoring". In: *Measurement* 118 (2018), pp. 354–361.
- [108] Luca Lombardo et al. "Wireless Sensor Network for Distributed Environmental Monitoring". In: *IEEE Transactions on Instrumentation and Measurement* (2017).

- [109] Robert Kelsall, Ian W Hamley, and Mark Geoghegan. *Nanoscale science and technology*. John Wiley & Sons, 2005.
- [110] Terry L Alford, Leonard C Feldman, and James W Mayer. *Fundamentals of nanoscale film analysis*. Springer Science & Business Media, 2007.
- [111] Masamitsu Watanabe, Masato Tomita, and Toshihiro Ichino. “Characterization of corrosion products formed on copper in urban, rural/coastal, and hot spring areas”. In: *Journal of The Electrochemical Society* 148.12 (2001), B522–B528.
- [112] Susan La-Niece. *Metal plating and patination: cultural, technical and historical developments*. Elsevier, 2013.
- [113] ISO. “Paints and varnishes – Determination of resistance to humid atmospheres of sulfur dioxide”. In: (1993).
- [114] SK Chawla and JH Payer. “The early stage of atmospheric corrosion of copper by sulfur dioxide”. In: *Journal of the Electrochemical Society* 137.1 (1990), pp. 60–64.
- [115] Patrik Schmuki and Sannakaisa Virtanen. *Electrochemistry at the Nanoscale*. Springer Science & Business Media, 2009.
- [116] Y Martín-Regueira et al. “Indoor atmospheric corrosion of copper and steel under heat trap conditions in Cuban tropical climate”. In: *Corrosion Engineering, Science and Technology* 46.5 (2011), pp. 624–633.
- [117] DW Rice et al. “Atmospheric corrosion of copper and silver”. In: *Journal of the Electrochemical Society* 128.2 (1981), pp. 275–284.
- [118] Erika Callsen. “Development of accelerated corrosion tests involving alternative exposure to hostile gases, neutral salt spray and drying”. In: (2012).
- [119] Huizhi Bao et al. “Crystal-Plane-Controlled Surface Restructuring and Catalytic Performance of Oxide Nanocrystals”. In: *Angewandte Chemie International Edition* 50.51 (2011), pp. 12294–12298.
- [120] Antonio R Mendoza and Francisco Corvo. “Outdoor and indoor atmospheric corrosion of non-ferrous metals”. In: *Corrosion Science* 42.7 (2000), pp. 1123–1147.
- [121] KP Fitzgerald, J Nairn, and A Atrens. “The chemistry of copper patination”. In: *Corrosion science* 40.12 (1998), pp. 2029–2050.
- [122] Sabrina Grassini et al. “Advanced plasma treatment for cleaning and protecting precious metal artefacts”. In: *Strategies for saving our cultural heritage. Proceedings of the international conference on conservation strategies for saving indoor metallic collections, Cairo. TEI of Athens, Athens. 2007*, pp. 127–131.
- [123] R Castell, EJ Iglesias, and J Ruiz-Camacho. “Glow discharge plasma properties of gases of environmental interest”. In: *Brazilian journal of physics* 34.4B (2004), pp. 1734–1737.

- [124] Brian N Chapman. *Glow discharge processes: sputtering and plasma etching*. Wiley, 1980.
- [125] Annemie Bogaerts et al. "Gas discharge plasmas and their applications". In: *Spectrochimica Acta Part B: Atomic Spectroscopy* 57.4 (2002), pp. 609–658.
- [126] Annemie Bogaerts and Renaat Gijbels. "Similarities and differences between direct current and radio-frequency glow discharges: a mathematical simulation. Invited Lecture Presented at the 2000 Winter Conference on Plasma Spectrochemistry, Fort Lauderdale, FL, USA, January 10-15, 2000." In: *Journal of Analytical Atomic Spectrometry* 15.9 (2000), pp. 1191–1201.
- [127] DB Graves and MJ Kushner. "Low temperature plasma science: not only the fourth state of matter but all of them". In: *Report of the Department of Energy Office of Fusion Sciences Workshop Low Temperature Plasmas*. 2008.
- [128] Michael A Lieberman. "Plasma discharges for materials processing and display applications". In: *Advanced Technologies Based on Wave and Beam Generated Plasmas*. Springer, 1999, pp. 1–22.
- [129] Liana Muresan et al. "Protection of bronze covered with patina by innocuous organic substances". In: *Electrochimica Acta* 52.27 (2007), pp. 7770–7779.
- [130] Katarina Maruvsic et al. "Comparative studies of chemical and electrochemical preparation of artificial bronze patinas and their protection by corrosion inhibitor". In: *Electrochimica Acta* 54.27 (2009), pp. 7106–7113.
- [131] I Constantinides, A Adriaens, and F Adams. "Surface characterization of artificial corrosion layers on copper alloy reference materials". In: *Applied Surface Science* 189.1-2 (2002), pp. 90–101.
- [132] ASTM international. "Standard Test Method for Corrosion Test for Engine Coolants in Glassware". In: (2012).
- [133] Xian Zhang, Inger Odnevall Wallinder, and Christofer Leygraf. "Mechanistic studies of corrosion product flaking on copper and copper-based alloys in marine environments". In: *Corrosion Science* 85 (2014), pp. 15–25.
- [134] Marta Chmielová, Jana Seidlerová, and Zdeněk Weiss. "X-ray diffraction phase analysis of crystalline copper corrosion products after treatment in different chloride solutions". In: *Corrosion science* 45.5 (2003), pp. 883–889.
- [135] G Di Carlo et al. "Artificial patina formation onto copper-based alloys: chloride and sulphate induced corrosion processes". In: *Applied Surface Science* 421 (2017), pp. 120–127.
- [136] Alejandro Echavarría et al. "Study of the copper corrosion mechanism in the presence of propionic acid vapors". In: *Journal of the Brazilian Chemical Society* 20.10 (2009), pp. 1841–1848.

- [137] CMB Martins and JI Martins. "Identification of corrosion products on a medieval copper-silver coin". In: *Protection of Metals and Physical Chemistry of Surfaces* 47.1 (2011), pp. 128–132.
- [138] Kanggen Zhou et al. "Selective precipitation of Cu in manganese-copper chloride leaching liquor". In: *Hydrometallurgy* 175 (2018), pp. 319–325.
- [139] M Biton et al. "On the electrochemical behavior and passivation of copper and brass (Cu70/ Zn30) electrodes in concentrated aqueous KOH solutions". In: *Journal of the Electrochemical Society* 153.12 (2006), B555–B565.
- [140] OA Jianu et al. "X-ray diffraction of crystallization of copper (II) chloride for improved energy utilization in hydrogen production". In: *International Journal of Hydrogen Energy* 41.19 (2016), pp. 7848–7853.
- [141] E Angelini, S Grassini, and M Parvis. "Silver artefacts: plasma deposition of SiOx protective layers and tarnishing evolution assessment". In: *Corrosion Engineering, Science and Technology* 45.5 (2010), pp. 334–340.
- [142] Teresa Palomar et al. "A comparative study of cleaning methods for tarnished silver". In: *Journal of cultural heritage* 17 (2016), pp. 20–26.
- [143] VK Gouda and AM Awad. "AN APPROPRIATE METHOD FOR SILVER TARNISH REMOVAL". In: *18 TH INTERNATIONAL CORROSION CONGRESS*. 2011.
- [144] Craig Hillman et al. "Silver and sulfur: case studies, physics and possible solutions". In: *SMTA Inter, October* (2007).
- [145] Amy E Marquardt et al. "Protecting silver cultural heritage objects with atomic layer deposited corrosion barriers". In: *Heritage Science* 3.1 (2015), p. 37.
- [146] Francesco Sponza. "Resistenza al tarnishing di leghe d'argento mediante comparazione elettrochimica". In: (2011).
- [147] Vincent Daniels. "Plasma reduction of silver tarnish on daguerreotypes". In: *Studies in Conservation* 26.2 (1981), pp. 45–49.
- [148] Mao Yangwu et al. "Tarnish Testing of Copper-Based Alloys Coated with SiO₂-Like Films by PECVD". In: *Plasma Science and Technology* 16.5 (2014), p. 486.
- [149] Hsien-Che Lee. *Introduction to color imaging science*. Cambridge University Press, 2005.
- [150] Edward J Giorgianni and Thomas E Madden. *Digital color management: encoding solutions*. Vol. 12. John Wiley & Sons, 2008.
- [151] Marc Ebner. *Color constancy*. Vol. 6. John Wiley & Sons, 2007.
- [152] Phil Green and Michael Kriss. *Color management: Understanding and using ICC Profiles*. Wiley, 2010.
- [153] Simone Bianco et al. "Computational Color Imaging: 6th International Workshop, CCIW 2017, Milan, Italy, March 29-31, 2017". In: *Proceedings*. Vol. 10213.

- [154] Charles Poynton. *Digital video and HD: Algorithms and Interfaces*. Elsevier, 2012.
- [155] Frantisek Krčma Radko Tino Katarína Vizárová. “Plasma Surface Cleaning of Cultural Heritage Objects”. In: *Nanotechnologies and Nanomaterials for Diagnostic, Conservation and Restoration of Cultural Heritage*. Ed. by Rawil Fakhrullin Giuseppe Lazzara. 1st ed. Elsevier, 2006.
- [156] F Fracassi et al. “Application of plasma deposited organosilicon thin films for the corrosion protection of metals”. In: *Surface and Coatings Technology* 174 (2003), pp. 107–111.
- [157] Sandra Sif Einarsdóttir, Kulturvård Konservatorsprogrammet, Kulturvård Konservatorprogrammet, et al. “Mass-conservation of Archaeological Iron Artefacts”. In: (2012).

This Ph.D. thesis has been typeset by means of the \TeX -system facilities. The typesetting engine was $\text{Lua}\mathcal{A}\mathcal{T}\mathcal{E}\mathcal{X}$. The document class was `toptesi`, by Claudio Beccari, with option `tipotesi=scudo`. This class is available in every up-to-date and complete \TeX -system installation.